

Characterization of Soiling Loss on Photovoltaic Modules, and Development of a Novel Cleaning System

Submitted in partial fulfillment of the requirements
for the degree of

DOCTOR OF PHILOSOPHY

by

Jim Joseph John
(Roll No. 10407612)

under the guidance of

Prof. Anil Kottantharayil
Prof. Govindasamy Tamizhmani
(Arizona State University)



Department of Electrical Engineering
INDIAN INSTITUTE OF TECHNOLOGY BOMBAY

2015

Thesis Approval

This thesis entitled

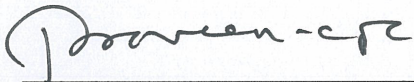
**Characterization of Soiling Loss on Photovoltaic Modules, and
Development of a Novel Cleaning System**

by

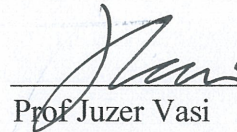
JIM JOSEPH JOHN
(Roll No: 10407612)

Is approved for the degree of

Doctor of Philosophy



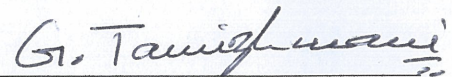
Prof Praveen C Ramamurthy
(Examiner)



Prof Juzer Vasi
(Examiner)



Prof Anil Kottantharayil
(Supervisor)



Prof Govindasamy Tamizhmani
(Co-Supervisor)



Prof Parag Bhargava
(Chairman)

Place: IIT Bombay
Date: 13th April 2016

Dedicated to
my Mother, Father,
Brothers, Wife and Son

Declaration

I declare that this written submission represents my ideas in my own words and where others ideas or words have been included, I have adequately cited and referenced the original sources. I also declare that Chapter 4 of this thesis contains the work we have published in IEEE Journal of Photovoltaics, vol. 5, No. 6, pp.1727-1734, Nov 2015 (DOI: 10.1109/JPHOTOV.2015.2463745) and in the proceedings of the SPIE Conference on Reliability of Photovoltaic cells, Modules, Components and Systems VII, 91790D, Oct 2014 (DOI: 10.1117/12.2063351). Chapter 5 contain the work published in IEEE Journal of Photovoltaics, vol. 6, No. 1, pp.236-243, Jan 2016 (DOI: 10.1109/JPHOTOV.2015.2495208) and in the proceedings of the 42nd IEEE Photovoltaic Specialists Conference 2015. Chapter 6 contains the work published in the proceedings of 26th European Photovoltaic Solar Energy Conference and Exhibition 2011, pp.3569-3571, ISBN:3-936338-27-2 (doi: 10.4229/26thEUPVSEC2011-4AV.2.27), and in the proceedings of 39th IEEE Photovoltaic Specialists Conference 2013, pp. 1481-1483, Jun 2013.

I also declare that I have adhered to all principles of academic honesty and integrity and have not misrepresented or fabricated or falsified any idea/data/fact/source in my submission. I understand that any violation of the above will be cause for disciplinary action by the Institute and can also evoke penal action from the sources which have thus not been properly cited or from whom proper permission has not been taken when needed.



JIM JOSEPH JOHN

Roll No. 10407612

IIT BOMBAY

April 12, 2016

Abstract

Given that electricity produced by photovoltaic (PV) technology is already contributing to 1% of world electricity demand in a short period of time, proving that the technological challenges are surmounted. It is inevitable that this percentage is going to increase considerably. Solar radiation is abundant in the Sun-belt countries and has huge scope of PV installations. But some of these countries have low frequency rain which aids in dust accumulation on PV modules. Occurrence of dust storms and high concentration of airborne particles that may get accumulated on PV modules can further worsen PV performance. Soiling on PV modules can be a potential showstopper for the PV technology deployment.

Till now, PV system has been designed for best energy yield by taking into consideration of irradiation and ambient temperature. This thesis discuss two strategies - one qualitative (Site Soiling Index) and another quantitative (World PV Soiling Loss rate map) methodology to evaluate the effect of soiling on PV modules at a geographical location. In order to understand the spectral and angular loss on PV modules, a outdoor and indoor characterization techniques are presented.

Spectral and angle of incidence (AOI) losses on naturally soiled crystalline silicon PV modules installed in Arizona are investigated in this thesis. The test modules designated as “moderately soiled (3 gm^{-2})” and “heavily soiled (74.6 gm^{-2})” showed short-circuit current (I_{sc}) losses of about 10% and 41%, respectively. The spectral reflectance and quantum efficiency (QE) losses were also quantitatively determined. In the wavelength range of 350 – 1100 nm, the average reflectance of moderately and heavily soiled modules increased (as compared to the clean surface) by 58.4% and 87.2%, respectively. In the moderately soiled module, the 26.3% (average) reduction in QE is mainly because of 23% of absorption and 5.5% of reflection in the dust. In the highly soiled module, the 75.3% (average) reduction in QE is mainly because of 62% of absorption and 31% of reflection

in the dust particles. It is also seen that the typical critical AOI of 57° for cleaned PV modules decreased to 38° for the moderately soiled module and 20° for the heavily soiled module. This influence is crucial for fixed tilt modules as they experience a wide range of AOI during its daily operation and a significant fraction of energy is generated at higher AOIs, especially on cloudy days.

Evaluation of soiling loss on photovoltaic modules in a geographical location involves collecting data from a fielded PV system of that location. This is usually a time consuming and expensive undertaking. Hence we propose collecting dust samples from various location of interest, preferably from the module surface, and use them as dust samples so that the soiling experiments can be conducted in laboratory. In this thesis, a low-cost artificial dust deposition technique is utilized that could be used to deposit dust on a module surface in a controlled manner which helps in predicting soiling loss associated with various dust properties including densities, chemical compositions and particle sizes. The soil samples covering diverse climatic conditions and six different geographic locations covering entire India were collected and investigated. Soiling loss on a silicon solar cell with Mumbai dust (17.1%) is about two times that of Jodhpur dust (9.8%) for the same soil gravimetric density of 3 gm^{-2} . The dust collected from Mumbai showed highest spectral loss, followed by Pondicherry, Agra, Hanle, Jodhpur and Gurgaon. The worst affected module technology was amorphous silicon (17.7%) followed by cadmium telluride (15.7%), crystalline silicon (15.4%) and CIGS (14.5%) for the same density (1.8 gm^{-2}) of dust from Mumbai.

This thesis discusses a novel PV module cleaning system using ambient moisture. The deliquescent property of salts are used to absorb moisture from the humidity. Clean water is extracted from the salt solution using a similar principle used in solar still. A pyramid made of glass is used to separate clean water from the solution. It is shown that the resultant water is of good quality with very low salinity and chloride values. A prototype using this technique of capturing water from ambient is developed to clean PV modules. After spraying water on PV modules, it is usually followed by a wiping, which is usually done manually or by some robots which uses electricity. A full automated (without electricity) wiping is achieved by using the superhydrophilic property of TiO_2 , which is coated on PV module glass surface.

Acknowledgements

Firstly, I would like to express my sincere gratitude to my advisor Prof. Anil Kottantharayil for the continuous support of my PhD study and related research, for his patience, motivation, and immense knowledge. His guidance helped me in all the time of research and writing of this thesis. I could not have imagined having a better advisor and mentor for my PhD study.

I would like to express my gratitude to my co-advisor Prof Govindasamy TamizhMani of Arizona State University, USA for his guidance in providing directions for my PhD. I would also like to thank him for accepting me as an intern at his prestigious Photovoltaic Reliability Lab (*ASU – PRL*) and at TuV Rheinland USA. Without this internship and his support it would not be possible to conduct this research.

Besides my advisors, I would like to thank the rest of my research progress review committee: Prof. Chetan Singh Solanki, Prof. Suryanarayan Doolla, and Prof. Juzer Vasi, for their insightful comments and encouragement, but also for the hard question which incited me to widen my research from various perspectives. I would also like to thank Prof K. L. Narasimhan and Prof B. M. Arora for supporting and helping me understand some of the fundamental aspects of Photovoltaic Technology.

I thank my fellow labmates Shashwata Chattopahyay, Rajeev Dubey, Vivek Kuthanazhi, Sonali Warade, Sonali Bhaduri, Abhishek Kumar, Rambabu and Firoz Ansari for the stimulating discussions and for all the fun we have had in the last four years. I would like to thank my colleague Mehul Raval for encouraging and helping me to pursue the novel cleaning system using ambient moisture. Also, I want to express my sincere gratitude towards Sonali Warade in helping with the experiments which lead to Chapter 5 and Chapter 6. Also, I thank my friends Sai Tatapudi, Brett Knisley, Sanjay S, Vidyashree Rajasekar, Sravanthi Boppana and Joseph Kuitche at ASU-PRL. In particular, I am grateful to Dr.Larry Kazmerski and Dr. Bill Tumas of NREL (National Renewable Energy

Laboratory), USA for enlightening me with a first glance of research during my 2 week visit.

I would like to acknowledge the support by the Solar Energy Research Institute for India and the United States (SERIUS) funded jointly by the U.S. Department of Energy subcontract DE AC36-08G028308 (Office of Science, Office of Basic Energy Sciences, and Energy Efficiency and Renewable Energy, Solar Energy Technology Program, with support from the Office of International Affairs) and the Government of India subcontract IUSSTF/JCERDC-SERIUS/2012 dated 22nd Nov. 2012. Part of this work was carried out at the National Centre for Photovoltaic Research and Education (NCPRE) at IIT Bombay, which is supported by the Ministry of New and Renewable Energy, Government of India. I would like to acknowledge CEN (Centre of Excellence in Nanoelectronics), Applied Materials Chemistry Lab, SAIF (Sophisticated Analytical Instrument Facility), Department of Earth Science and Department of Metallurgical Engineering & Material Science at IIT Bombay for allowing us to use their facility.

Last but not the least, I would like to thank my family: my wife Jincy, my son Neil, my Mom Annamma John and Dad Joseph John, parent-in-law Lisy and T C Kuriakose and to my brothers Jinu and Jovin and sister-in-law Jiny for supporting me spiritually throughout writing this thesis and my life in general.

Jim Joseph John

Contents

Abstract	ii
Acknowledgment	iv
List of Figures	xiii
List of Tables	xv
List of Abbreviations	xv
1 Introduction	1
1.1 Background	1
1.2 Outline of Thesis	6
2 Understanding Soiling on Photovoltaic Module	9
2.1 Understanding the Soiling Mechanism	9
2.1.1 Size Distribution of Dust Particles	10
2.1.2 Various Sources of Dust	11
2.1.3 Composition of Dust Particles	12
2.1.4 Processes of Soiling	13
2.1.4.1 Transportation of Dust Particles	13
2.1.4.2 Initial Adhesion Mechanisms	14
2.1.4.3 Changes in Initial Adhesion Mechanisms	15
2.1.4.4 Alterations on the Surface	16
2.1.4.5 Restorative Methods	16
2.2 Factors that Affect Soiling on PV Modules	17
2.2.1 PV Module and System Characteristics	17

2.2.1.1	Tilt Angle	18
2.2.1.2	Orientation	19
2.2.1.3	Glazing Surface Characteristics	19
2.2.1.4	PV Technology	19
2.2.1.5	PV Module Cell Configuration	20
2.2.2	Environmental Effects	20
2.2.2.1	Height of Installation	22
2.2.2.2	Airborne Dust Concentration	22
2.2.2.3	Average Wind Speed	22
2.2.2.4	Probability of Dust Storm	23
2.2.2.5	Distance of Domestic Dust Source	24
2.2.2.6	Occurrence of Dew	24
2.2.2.7	Module Dust Particle Size Distribution	25
2.3	Conclusion	25
3	Effect and Strategies for Quick Estimation of Soiling on PV Modules	27
3.1	Impact of Soiling on PV Modules Installed in Mumbai	27
3.1.1	Experimental Setup	28
3.1.2	Results - Soiling Rate Observed in Mumbai	29
3.2	Strategies for Quick Estimation of PV Module Soiling Rate	32
3.2.1	Site Soiling Index	32
3.2.2	World PV Soiling Map	35
3.3	Conclusion	36
4	Outdoor Characterization - Quantification and Modeling of Spectral and Angular Losses of Naturally Soiled PV Modules	38
4.1	Introduction	38
4.2	Methodology to Estimate the Spectral and Angular Loss	40
4.2.1	Determination of Soil Gravimetric Density	41
4.2.2	Characterization of Spectral Loss	42
4.2.3	Characterization of Angular Loss	45
4.3	Results and Discussions	46
4.3.1	Comprehensive Spectral Loss Calculation of Soiled PV Module	47

4.3.2	AOI Loss of Soiled PV Module	52
4.4	Conclusion	54
5	Indoor Characterization of Different Types of Dust found on PV Modules from India	56
5.1	Introduction	56
5.2	Methodology	58
5.2.1	Preparation of Soil Suspension	59
5.2.2	Artificial Dust Deposition	59
5.2.3	Characterization	60
5.2.4	Uniformity and Repeatability	62
5.3	Results and Discussion	63
5.3.1	Sediment Characterization	63
5.3.2	Impact of Dust Samples from Mumbai and Jodhpur on Performance	64
5.3.2.1	1-Sun Response	64
5.3.2.2	Quantum Efficiency	66
5.3.3	Impact of Dust Samples from Gurgaon, Hanle, Agra and Pondicherry on PV Performance	66
5.3.4	Simulated Soiling Loss of Different PV Module Technologies	70
5.3.4.1	Soiling Loss for Different Gravimetric Densities	70
5.3.4.2	Soiling Loss for Different Dust Types	71
5.4	Conclusion	73
6	Novel PV Module Cleaning System using Ambient Moisture	75
6.1	Concept and Approach	76
6.2	Average Annual Relative Humidity of the World	77
6.3	Moisture Extraction	78
6.3.1	Moisture Absorption Experiments	79
6.3.2	Filtration	81
6.4	Prototype Design	83
6.5	Development of Wiping coating	87
6.5.1	Experiment	89
6.5.2	Results	92

6.6	Conclusion	93
7	Summary	94
7.1	Outdoor Characterization of Spectral and Angular loss of Naturally Soiled PV Modules	95
7.2	Development of Artificial Dust Deposition System and Indoor Characterization of Dust Samples Collected from PV Modules Installed in Different Parts of India	96
7.3	Novel PV Module Cleaning System Using Ambient Moisture	97
8	Future Works	99
8.1	Strategies for Quick estimation of the Extent of Soiling	99
8.2	Artificial Dust Deposition Using Water	100
8.3	Improvements for the PV Module Cleaning System	101
	Appendices	103
A	Literature Reviewed for the World PV Soiling Loss Rate Map (used in Section 3.2.2)	104
	Publications and patents	114
	Bibliography	118

List of Figures

1.1	World map showing the sunbelt countries of the World [5].	3
1.2	World map showing the dust storm frequency, data from 2225 meteorological stations [6].	3
1.3	World map showing the PM2.5 particle concentration (2010) [7].	5
1.4	World map showing the PM10 particle concentration (2014)[8].	5
2.1	Process involved in soiling or dust deposition on surfaces such as PV modules.	13
2.2	Schematic of different modes of aeolian transport of particles [13].	14
2.3	Cementation by water soluble particles [11].	16
2.4	Weathering of soda-lime glass [24].	17
2.5	PV module cell configuration for (a) thin-film and (b) c-Si PV modules. . .	21
2.6	Dust accumulation on PV modules after a dust storm [34].	24
2.7	Seasonal occurrence of dew as a fraction of days [37]. DJF (December, January, February), MAM (March, April, May), JJA (June, July, August), and SON (September, October, November).	25
3.1	Soiling station installed in Mumbai, having 2 modules of each PV module technologies, such as monocrystalline silicon (mono c-Si), multi-crystalline silicon (multi c-Si), amorphous silicon (a-Si) and CIGS.	28
3.2	Soiling loss calculated based on I_{sc} , P_{max} and daily energy (97 non-monsoon day data) for the year 2013.	30
3.3	Soiling rate observed in Mumbai for the non-monsoon month of February to June for the year (a)2013 (Data interval - 10 days) and (b)2015 (Data interval - 20 days).	31
3.4	World PV Soiling Loss Rate Map with data from 64 literature, shown in Appendix A.	37

4.1	Different types of soil layer formation on PV modules at different sites in India. (a),(b) and (d) are c-Si PV modules, found in Delhi and (c) is a-Si PV module found in Mumbai.	39
4.2	The methodology used in this study.	41
4.3	Illustration of optical losses on (a) cleaned and (b) soiled PV Module. . . .	43
4.4	Outdoor experimental setup for AOI measurement [Soiling level: A – Heavy (11.8 g/m^2), B – Moderate (4.85 g/m^2), C – Moderate (2.74 g/m^2), D –Light (1.71 g/m^2); E – Cleaned].	46
4.5	Spectral reflectance of the moderately (a) and heavily (b) soiled PV module before and after cleaning.	48
4.6	Reflectance, Absorption and Transmittance spectra of the heavily (a) and moderately (b) soiled PV module.	50
4.7	Non-uniform soiling of PV cells leading to difference in transmittance and I_{sc} data.	51
4.8	Comparison of quantum efficiency of heavily, moderately and lightly soiled PV module with the cleaned PV module.	52
4.9	AOI curve of cleaned and moderately soiled PV module.	53
5.1	Detailed methodology used in this study.	58
5.2	The experimental setup that was used to deposit dust on the solar glass samples.	59
5.3	Uniformity of the sample was evaluated by calculating J_{sc} from QE spectra at 5 different locations in the sample. The sample shown in (a) has a SGD of 15 g/m^2 . Repeatability of the deposition technique was checked by depositing 3 soil gravimetric densities (H – Heavy (15 g/m^2), M - Moderate (5 g/m^2), L - Light (1 g/m^2)) thrice shown in (b) and J_{sc} value is calculated.	62
5.4	Analyzed XRD data of dust samples from Agra, Mumbai, Hanle, Gurgaon, Pondicherry and Jodhpur.	65
5.5	Comparison of soiling loss (using I_{sc}) of soiled glass samples from Mumbai and Jodhpur with different soil gravimetric densities.	66
5.6	I-V curves of mono c-Si solar cell under clean and soiled glass samples from (a) Mumbai and (b) Jodhpur with different soil gravimetric densities. . . .	67

5.7	Comparison of QE curve of mono c-Si solar cell with different dust densities from (a) Mumbai and (b) Jodhpur.	68
5.8	Comparison of soiling loss (I_{sc}) due to dust from Gurgaon, Hanle, Jodhpur, Agra, Mumbai and Pondicherry of same gravimetric density (1.8 g/m^2). . .	69
5.9	Comparison of difference in QE spectra from clean glass and dust deposited glass samples. The gravimetric density of 1.8 g/m^2 is maintained for all dust coated glass. Dust samples are collected from Gurgaon, Hanle, Jodhpur, Agra, Mumbai and Pondicherry. The graph is split into zones I, II and III.	70
5.10	Spectral response of a-Si, mono c-Si, CdTe and CIGS modules, and AM1.5G spectrum divided into 3 zone- Zone I, Zone II and Zone III.	71
6.1	Illustration of a simple filtering process comprising of evaporation and condensation.	77
6.2	Average annual Relative Humidity seen in the (a)World and (b)Asia. . . .	78
6.3	Experiment setup to quantify the weight gain of various salts such as NaCl , MgCl_2 and CaCl_2 , due to moisture absorption.	79
6.4	Weight gain data for 100 hours experiment for CaCl_2 (A), MgCl_2 (B) and NaCl (C) (CRH = 75.5%).	80
6.5	Weight gain data for 300 hours experiment for CaCl_2 (A), MgCl_2 (B), NaCl (C) and equal mixtures of MgCl_2 and CaCl_2 (A+B), NaCl and CaCl_2 (A+C), and NaCl and MgCl_2 (B+C).	81
6.6	Weight gain data CaCl_2 (A), MgCl_2 (B), and equal mixture of MgCl_2 and CaCl_2 (A+B) for low relative humidity and high temperature.	81
6.7	Filtration experiment using solar energy image showing evaporation (a), and condensation happening on the glass surface (b). Circled area shows the clean water collected during the evaporation and condensation.	82
6.8	Filtration experiment using electric heater image showing evaporation and condensation happening on the glass surface (a). Circled area shows the container where the clean water gets collected during evaporation and condensation. The resultant anhydrous CaCl_2 is seen in (b) which can be reused for absorption.	83

6.9	Schematic of the moisture absorbing and filtration stage, along with the salt plate	84
6.10	Prototype of water from humidity system, storage tank and pipe based dispersing mechanism.	86
6.11	(Schematic (a) and Prototype (b) of the tracker based wiping mechanism. .	87
6.12	Illustration of the PV Module cleaning system prototype with the coating.	88
6.13	Schematic showing the electrospinning equipment.	90
6.14	Electrospinning equipment used for this work.	91
6.15	PVAc- TiO_2 composite nanofiber coated on glass sample. Image taken using Zeta 3D microscope.	91
6.16	SEM image showing porous TiO_2 fibers with width of fiber $< 1\mu m$	91
6.17	Image of the two solar glass coupons with TiO_2 coating (Right) and without TiO_2 coating (Left).	92
8.1	FTIR result of dust samples after artificial deposition using acetonitrile and water.	101

List of Tables

2.1	Earlier classification of particles found in the atmosphere by Bagnold[13].	10
2.2	Classification of sediments based on particle size distribution [14].	10
2.3	Most common outdoor dust particle sources and its characteristic elements [18].	12
3.1	Reference table to determine Site Soiling Index (SSI). Source of the data are denoted as PS- PV System characteristics, PM - Module Data Sheet, WD - Weather data, SI- Site information, and LM - Lab Measurement.	34
3.2	SSI calculation for IITB, Powai, Mumbai and ASU-PRL, Mesa, Arizona.	35
4.1	Gravimetric density of soiled PV Module used in this study.	41
4.2	Comparing AOI curves of cleaned and soiled c-Si PV modules.	54
5.1	Calculated J_{sc} of soiled glass sample in Figure 5.3(a) (15 g/m^2), showing uniformity of deposition.	63
5.2	Calculated J_{sc} of soiled glass sample in fig 5.3(a) (15 g/m^2), showing repeatability of deposition.	63
5.3	Particle size distribution and sediment types.	64
5.4	Sediment type classification of dust samples.	69
5.5	Simulated soiling loss of dust samples from Mumbai.	72
5.6	Simulated soiling loss of dust samples from Jodhpur.	72
5.7	Simulated soiling loss of dust samples (1.8 g/m^2) from 6 locations.	73
6.1	Critical Relative Humidity of commonly available salts.	76
6.2	Test result of filtered water, compared with potability parameters.	83
6.3	WCA and weighted avg transmittance of TiO_2 samples on plain glass.	92
6.4	WCA and weighted avg transmittance of TiO_2 samples on textured glass.	92

List of Abbreviations

a-Si	amorphous silicon
A	Area of the solar cell
$A_{H'}$	Area of Heavily soiled cell
$A_{M'}$	Area of Moderately soiled cell
A'_g	Absorbed by the cleaned glass
A''_g	Absorbed by the soiled glass
ASU-PRL	Arizona State University Photovoltaic Reliability Lab
AOI	Angle Of Incidence
ARC	Antireflective coating
BIPV	Building Integrated Photovoltaics
c-Si	Crystalline silicon
$CaCl_2$	Calcium Chloride
CdTe	Cadmium Telluride
CF	Certainty Factor
CIGS	Copper Indium Gallium Selenide
E_{dni}	Direct Normal Solar Irradiance
E_o	Reference Global Solar Irradiance
E_{poa}	Global Solar Irradiance in the plane-of-array
EQE	External quantum efficiency
EQE_{CPVM}	External quantum efficiency of Cleaned PV Module
EQE_{SPVM}	External quantum efficiency of Soiled PV Module
EQE_{MCPVM}	Measured External quantum efficiency of Cleaned PV Module
EQE_{MSPVM}	Measured External quantum efficiency of Soiled PV Module
η	Efficiency
$f_2(\text{AOI})$	Relative optical response

FF	Fill factor
H'	Heavily soiled
HSC	Heavily Soiled solar cell
IQE	Internal quantum efficiency
I - V	Current - voltage
I_{sc}	Short circuit current
$I_{sc,H'}$	Short circuit current of Heavily soiled cell
$I_{sc,M'}$	Short circuit current of Moderately soiled cell
IEC	International Electrotechnical Commission
IPA	Isopropyl Alcohol
J_{sc}	Short circuit current density
$J_{sc,H'}$	Short circuit current density of Heavily soiled cell
$J_{sc,M'}$	Short circuit current density of Moderately soiled cell
LM	Lab Measurements
M'	Moderately soiled
$MgCl_2$	Magnesium Chloride
mono c-Si	monocrystalline silicon
multi c-Si	multicrystalline/polycrystalline silicon
Mw	Molecular Weight
MW	Mega-Watt
NASA	National Aeronautics and Space Administration, USA
NE	North East
NCPRE	National Center for Photovoltaic Research and Education
PM	Module Data Sheet
PM2.5	Particulate Matter 2.5 micrometer or less in diameter
PM10	Particulate Matter 10 micrometer or less in diameter
PS	PV System characteristics
PV	Photovoltaics
PVMM	Photovoltaic Module Monitoring
PVAc	Polyvinyl Acetate
QE	Quantum Efficiency
R_{g-a}	Reflectance of the cleaned glass

R_{a-d}	Reflectance at the air-dust interface
R_{MCPVM}	Measured Reflectance of Cleaned PV Module
R_{MSPVM}	Measured Reflectance of Soiled PV Module
A_d	Absorbed by dust particles
S	Severity
SGD	Soil Gravimetric Density
SI	Site Information
SL	Soiling loss
SR	Soiling loss rate
SSI	Site Soiling Index
STC	Standard test conditions
SWIR	Short-wave Infrared
T_c	Measured module temperature
T_{HSC}	Transmittance of the Heavy soiled solar cell
T'_g	Transmittance of the cleaned glass
T''_g	Transmittance of the soiled glass
$T_{H'}$	Transmittance of Heavily soiled cell
$T_{M'}$	Transmittance of Moderately soiled cell
UNCCD	United Nations Convention to Combat Desertification
USA	United States of America
VNIR	Very near Infrared
W	Weightages
WCA	Water Contact Angle
WD	Weather Data
WHO	World Health Organization
V_{oc}	Open circuit voltage

Chapter 1

Introduction

1.1 Background

The current energy systems depend heavily on the declining stock of fossil fuels (coal, oil and natural gas), leaving about 2.7 billion people [1] in the world without access to adequate electricity, and is, therefore not sustainable economically, socially and environmentally. Moreover, the highly carbon-intensive state of the energy sector throughout the developing countries is susceptible to large swings in oil prices and also cost billions in subsidies. Greening the energy sector aims at a renewable and sustainable energy generation system. Renewable energy technologies is looked upon as the answer to address the current concerns regarding energy security, the environment and global climate change. Solar electricity, also known as photovoltaics (PV), has shown since 1970s that the substantial portion of the world electricity demand can be met without burning fossil fuels or creating nuclear fission reactions. PV systems can be used for wide range of applications, scales, climates and geographical locations.

The word ‘photovoltaic’ is a marriage of two words: the Greek word ‘photo’, meaning light, and ‘voltaic’, meaning electricity. Photovoltaic technology (PV) is used to describe the hardware that converts solar energy into usable electrical energy from light. Photovoltaic is the direct conversion of light (photons) into electricity (voltage) using semiconductor materials. All inorganic PV cells have two layers of semi-conductors, one n-type and another p-type. When light shines on the semi-conductor, the electric field across the junction between these two layers causes electricity to flow, generating DC (direct current). Photovoltaic cells are the major constituent of a photovoltaic module. A

typical silicon photovoltaic cell produces less than 3 watts at 0.5 volts DC, therefore cells must be connected in series or parallel configurations to form PV modules to produce enough power for high-power applications. Modules have peak output powers varying from few watts to more than 350 watts, depending on the application. If the application requires output power to range from few hundred watts to megawatt range, modules are connected in series, parallel or series-parallel configurations to form PV arrays.

PV systems often employ an energy storage mechanism so that when the sun illuminates the PV arrays, the electrical energy is captured and stored. The most commonly used storage mechanism is rechargeable batteries. This type of PV systems is commonly known as stand-alone PV systems, off-grid PV systems, or battery based PV systems. It is also a common practice that the PV systems are connected to the utility grid. Such systems may deliver excess PV energy to the grid or use the grid as a backup system in case of insufficient PV generation. This type of PV system which is commonly referred to as grid connected PV systems is a cost effective solution provided a utility grid is available.

PV is generally considered to be an expensive method of producing electricity. However, in remote locations PV is very often the most economical solution to provide the electricity. The growing PV market all over the world indicates that solar electricity has entered many areas in which its application is economically viable. Additionally, the rapidly growing application of photovoltaic in utility grid-connected situations shows that photovoltaic are very attractive for a large number of people, companies and governments who want to contribute to the establishment of new and more environmentally friendly electricity supply systems. In addition to this, many Research and development centres are working towards reductions of cost envisaging mass production of photovoltaic systems, leading to further attractiveness of this technology and its extension to other fields of applications.

The global growth of installed PV system has been trending in an exponential manner for more than two decades. In the year 2014, the total installed capacity was more than 178 GW and the projected capacity for 2015 is 233 GW [2]. Now solar electricity covers more than 1% of the world electricity demand which is equivalent of 33 large coal fired power plants of 1GW each. India is currently witnessing a transition in its solar PV market with its installed capacity crossing above 4GW [3] as of June 2015. Government

of India has recently revised its National Solar Mission to set an aggressive target of 100GW of installed PV by the year 2022 [4], out of which 40GW is roof-top solar PV and 60GW is ground mounted large grid-connected PV system.

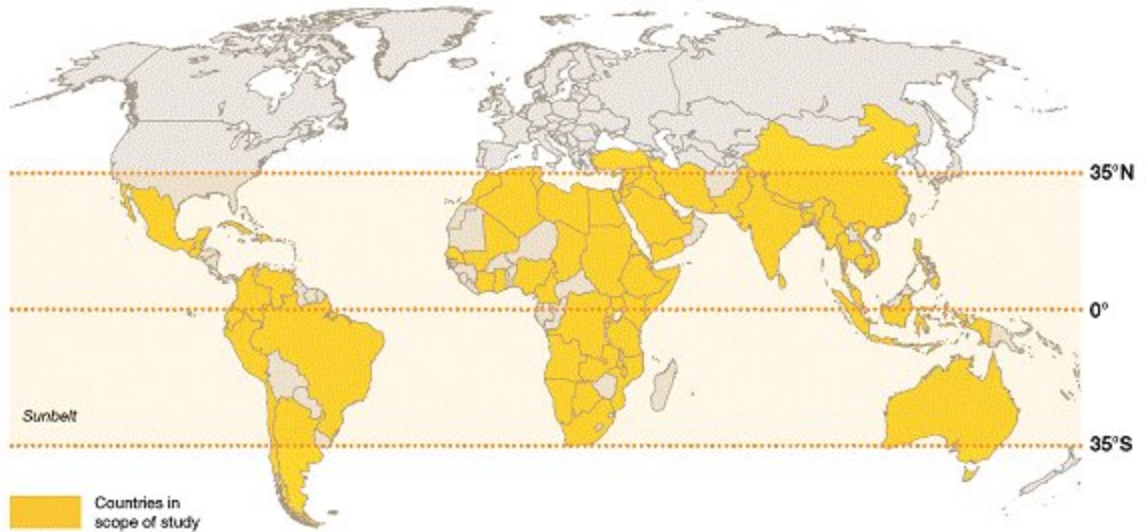


Figure 1.1: World map showing the sunbelt countries of the World [5].

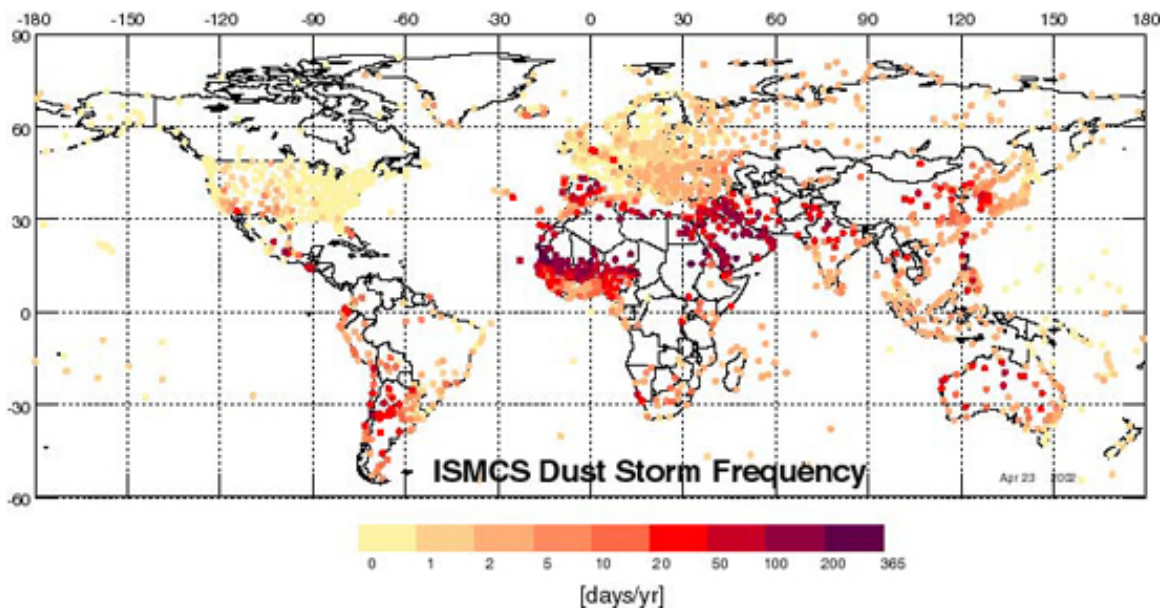


Figure 1.2: World map showing the dust storm frequency, data from 2225 meteorological stations [6].

The main advantage of PV system is that it uses solar radiation. Solar radiation is abundant especially at the Sun Belt regions around the equator which is mostly arid and has abundant sunlight. However, most of these areas exhibit high ambient temperature and low frequency rain which aids dust accumulation. These two environmental factors

can be detrimental to the performance of PV systems. Temperature effect of the PV modules are considered while designing the PV system, whereas the dust accumulation, referred in this thesis as "Soiling", on the PV modules is generally not considered or put arbitrarily (3%) during the design, deployment and operation of the PV system. Dust inherently stops the sunlight from reaching the PV cells, which can significantly reduce the power output of PV modules. Only recently has the issue of soiling on PV modules come to the forefront because of the increased growth of the PV installation in the sun belt countries, see Figure 1.1 (reproduced from reference [5]). Figure 1.2 (reproduced from reference [6]) shows the dust storm frequency (days/year) estimated using daily measurement from 2225 meteorological stations from the International Station Meteorological Climate Summary (ISMCS) data set. Many areas of Sun Belt regions such as the Middle East, North Africa, Northern India, South America and east part of China show high frequency of dust storm. Apart from dust storms, domestic pollution also can significantly contribute to soiling. The PM2.5 and PM10 map of the world, in Figure 1.3 (reproduced from reference [7]) and Figure 1.4 (reproduced from reference [8]) shows the concentration of particulate matter (PM) smaller than $2.5\mu\text{m}$ and $10\mu\text{m}$ respectively in the atmosphere, and indicates the degree of domestic pollution. In chapter 4 of this thesis, it is shown that urban places like Mumbai can show almost two times loss in PV performance due to soiling as compared to arid regions like Jodhpur, India for the same density of dust accumulation. This is attributed to the particle size distribution of the dust samples found in these locations. It is seen that large concentration of small particles in the dust deposited on the PV panels are more detrimental, as a result, the PM2.5 and PM10 particles can serve as an indicator of the severity of soiling at the geographical location.

The performance of the PV system is evaluated by the total energy output measured for a given time period. The energy yield by the PV system is used as a comparison parameter between different PV technologies, installation methods, tilt and orientations, and balance of systems. The decisions between various PV system designs greatly depend on the energy yield. Therefore, soiling is an important parameter which determines the energy yield from PV modules. Soiling loss on PV module is an environment dependent parameter that can be a potential showstopper for PV system deployment, simply because it is not easy to estimate the amount of dust accumulation. The decision to employ any

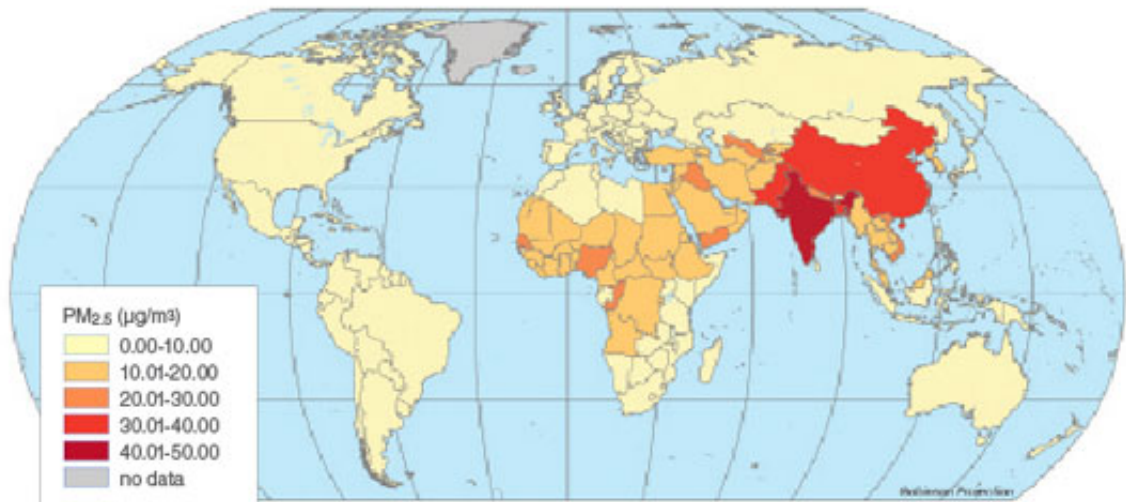


Figure 1.3: World map showing the PM_{2.5} particle concentration (2010) [7].

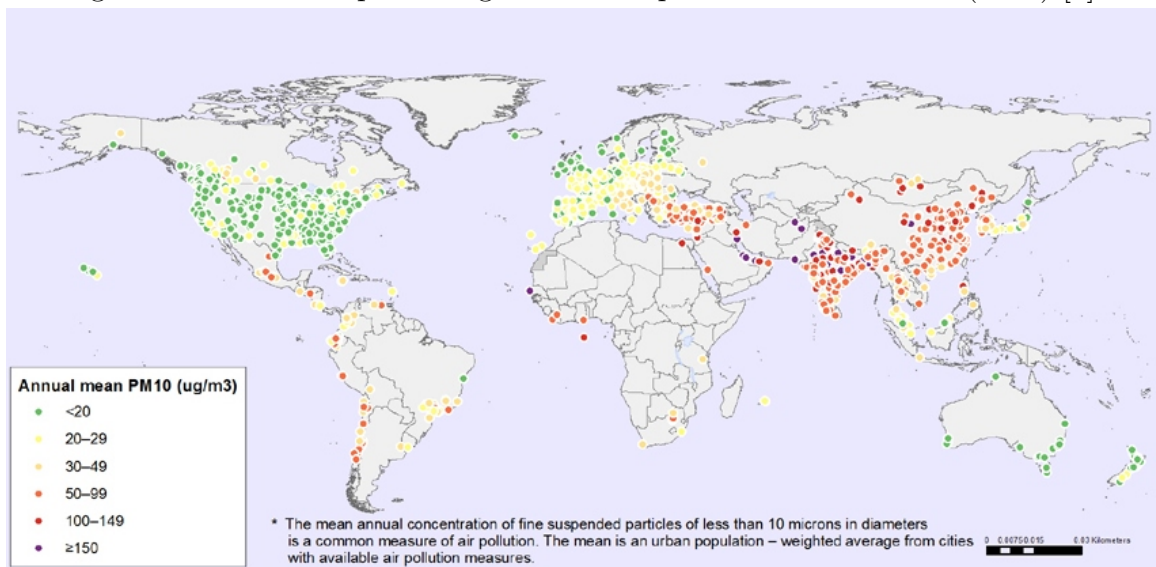


Figure 1.4: World map showing the PM₁₀ particle concentration (2014)[8].

restorative strategies depends on the financial loss due to reduction in the energy yield and the cost of implementing these strategies. During the design stage of the PV system, an annual soiling loss of 3 to 6% is considered. This value can mislead as this is averaged over dry and rainy days and is usually arbitrarily accounted with no valid data. In this thesis (Chapter 2, Section 2.3) it is reported that during the span of 100 non-rainy days the energy loss due to soiling can be above 32% for Mumbai. Energy loss of 50% from PV system due to soiling has been reported in places like Iraq and Libya [9]. Hence, energy yield loss due to soiling is an important parameter to be considered, and is dependent on the geographical location.

The soil layer formed due to dust accumulation on PV modules obstruct the incoming

radiation and alter the solar spectrum which affects PV cells as they are spectrally dependent devices. Spectral loss due to the soil layer on a fielded PV module is reported in chapter 3 of this thesis by using combination of outdoor and indoor spectral measurement techniques.

In the advent of huge growth in the PV installation throughout the world, the environment in which the PV modules are installed is becoming more important. The question that usually arises from PV system designers and operators is that how much soiling loss should be accounted for and how to determine the rate at which dust is accumulated. The most common practice for determining the soiling loss or the frequency of cleaning PV modules is to keep two separate set of panels which are monitored separately. One set of PV modules are cleaned everyday and the other is left to be naturally soiled. From this experimental setup, PV system operators determine the frequency of cleaning. The rate of soiling is not uniform throughout the year because of the seasonal variations. Hence, this systematic experiments will have to run for a minimum of 1 year. Cattle et al. [10] showed that dust accumulation can vary significantly within a single geographical area due to single source of dust. This level of detailed study can be very useful for planning PV system installation but this data took several years to collect. Therefore, a faster testing and evaluation method would be valuable in locating, designing and installing PV systems. Specific knowledge of the interaction between the accumulated dust at a location with the incident light would assist in these predictions. In this thesis, a low-cost accelerated method is discussed to understand the properties of dust and its interactions with various PV technologies. PV Engineers are looking for ways to resolve this issue by developing novel cleaning techniques and anti-soiling coatings. In chapter 5 of this thesis, we propose a new technique for cleaning of PV modules.

1.2 Outline of Thesis

Soiling loss on PV modules is usually treated as a trivial problem but can be a serious problem in certain geographical regions as explained in the above section. This thesis discuss this problem in detail and discusses a novel solution. In the first chapter, we introduce the context of the problem and how it can be a showstopper for PV technology deployment.

The second chapter attempts at understanding the mechanisms involved in the deposition of dust on PV modules. This chapter identifies and classifies the factors that facilitate the deposition of dust such as PV module and system characteristics, and geographical location dependent parameters.

Results of an outdoor PV modules experiment performed in Mumbai to understand the severity of soiling loss on PV modules is reported in Chapter 3. Soiling loss observed in Mumbai during the non-monsoon days is about 35-40% in about 100 days. Two different methods to quickly estimate the extent of soiling loss in a geographical location is proposed. The first method involves assigning scores to various parameters and calculating an index called Site Soiling Index. Also, there are lot of independent research centers and PV power plants conducting experiments to determine the soiling rate at their location. The second method involves creation of a web platform that consolidate all these results in an easily accessible interactive resource. This web platform can serve as a source of data for PV designers and operators who are installing a PV system near these research centers or power plants.

The fourth chapter looks into how the solar cell is affected by the soil layer on a PV module in terms of Quantum Efficiency. This study also shows what part of the spectrum is being absorbed, reflected and/or scattered by the soil layer. It is known and well understood that angle of incident sun ray with respect to normal of the PV module surface should be as small as possible (angle of incidence should be ideally zero degrees) in order to minimize reflection loss. This loss is determined by the PV module top cover, usually glass, and the air interface. But when the PV modules are soiled, the Angle Of Incidence (AOI) characteristics changes and is discussed in detail in this chapter.

Dust or soot from the air pollution causes significant loss in the PV modules. Evaluating the performance loss of photovoltaic modules in a location involves collecting data from an existing PV system. This is usually a time consuming and a costly affair. In chapter five, we propose collection of dust from an area, preferably from the module surface and use it as dust sample. Here a low-cost artificial dust deposition technique is introduced that could be used to predict the soiling loss associated with various dust densities. This approach produced uniform soil coatings of various densities. Using the collected dust, dust of varying densities was deposited which showed short-circuit current loss ranging from 4% to 49%. Dust from different parts of India was deposited using this

technique. Spectral loss studies were done on these dust samples.

An indigenous PV module cleaning system is developed and discussed in chapter six. This chapter also discusses coupling this design with the self-cleaning coating developed in the lab.

Chapter 7 summarizes the findings of this thesis. Future directions for research in this area are discussed in chapter 8.

Chapter 2

Understanding Soiling on Photovoltaic Module

In the previous chapter, the importance of considering soiling on PV modules installed in different geographical locations were discussed. In this chapter, a literature review is done to understand the dust and its various types, followed by mechanism involved in dust accumulations on PV modules, referred to in this thesis as "soiling mechanisms/process of soiling". There are many literature discussing various factors involved in aiding soiling on PV modules. All these factors are classified into two categories, viz. PV module and system characteristics, and geographical location effects.

2.1 Understanding the Soiling Mechanism

Particles of various sizes and constituents are present all around us in great abundance. Particles found in the atmosphere, in general, is of less than $500\mu\text{m}$ in diameter [11] which is about 10 times the diameter of human hair. These particles can be a mixture of various constituents such as pollen, fibers, metals, metal oxides, hydrocarbons, and organic matter [12]. Atmospheric particles are generated through various mechanisms such as mechanical abrasions, chemical reactions, and combustion processes. The particle size, constituents and shape can vary throughout different geographical locations of the world. Moreover, the deposition mechanism and the deposition rates can vary dramatically with geographical locations.

Table 2.1: Earlier classification of particles found in the atmosphere by Bagnold[13].

Particles	Size (mm)	Rate of Fall (m/s)
Pebbles, etc	1mm and above	10 and above
Sand	0.02 to 1	0.01 to 10
Dust	0.001 to 0.02	0.0001 to 0.01
Thin Smoke/Haze	10^{-6} to 10^{-4}	Do not fall

Table 2.2: Classification of sediments based on particle size distribution [14].

Diameter (μm)	Sediment Type
0 - 4	Clay
4 - 8	Very Fine Silt
8 - 16	Fine Silt
16 -31	Medium Silt
31 - 63	Coarse Silt
63 - 125	Very Fine Grained
125 - 250	Fine Grained
250 - 500	Medium Grained
500 - 1000	Coarse Grained

2.1.1 Size Distribution of Dust Particles

An earlier study (1954) by Bagnold in his book titled "The physics of blown sand and desert dunes" [13] has classified particles found in the atmosphere as shown in the table 2.1. Particle size range from pebbles, of large size, through sand grains to dust and to very small particles that form thin smoke and hazes. Each type of these particles has their rate at which they will fall on any given surface. The small particles which form thin smoke and haze are suspended in the atmosphere and do not fall. As the particle size increases, the rate of fall of these particles increases. In this thesis, all these atmospheric particles collectively will be referred to as "dust particles".

In a recent review paper by Blott et al. [14] published in the Journal of the International Association of Sedimentologists, they have classified dust particles into sediment types based on particle size distributions (see 2.2). Particle sizes of less than $4\mu\text{m}$ are known as clay, particles of size between 4 to $63\mu\text{m}$ are silt and the larger particles of 63 to $1000\mu\text{m}$ are known as grained or sand. Each of these sediment types are further classified as very fine, fine, medium and coarse. The sediment types that will be used in this thesis is as shown in table 2.2.

2.1.2 Various Sources of Dust

Dust's origin may be natural, or a consequence of human activities. Dust particles as they are formed are known as primary particles. Particles that originate due to atmospheric conversion processes are known as secondary particles. Primary particles are introduced into the atmosphere in solid or liquid form, while secondary particles are results of gas-to-particle conversion of emitted precursors.

Aeolian process is the dominant source of dust in the atmosphere where wind assisted emission, transport and deposition of sand and dust takes place. This process takes places whenever there is winds of sufficient speeds and availability of dust particles. The natural particles arises from erosion of rocks, sandstorms or deserts, from forest fires, grain of pollen and volcanic activity. According to NASA Goddard Space Flight Centre [15], satellite image shows that every year 64 million tons of airborne dust particle arrive in North American airspace from foreign sources (such from African continent) and this is as much as they are produced domestically. Atmospheric dust concentration can range from $30 \mu\text{g m}^{-3}$ for remote and rural locations, to $170 \mu\text{g m}^{-3}$ for polluted urban areas, and can be as high as $100,000 \mu\text{g m}^{-3}$ in sand storms [16].

Grained or coarse particles originate from mechanical processes, including grinding, breaking and wear of material, transportation, and dust re-suspension, and contain largely earth crust compounds. Small or fine particles are from combustion, photochemical processes, and gas-to-particle conversion. They contain soot, organic compounds, sulfates and nitrates, as well as trace metals and other toxins. Some events such as forest fires, generate particles with broad size distributions inclusive of coarse and fine particles. In most cases, coarse and fine particles are results of different generation events. According to Buekens et al. [16], there is little correlation between the number of particles and mass of coarse and fine dust. Coarse and fine particles have different chemical composition and origins, and are transported and removed by different mechanisms.

Another important factor controlling dust emission at the source areas is the vegetation cycle. The dust storm frequency is highest in desert/bare ground [17]. It is inversely correlated with the leaf area index, which describes the density of the vegetation. The emissions of dust are correlated with the vegetation types of the areas considered.

Table 2.3: Most common outdoor dust particle sources and its characteristic elements [18].

Source of Dust	Characteristic Elements Emitted
Road Transport	
Motor Vehicle emissions	Br, Pb, Ba, Mn, Cl, Zn, V, Ni, Se, Sb, As
Engine Wear	Fe, Al
Catalytic Converters	Rare earths, Pt
Tyre Wear	ZnO, Carbon Black
Road Side Dusts	Al, Si, K, Ca, Ti, Fe, and Zn
Industrial Facilities	
Oil Fired Power Plants	V, Ni
Coal Combustion	Se, As, Cr, Co, Cu, Al, S, P, Ga
Oil Refineries	V
Nonferrous Metal Smelters	As, Sb, Cu, Zn, Pb, Cd, Hg
Iron and Steel Mills	Zn, Pb
Copper Refinery	Cu, Zn
Waste Incineration	Zn, Pb, Cu, Cd, Hg, K
Mineral and Material Processing	Si, Al, Ca, Mg, K, Sc, Fe, Mn
Sea Spray	Na, Cl, S, K
Resuspended Soil	Si, Al, Ca, Mg, Fe, Ti, Sr, Mn, Sc

2.1.3 Composition of Dust Particles

Elemental composition has been used by Schwela et al. to identify common sources of dust particles, as shown in table 2.3 (reproduced from [18]). Kazmerski et al. [19] had have reported elemental composition of dust particles from PV modules deployed in Egypt. The area from where the dust was collected in Egypt has a large cement industry and therefore showed elements associated with cement such as Sulphur, Calcium, Silicon, Oxygen, Aluminum, Potassium, Sodium and Iron. Since cement is an important constituent in buildings, these elements are expected in all Urban areas. This paper has also shown that minerals that are commonly found in dust particles deposited on PV modules installed in Libya, Iraq and Saudi Arabia are Quartz, Calcite, Chlorite, Gypsum and Dolomite. A similar study has been done for dust particles found in various parts of India, which will be discussed later in the thesis.

Dominant minerals in arid soils are illite, kaolinite, smectite, calcite, quartz, feldspar, hematite and gypsum. Phyllosilicates (illite, kaolinite and smectite) makes up the largest chemical weathering minerals in sedimentary rocks [20]. The crust of the earth constitutes approximately 90 percent of phyllosilicates and tectosilicates (quartz and feldspar).

2.1.4 Processes of Soiling

The understanding and eventual control of dust deposition on PV modules surface will significantly depend on understanding the processes involved in dust accumulation (or soiling). The soiling process involves the following steps:

1. Dust transportation
2. Initial adhesion
3. Changes in initial adhesion mechanisms
4. Alterations on the surface
5. Restorative methods



Figure 2.1: Process involved in soiling or dust deposition on surfaces such as PV modules.

2.1.4.1 Transportation of Dust Particles

The process of delivering the dust to the surface of PV module is mainly due to wind, known as Aeolian process. The uptake of the airborne particles from the ground depends on the near-surface dynamics [21]. This is controlled by the wind speed, wetness and texture of soil. The transportation of the particles occur in several modes, as shown in Figure 2.2 (reproduced from reference [13]), which depend mainly on wind speed and particle size. As the wind speed increases, sand particles of approximately 70 to 500 μm are moved, lifted and hop along a surface in a process called saltation. These particles can mobilize particles of wide range of sizes by predominantly ejecting them from soil surface due to impacts of the saltating particles. After ejection, dust particles tend to enter into short-term (20 to 70 μm) or long-term suspension ($< 20 \mu\text{m}$). Dust particles in long-term suspension can remain in the atmosphere for several weeks and can be transported thousands of kilometers from their point of origin [22]. Due to the impact of saltating

particles, it can also mobilize larger particles ($>500 \mu\text{m}$). These large particles can roll or slide along the surface, or after a short hop of less than a centimeter can settle back to the soil in a mode of transport known as creep. Even though these four modes are defined separately, they are not discrete, each mode morphs continuously into the next with wind speed and particle sizes.

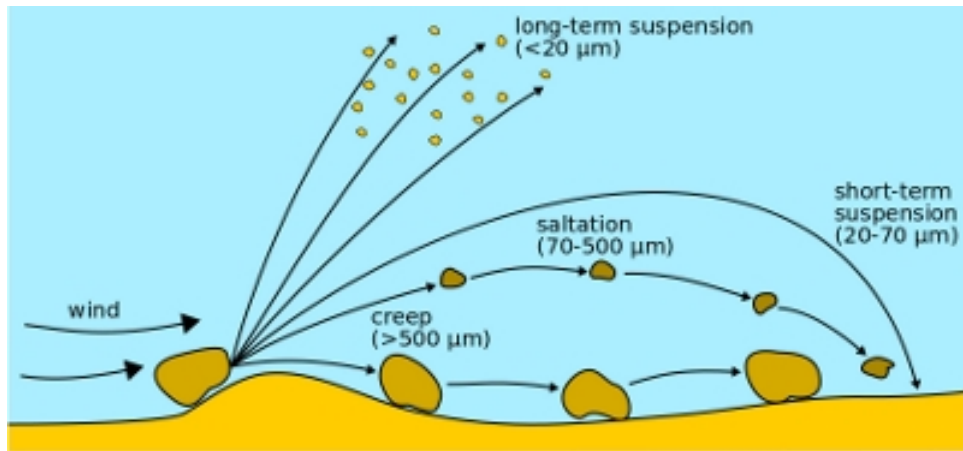


Figure 2.2: Schematic of different modes of aeolian transport of particles [13].

2.1.4.2 Initial Adhesion Mechanisms

The initial adhesion will depend on the properties of surface and dust particle, its composition, chemistry, degree of smoothness or roughness, electrical properties (conductivity and charge), orientation, optical properties, hardness/softness, temperature, mechanical motion and to its micro or nano characteristics [11]. Large particles are mainly impacted by gravitational and inertial effects, while the smaller particles interact largely due to inter-particle forces. Some of the most common dust deposition mechanisms are as follows [23]:

1. Gravitational Settlement - For the coarse particles in the atmosphere, effect of gravity becomes dominant than other effects. Diameter, density, shape are the important parameters which will decide the falling rate through air.
2. Brownian Motion - This applies to very small particles in which the forces are no longer balanced on all sides, resulting in the particles undergoing random and irregular movements.

3. Eddy Diffusion – Dust particles are also under the influence of turbulent airflow. The flux of these particles to the laminar region near a surface gives the particles a high probability of being deposited on that surface. The eddy force acting on the surface imparts sufficient force to a particle to bring to a plain surface where there are no force to take it away from the surface.
4. Electric charge and states – Dust particles can gain charge in number of ways, including induced charge in movement. When these particles come in contact with an opposite charge particle or surface, it gets attracted to it.
5. Coalescence – In situation where there are large number of dust particles, collisions between particles can occur and these particles can cause particles to coagulate to form larger particles. This process can lead to large particles that they fall out of suspension.

2.1.4.3 Changes in Initial Adhesion Mechanisms

The adhesion mechanisms tend to change with time due to the influence of the environment. Cuddihy et al. [24] explained four soiling mechanics that can change the adhesion mechanisms between deposited dust particles and the surface.

1. Cementation by water soluble particles - Dust particle in the atmosphere contains both inorganic and organic particulates that contain water soluble and insoluble salts. At high humidity or during the morning dew, particles on the surface form droplets of salt solutions that can retain water insoluble particles. This mixture when dried from the heat of the sun, the precipitated salt acts as a cement to anchor insoluble particles to the surface. Repetitive cycles of dew formation and evaporation and high relative humidity resulted in a gradual buildup of cemented layers, as illustrated in fig 2.3 (reproduced from [11]).
2. Organic Deposition - In certain ambient conditions, an ultrathin layer of organic deposition tend to coat the surface before the initial adhesion or deposition of dust. This makes removing salt deposit more difficult, and in turn, necessitating to more frequent cleaning using combinations of surfactant and detergent solutions to remove the organic layer.

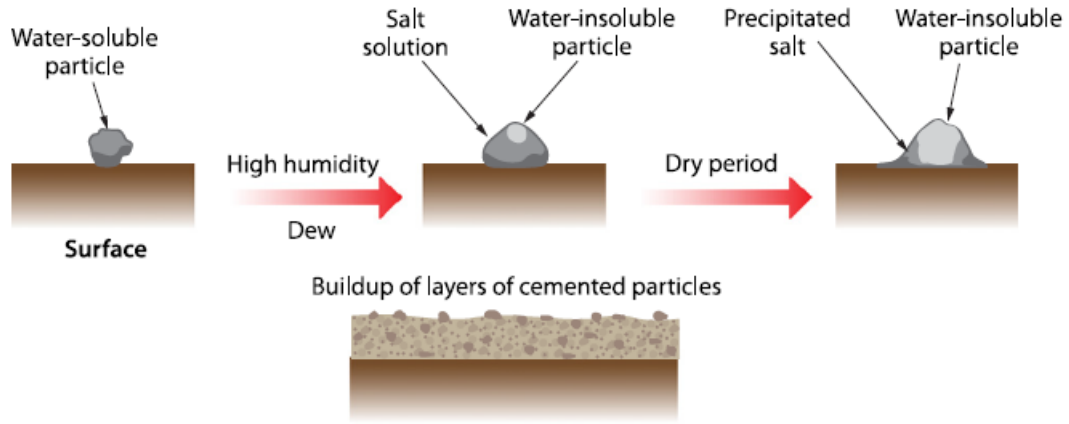


Figure 2.3: Cementation by water soluble particles [11].

3. Surface Tension - Surface tension forces can produce large forces and internal pressure within water droplets. This can attract water soluble salts which facilitates cementation process.
4. Particle Energetics - The energetics of particles, and therefore particle-particle attraction increases with decreasing particle size below $10 \mu\text{m}$. The attractive forces are considered to be van der Waals' forces. Cuddihy showed through an experiment that the wind speeds of upto 150 m/s are not effective in removing these small particles.

2.1.4.4 Alterations on the Surface

The adhesion mechanisms can alter the surface by means of weathering or leading to more accumulation. Weathering of soda-lime glass, most common glazing material in PV modules, is schematically illustrated in Figure 2.4 (reproduced from [24]). The result of glass weathering is the formation and deposition of water soluble sodium salts on the surface. This can lead to further soiling due to cementation and weathering of glass. Any of the soiling mechanics explained in the above section can aid in further soiling that leads to more accumulation of dust, thereby changing the surface characteristics.

2.1.4.5 Restorative Methods

Rain and manual water cleaning are well known cleaning or restorative methods for PV modules. Rain can compound the problem of soiling if the duration is brief and the intensity is light. In light rains, the rain droplets can collect airborne particulate matter

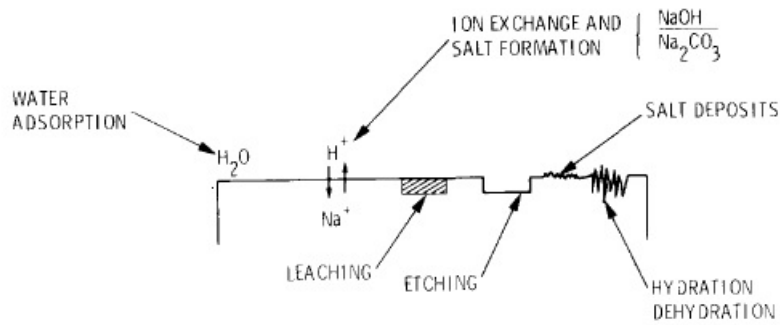


Figure 2.4: Weathering of soda-lime glass [24].

and deposit high concentrations of residue when striking the surface of the PV modules. If the rain does not persist to wash off this residue, when dried, large spots will populate the surface. Similarly, if the panels are cleaned using water and is not dried immediately, the residual water droplets can attract more dust particulates on to the surface of PV modules.

2.2 Factors that Affect Soiling on PV Modules

There are various factors that can contribute to energy loss due to soiling. They can be broadly classified into two main categories, viz. PV module and system characteristics, and the effect of the environment.

2.2.1 PV Module and System Characteristics

Solar PV system are generally expected to be designed for maximum energy yield. As a result, PV module and system characteristics are fixed and some of these characteristics can aid in soiling loss, especially if regular cleaning regimes are not followed. Given the advantage of PV system that it can be placed in any open-shade free area, roof-top systems are placed in inaccessible area which hinders regular cleaning. Some of the characteristics that can contribute to soiling loss are given below:

- Tilt angle
- Orientation
- Glazing surface characteristics

- PV technology
- PV module cell configuration

2.2.1.1 Tilt Angle

PV modules are installed in a fixed tilt or on solar trackers. Solar trackers are expensive and need regular maintenance, as a result, most PV systems are mounted on fixed tilts (tilt angle is calculated based on the latitude of the location). The fixed tilt angle is similar to the latitude angle of the place of installation. There are also PV power plants which have manual tracking based on the seasons. The seasonal tracking is usually 2 or 3 tilts per year. For Mumbai, the seasonal tilt angles are approximately 0 degree during June and July, nearly latitude angle (19°) for the months of March and September, and largest tilt angle of approximately 45° for December and January.

Depending on the PV system design, the tilt angles of the PV modules can change. Negash et al. [25] has done a systematic study to show the PV energy loss due to dust for different tilt angles such as 0, 5, 11.6, 15, 21.5, 25, 30 and 35 degrees. The loss was highest for 0 degree tilt angle at 33.5% and decreased gradually till 25 degrees to 14.5%. At 30 degree tilt angle, the energy loss slightly increased to 17.8% and then decreased again to 14.9% at tilt angle of 35 degree. This unexpected increase in soiling loss, not addressed in the paper, may be due to increased non-uniformity in the dust distribution throughout the PV panel surface. Qasem et al. [26] had shown that at 30 degree tilt angle the non-uniformity in the dust distribution at the top, middle and bottom section of the module is the highest at 4.4% as compared to less than 2% and 1% at 0 and 15 degree tilt respectively. Cano et al. [27] through their experiment concluded that the 0 degree tilt angle showed the highest loss. It can be observed from the study by Negash et al. and Cano et al. that beyond 15 degree tilt angle, the soiling loss decreases but not very significantly. Hence, it can be stated that for fixed tilt PV system installed in a dusty environment and at locations of latitude angle less than 15 degree, the optimum tilt angle would be 15 degree. Similar consideration have to be made for seasonal tilt PV systems where the tilt would be less than 15 degree.

2.2.1.2 Orientation

In the northern hemisphere, all PV system should be oriented to the south direction for maximum energy yield. For the southern hemisphere, the PV modules should face north looking towards the equator. This is done so that the PV panels face the sun most of the time. Elminir et al. [28] studied the dependence of dust deposition with module orientation and tilt angle. In this study, they observed that the glass samples oriented North-East (NE) accumulated greater dust than any other orientation. They attributed this to the influence of the more prevalent NE winds, which were bringing the emissions from the local cement factories. Goosens et al. [29] through his wind tunnel experiment concluded that wind direction and PV module orientation significantly impact dust deposition.

2.2.1.3 Glazing Surface Characteristics

The surface of glazing material on PV module determine distribution of dust. Textured surfaces tend to trap dust particles in the voids and thereby forming non-uniform deposition of dust. Non-uniform soiling is more detrimental to the PV module performance than uniform soiling. This is because the PV cells in the modules are connected in series and the cell that is seeing heaviest soiling will regulate the current flowing through the PV module. Tony et al. [30] compared the soiling behavior of textured and non-textured solar glass. They observed that the textured glass exhibited a greater variation in soiling pattern compared to flat glass and as a result, high pressure water spraying was used to clean the textured PV modules in addition to manual cleaning. However, the flat glass PV module showed no further improvement with an additional high pressure water cleaning.

2.2.1.4 PV Technology

Qasem et al. [26] showed that soiling reduces the PV output by attenuating irradiance in a spectrally dependent manner. The effect was not the same magnitude for all types of PV technology because the spectral transmittance of the soil layer affects various spectral response curves differently. Most dust types studied by Qasem, showed higher spectral loss around the 450 - 500nm range compared to the other wavelength range. As a result, the soiling effect was worse for the PV modules with wider bandgap absorbers like a-Si and

CdTe, which showed 33% reduction in photocurrent when a concentration of 4.25 mg/cm^2 of dust was applied. In comparison, c-Si and CIGS technologies showed 28.6% and 28.5% reductions at the same dust density.

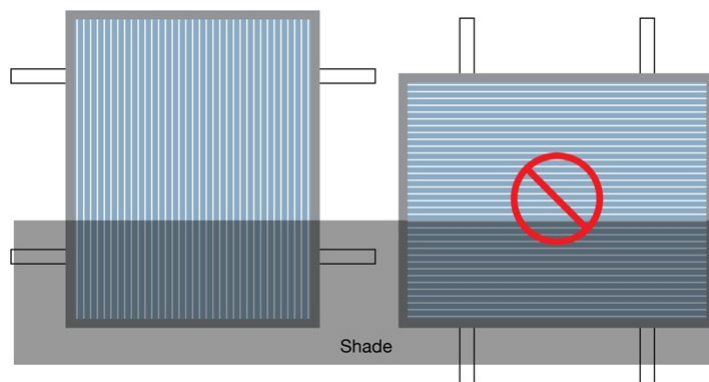
2.2.1.5 PV Module Cell Configuration

PV cells in c-Si PV modules are usually 5 or 6 inch squares which are connected in series, whereas thin film PV cells are thin strips of approximately 1000 mm x 4 mm. C-Si PV modules have usually 60 or 72 cells in series whereas thin film PV modules have approximately 100 cells in series. Thin film PV modules with PV cells perpendicular to ground are usually installed in portrait mode as shown in Figure 2.5(a) to avoid one entire cell being shaded due to nearby structure or due to accumulated dust at the bottom. It is quite difficult for a single cell in c-Si PV module (either in the portrait or landscape installation mode) to be soiled because of its cell dimension and configuration, see Figure 2.5(b). Since thin film modules like a-Si or CdTe are always installed in Portrait mode and if there is non-uniform soiling (assuming high density at the bottom of the module), a very small percentage of single cell gets affected due to soil layer since every cell stretches from top to bottom. But in the case of c-Si PV module, either in portrait or landscape mode (assuming no bypass diode), significant portion of the cell gets shaded as it has larger fraction of the cell exposed to the soil layer. As a result, a non-uniform shading may affect the c-Si PV module more than thin-film PV modules. If there are 3 bypass diodes in a module and it is installed in landscape mode, one of the bypass diodes may kick-in, as a result the PV module will function at two-third of its capacity.

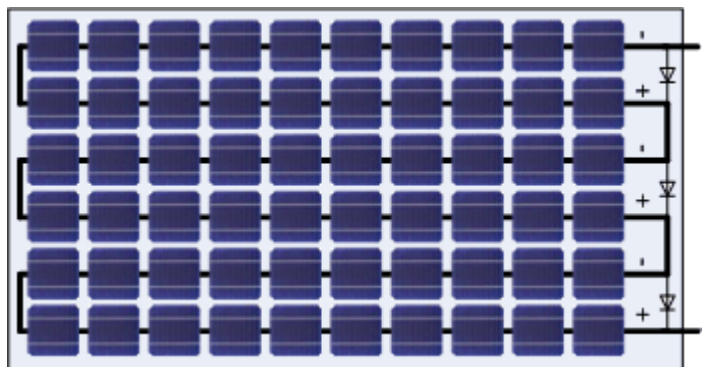
2.2.2 Environmental Effects

Soiling on PV modules surface is very dependent on the environmental and geographical location. This parameter can also change with time. There are many site dependent factors that influence the dust settlement on PV module surface which is shown below:

- Height of installation
- Average wind speed
- Occurrence of dew



(a) Thin film PV module installation mode -, Portrait (Left) and Landscape (Right).



(b) c-Si PV module 60 cell configuration in landscape mode.

Figure 2.5: PV module cell configuration for (a) thin-film and (b) c-Si PV modules.

- Airborne dust concentration
- Location and distance of source
- Probability of dust storm
- Dust particle size distribution

2.2.2.1 Height of Installation

Quang et al. [31] studied the vertical dust particle concentration profiles around urban office buildings in Australia. They showed that the PM2.5 particles are highest below 5 meters from the ground level. This was mainly due to vehicular traffic. A different study by McGowan et al. [32] showed the vertical distribution of PM10 dust concentrations. The trend was similar to the earlier study, where the PM10 concentration was highest below 5 meters (approximately $125 \mu\text{g m}^{-3}$), which then decreases to $95 \mu\text{g m}^{-3}$ at around 100 meters. These two studies shows that height of PV installation may contribute to the amount of soiling on its surface.

2.2.2.2 Airborne Dust Concentration

Particulate matter less than 10 micrometers (PM10) or less than 2.5 micrometers (PM2.5) in diameter are the most commonly measured parameter to estimate the airborne dust concentration. Boyle et al. [33] studied the ambient concentration of PM10 particles collected at the same time as naturally accumulated dust on PV modules. The result show that PM10 particles are partially related to the mass of dust accumulated. Kazmerski et al. [19] showed that the dust particle size distribution found on PV module surface and airborne dust particle are different. Nevertheless, the PM2.5 and PM10 particles can serve as a fairly good estimate of concentration of dust in the ambient that can settle on the PV module surface.

2.2.2.3 Average Wind Speed

Wind velocity has an important impact on PV module performance. Goosens et al. [29] have done extensive wind tunnel experiments to understand the effect of wind velocity and airborne dust concentration on PV performance. High wind speeds lead to high

dust accumulation on PV module, leading to sharp decrease in performance. In cases of low wind speeds, dust accumulation is smaller which result in less drop in performance. Their study also showed that wind also has an impact on the sedimentological structure of the dust coating on the module surface: light transmittance is higher in soil layer created in high wind speed than in soil layer created in low wind speed, resulting in larger performance drops during high winds. Even though the light transmittance was higher in many areas, high wind speed created non-uniform soiling. Since the cells in c-Si PV modules are in series, the cell which sees maximum soiling determines the current flowing out of the PV modules. Their experiments also indicated that the former effect is much more important than the latter, so in general the drop in PV module performance due to dust accumulation is greater in high wind speed.

From the experiment of Goosens et al., we can conclude that an average wind speed of less than 0.55m/s (or 2 km/hr) is favorable wind speed which produce less dust accumulation. Average wind speeds of above 1.67 m/s (or 6 km/hr) tend to bring heavy dust accumulation provided there is presence of high concentration of airborne dust concentration.

2.2.2.4 Probability of Dust Storm

Major dust storms occur when prolonged drought causes the soil surface to lose moisture and there is a co-occurrence of strong winds. This allows the mass entrainment of fine particles into the air through suspension. Dust storms can be hundreds of kilometers wide and up to a kilometer high. Although the occurrence of dust storms are quite rare, its frequency is increasing due to climate change. The effect of dust storms on PV modules are quite severe as these storms deposit huge amount of dust on PV modules, as shown in Figure 2.6 (reproduced from [34]). The regions in the world that are susceptible to dust storms, according to United Nations Convention to Combat Climate Change (UNCCD) [35], are the Northwest China, Canada's Prairie region, Dust bowl regions of USA, Sahelian regions of Africa, Southern Australia, Central Asia, and Middle-east countries.



Figure 2.6: Dust accumulation on PV modules after a dust storm [34].

2.2.2.5 Distance of Domestic Dust Source

For large ground mounted PV systems, the most common domestic dust source are the dust emitted from the road (paved or unpaved) or highways, emissions from vehicular traffic and nearby vegetation. However, in the urban areas, the main source of dust is vehicular traffic, constructions, households and industrial emissions. Sioutas et al. [36] had studied the concentration of Black carbon particles with distance from highway. The measurements done at a distance of 10 m, 20 m, 30 m, 90 m, 150 m and 300 m yielded dust densities of 22, 18, 11, 7, 6.5 and 6 $\mu\text{g m}^{-3}$ respectively.

2.2.2.6 Occurrence of Dew

The mean seasonal fraction of days in the world during which the formation of dew occurs on a surface, as shown in Figure 2.7 ,was studied by Vuollekoski et al. [37]. The regions shown in blue colour have high daily occurrences of dew formation. Apart from very warm and dry deserts, the meteorological conditions on almost all continental areas favor the formation of dew. The lack of dew formation is generally caused by inefficient nocturnal cooling of the surface as a result of high incoming long-wave radiation, which occurs due to a high cloud fraction and high humidity in the atmosphere (although high humidity at surface level favors dew formation). The lack of oceanic dew formation is probably caused by higher wind speeds and the weaker diurnal cycle in air temperature, denser average cloud cover and higher humidity compared to land areas, resulting in amplified long-wave radiation downwards, and therefore weaker cooling. The above study shows that all installed PV modules are susceptible to dew formation, thereby, increasing the chance of attracting dust on module surface.

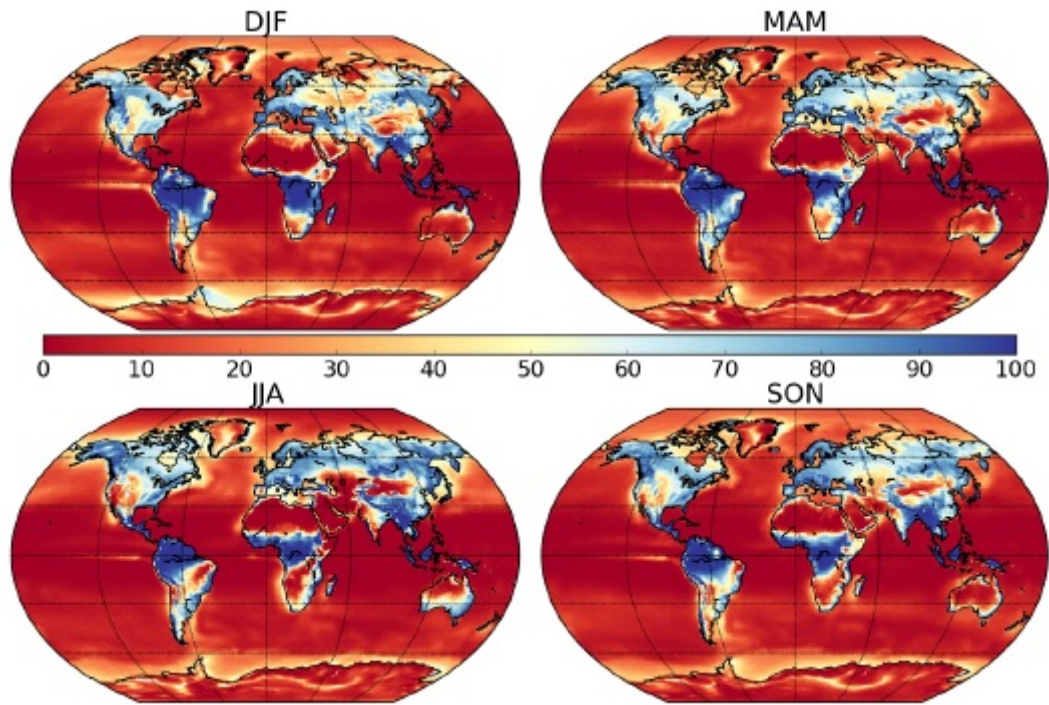


Figure 2.7: Seasonal occurrence of dew as a fraction of days [37]. DJF (December, January, February), MAM (March, April, May), JJA (June, July, August), and SON (September, October, November).

2.2.2.7 Module Dust Particle Size Distribution

Kazmerski et al. [19] showed that the particle size distribution of dust on module surface is different from airborne dust for a study done in Saudi Arabia. The airborne particle size distribution showed a higher concentration peaking at approximately $80 \mu\text{m}$ whereas the module dust showed a peak at $15 \mu\text{m}$. The chapter four of this thesis will show that higher amount of clay sediments (of size less than $4 \mu\text{m}$) are more detrimental to PV module performance than grained particles of size greater than $100 \mu\text{m}$.

As a result knowledge of the particle size distribution on module surface is important. Compared to other parameters the measurement of this is non-trivial and would require laboratory measurements.

2.3 Conclusion

It can be seen from the above sections, that there are many PV system and environmental parameters that aid in the process of soiling. Hence, it can be difficult to estimate or predict the rate at which soiling occurs on panels deployed in a geographical location.

Also, it is important to understand the effect of soiling on a PV module.

The impact of soiling is usually judged by the amount of energy lost by the PV module. But in order to develop mitigation strategies, it is important to understand the spectral and angular losses associated with soiling on a PV modules. In this thesis, a combination of outdoor and indoor technique is developed to understand the spectral loss on PV modules with various soil gravimetric densities. It is also important to understand the effect of soiling due to module's orientation with respect to incident sunlight. The angular loss study can be fully done outdoor. Both these studies will be important if a preventive or restorative mitigation strategy have to be devised.

The rate at which dust accumulates on PV modules may not be same throughout the year due to the various environmental factors. Hence, it poses a challenge to estimate an optimum cleaning frequency for a given location. It may be expensive to setup a test station which determines the soiling rate. In this thesis, we discuss two methodologies to estimate the soiling rate.

Chapter 3

Effect and Strategies for Quick Estimation of Soiling on PV Modules

In the earlier chapter, the process of soiling and various factors that affect soiling on PV System are discussed. In this chapter, we understand the impact of soiling on PV modules and how we can estimate it. There are various methods to accurately measure the soiling rate on PV modules. Various research groups around the world use mainly 3 parameters viz. using short-circuit current, maximum power and daily energy. A comparison of soiling loss calculated using these parameters are done by means of actual field measurements carried out at the NCPRE Photovoltaic Module Monitoring (PVMM) station in Mumbai.

All methods currently available are time consuming and expensive methods to estimate soiling rate. Two methods are proposed to quickly estimate the severity of soiling and suggest cleaning frequency. The first method relies on data of the PV system itself and site specific information whereas the second method involves creation of a platform that reports measured soiling rates as reported by different groups in the world.

3.1 Impact of Soiling on PV Modules Installed in Mumbai

In this section, performance loss of different PV module technologies due to dust accumulation installed in an urban location like Mumbai is studied.



Figure 3.1: Soiling station installed in Mumbai, having 2 modules of each PV module technologies, such as monocrystalline silicon (mono c-Si), multi-crystalline silicon (multi c-Si), amorphous silicon (a-Si) and CIGS.

3.1.1 Experimental Setup

The experimental setup is located in the campus of IIT Bombay, Mumbai. Mumbai is the most populous urban city in India with a population above 20 million people. In a big city like Mumbai, there are many activities that can generate dust around the city such as thermal power plants, unpaved and paved road dust, construction, landfill open burning, vehicular pollution and industries. In the campus, the main source of dust is the constructions, that can produce high density of cement related particles in the dust. The setup is located on a rooftop approximately 22 meters above the ground. Two similar PV modules of different technologies, viz. mono-crystalline silicon modules, multi-crystalline silicon modules, CIGS modules (cell and frame construction), and amorphous silicon modules (a-Si) have been kept at tilt angle of 19 degrees (same as the latitude angle) as shown in Figure 3.1. Out of the two modules of each technology, one is cleaned every day and other is left for natural soiling. A multi-channel I-V curve tracer (Daystar MT5 3200) is connected to the individual modules to measure the I-V curves every 10 minutes. The measurements were done on non-monsoon months from February to June 2013 and 2015. Monitoring of the a-Si module started late in the month of April. The soiling loss (SL) is calculated as per the equation given below:

$$SL(\%) = \left(1 - \frac{X_{soiled}}{X_{cleaned}}\right) \times 100 \quad (3.1)$$

where X - I_{sc} or P_{max} or daily energy (kWh).

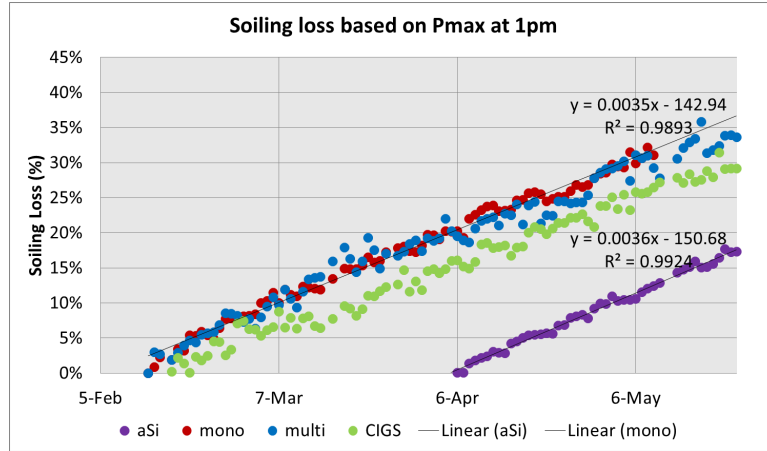
The solar noon is the time when the sun crosses the meridian and is at the highest elevation in the sky, which is at 12 o'clock apparent solar time. The solar noon of a location depends on the longitude and date. The I_{sc} and P_{max} values obtained at solar noon are considered for the SL calculation. Temperature correction of these parameters is not done since both modules gave very similar I-V characteristics initially and had similar temperature coefficients. Any temperature difference between these two modules, will be mainly due to dust accumulation.

Soiling loss calculated based on I_{sc} measurement is the widely used parameter for these calculations as it is a simple measurement. Gostein et al. [38] showed that even though I_{sc} based calculation is simple but only approximates true power loss in case of uniform soiling. Their experiments showed that I_{sc} measurements can severely over- or under-estimate true power loss for non-uniform soiling on c-Si PV modules.

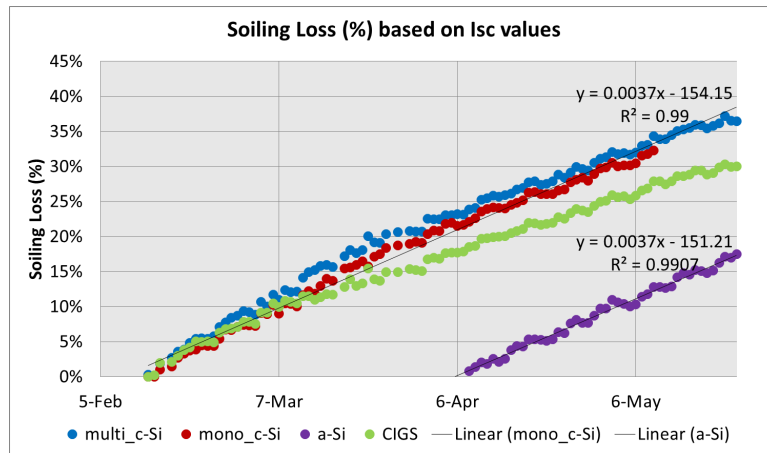
3.1.2 Results - Soiling Rate Observed in Mumbai

Figure 3.2 show the soiling loss calculated based on the I_{sc} , P_{max} and daily energy. In all the three graphs, the SL of the mono c-Si (0.36%/day) and the multi c-Si modules (0.35%/day) show similar soiling rate. This is expected since both these technologies have similar spectral response.

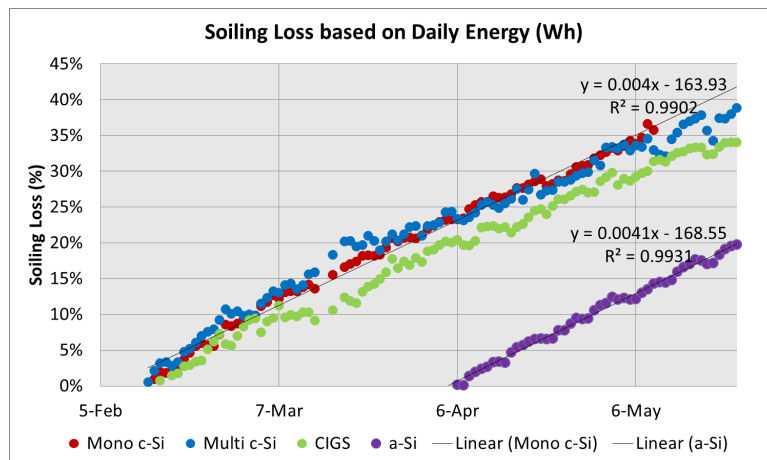
For c-Si technology, the cumulative SL over 97 days based on I_{sc} (37%) was higher than cumulative SL based on P_{max} (34%). The a-Si technology showed soiling rate of 0.36% per day similar to the c-Si technology. For a-Si module, the soiling rate and cumulative soiling loss (17%) calculated from the I_{sc} and P_{max} are identical. The cumulative SL of the CIGS module was less by 6% as compared to c-Si modules. The CIGS module was made from CIGS polycrystalline solar cell using technology from Global Solar Energy, USA. The comparatively higher performance in CIGS module maybe due to a the use of smoother solar glass whereas solar glass used in c-Si modules where slightly textured. Soiling on PV modules may lead to change in temperature of the PV module and as a result, both type of technologies can behave differently because of their different temperature coefficients.



(a)



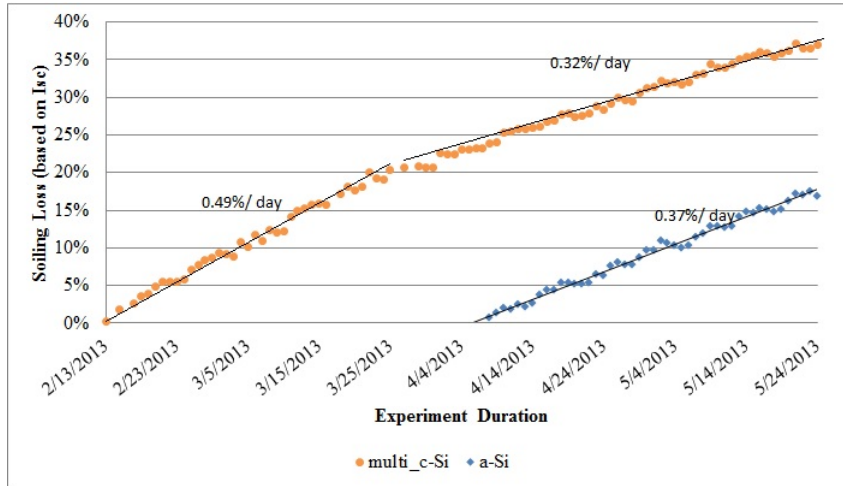
(b)



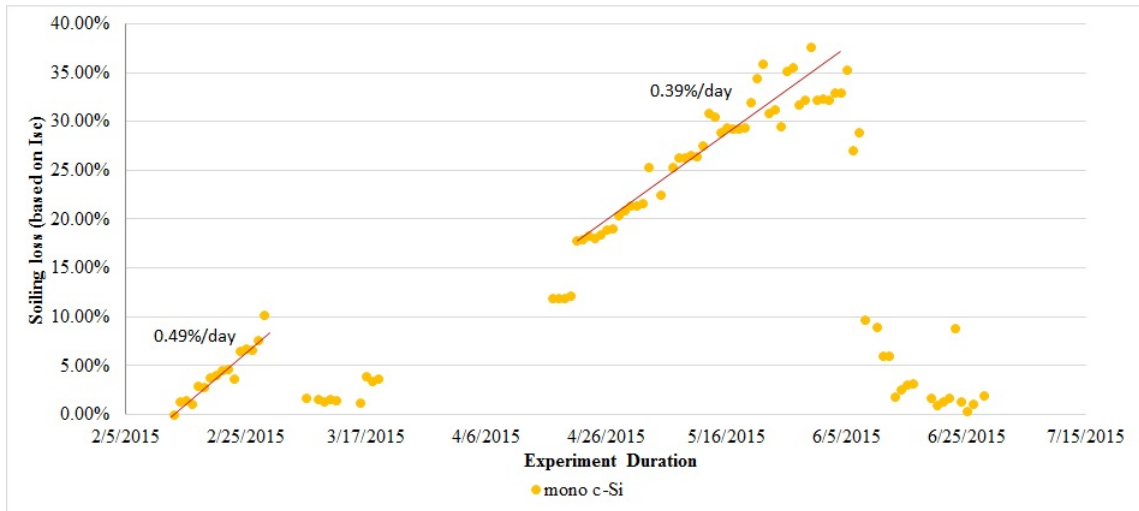
(c)

Figure 3.2: Soiling loss calculated based on I_{sc} , P_{max} and daily energy (97 non-monsoon day data) for the year 2013.

The cumulative SL and the soiling rate based on daily energy generation is high in all technologies as the AOI loss due to the soiled layer significantly influences the energy output [39] during morning and evening hours.



(a)



(b)

Figure 3.3: Soiling rate observed in Mumbai for the non-monsoon month of February to June for the year (a)2013 (Data interval - 10 days) and (b)2015 (Data interval - 20 days).

Similar experiment was repeated for the year 2015, it was found that the soiling rate for the month of February was high at 0.49% per day and then reduced to about 0.39% per day (see fig 3.3(b)). A similar high soiling rate for the month of February in 2013 can also be seen in fig 3.3(a). Figure 3.3(b) shows discontinuity between the two slopes because of irregular rain showers during that time. In conclusion, it can be seen that in a place like Mumbai, the soiling rate is consistently above 0.32% per day for the non-monsoon days.

3.2 Strategies for Quick Estimation of PV Module Soiling Rate

It has been shown in the earlier sections and through literature [40] that the soiling on PV modules is not same in all geographical locations. There are various methods [27] [38] [41] to estimate the soiling rate or soiling loss at a given location. Cano et al. [27] build a test station containing 10 mini-modules at different tilt angles. The objective of his experiment was to find the soiling rate for various tilt angles. The soiling rate was measured by logging the short-circuit current. Gostein et al. [38] and Lee et al. [41] logged I-V curve and module temperature of commercially available PV modules (1 soiled and 1 cleaned automatically daily), and then studied the temperature corrected I_{sc} and P_{max} . All techniques mentioned are hardware intensive, expensive, time consuming, and require systematic experiment to be conducted. In this section, two methods are proposed to quickly estimate soiling rate at a given location. These methods mentioned may not provide very accurate information but serves a starting point for PV system maintenance team to follow.

3.2.1 Site Soiling Index

In section 2.2, various parameters that affect soiling on PV modules are listed. All these values are measured quantity, and can be obtained from various sources such as meteorology data, site information, PV module data sheet and PV system characteristics. Some of the parameters are tilt angle, module direction, glazing material characteristics, PV technology, PV cell configuration, height of installation, average wind speed and direction, airborne dust concentration, dust storm frequency, distance of domestic dust sources, occurrence of dew, and dust particle size distribution. Any of these parameters have been individually studied by various research groups. In order to do a quick estimation of the impact of soiling on PV module, a qualitative method is proposed. This includes assigning weightages (W) to various identified parameters. Weightages can be assigned as high (3), medium/moderate (2) and low (1) chance of occurrence. Since all parameters will not have the same effect on the PV performance, each parameters needs to be assigned a severity value (S). The severity value is either 1 or 2, '1' indicates less severe and '2' means crucial parameter. A preliminary guide to assign weightage values to the various param-

eters is shown in table 3.1. One may argue about limiting the ranges of weightages and severity to 3 and 2 respectively. This maybe debated by various stake holders and more research maybe done to come to a consensus. The methodology presented here would serve as a starting point for these discussions. Some parameters need referring to weather station data and other non-trivial sources. Hence, another term “ Certainty Factor (CF)” is proposed. CF evaluates the confidence level of the user who assigns the weightage to each parameter. CF can be assigned as either 1 (some assumptions are made, based on faraway weather station or NASA weather data) or 2 (highly certain, based on actual measurement from the installation site). Using the terms weightage (W), severity (S) and certainty factor (CF), an index called “ Site Soiling Index (SSI)” is proposed as:

$$SiteSoilingIndex, SSI = \frac{\Sigma W \times S \times CF}{\Sigma W_{max} \times S \times CF_{max}} \quad (3.2)$$

SSI can be defined as a normalized index that shows the severity of soiling for a geographical location given its PV system characteristics and microclimate that aids in determining the cleaning frequency. SSI may be defined monthly or seasonally for a site as there maybe variations in the environmental parameters. For example, SSI values of PV systems located at IIT Bombay campus, Mumbai and Arizona State University Mesa Campus, Arizona are calculated as shown in table 3.2. IIT Bombay has an SSI for the non-monsoon days (February - May) calculated as 0.64 @ CF of 79% (0.77@CF=100%). Similarly, Arizona state university (ASU) Mesa campus has an SSI of 0.54 @ CF of 79% (0.61 @CF =100%). These two SSI values indicate that the cleaning frequency for PV system in IIT Bombay should be much higher as compared to a system located at ASU. Measured soiling rate for PV system installed in IIT Bombay is 0.35% per day whereas the system in ASU showed a soiling rate of 0.06% per day. It maybe noted that SSI index does not reflect 6 times soiling rate effect of IIT site compared to ASU site. This shows that there is more scope for improvement, one way to maybe resolve this, is to increase the weightage ranges of some parameters like airborne concentration and source of dust. Moreover, each of these parameters needs to be carefully studied to improve the methodology. The certainty factor is similar and high in both cases, because most of the weightages assigned were based on actual measurements. It should be also noted that rain is not considered here intentionally because it is assumed that there will be no soiling loss during rainy days. Hence, SSI maybe valid for only non-rainy months. As this work

Table 3.1: Reference table to determine Site Soiling Index (SSI). Source of the data are denoted as PS- PV System characteristics, PM - Module Data Sheet, WD - Weather data, SI- Site information, and LM - Lab Measurement.

Parameter	Criteriaon for Low, Medium and High Chances			Source
	High (3)	Medium (2)	Low(1)	
Module Positioning				
Tilt angle (Fixed Tilt)	For tilt angle less than 15 deg	For tilt angle between 15 deg and 45 deg	For tilt angle close to 90 deg (For BIPV) (60 to 90 deg)	PS
Module and Wind Direction	Module and Wind direction (approximately throughout the month/year) in opposite direction, helping dust accumulation leading to non-uniform soiling	Module and Wind direction (approximately throughout the month/year) in same direction with minor variation to the west or east	Module and Wind direction (approximately throughout the month/year) in same direction	PS, WD
Surface of PV module glazing material	Textures or ridges that aid in trapping dust	Minor textures on the glass surface	Surface that is treated to reduce the amount of dust settling on it (anti-soiling coating)	PM
PV Technology	a-Si	CdTe	CIGS or any c-Si	PM
PV Cell configuration	Series connected cells with one complete cell at the bottom of the module	Series connected cell, with one cell have presence at both top and bottom of the PV module	Parallel connected cells	PM
Environmental/Geographical Location Effect				
Height of installation	Ground Mounted (Distance from ground to middle of the panel is 5 meter or less)	If the panels are mounted on the roof of a building of height between 5 and 50 meters	If the panels are mounted on the roof of a very tall building (above 50 meters)	SI
Average Wind Speed	Above 6 km/hr (1.67 m/s)	2 to 6 km/hr	Less than 2 km/hr (0.55 m/s)	WD
Average daily Airborne dust concentration (PM2.5 and PM10)	Above $170 \mu\text{g}/\text{m}^3$	30 to $170 \mu\text{g}/\text{m}^3$	Less than $30 \mu\text{g}/\text{m}^3$	WD
Occurrence of Dew (mean fraction of days)	More than 180 occurrences per year (>50%)	40-180 occurrences in a year	Less than 40 occurrences in a year (<10%)	WD
Distance of nearest dust source of continuous emission	less than 10 m (Highways, factories, etc)	10 to 90 m (Highways, factories, etc)	More than 90 m (Highways, factories, etc)	SI
Places with probability of dust storms (as per UNCCD)	Northwest China, Canada's Prairie region, Dust bowl regions of USA, Sahelian regions of Africa, Southern Australia, Central Asia, and Middle-east countries	Once in a while occurrence of dust storm	No dust storms	WD
Sediment Properties- Size distribution	High Presence of particle size less than $4\mu\text{m}$ (>15% of clay sediments)	High presence of silt sediments (>80%) and grained particles (>10%)	High Presence of particle size greater than $63\mu\text{m}$ (>20% of grained sediments)	LM

Table 3.2: SSI calculation for IITB, Powai, Mumbai and ASU-PRL, Mesa, Arizona.

Parameter	Weightage (W)		Severity (S)	Certainty Factor (CF)		$\sum(W \times S \times CF)$	
	IITB	ASU		IITB	ASU	IITB	ASU
Module Positioning							
Tilt Angle (Fixed)	2	3	2	2	2	8	12
Module and Wind Direction	2	2	1	1	1	2	2
Glazing Material Surface	2	2	2	2	2	8	8
PV Technology	1	1	1	2	2	2	2
PV Cell Configuration	3	3	2	2	2	12	12
Environmental/Geographical Location Effect							
Height of Installation	2	3	1	2	2	4	6
Average Wind Speed	2	2	1	1	1	2	2
Airborne Dust Concentration	3	1	1	1	1	3	1
Occurrence of Dew (Mean Fraction of Days)	3	1	2	1	2	6	4
Distance of nearest dust source	3	2	2	2	2	12	8
Chance of Dust Storm	1	1	2	1	1	2	2
Sediment Properties - Size Distribution	3	1	2	2	1	12	2
				19 out of 24	20 out of 24	73 out of 114	61 out of 114
				79%	79%	0.64	0.54

progresses, it may make sense to define a monthly SSI value instead of one yearly value.

3.2.2 World PV Soiling Map

Many countries are scaling up their PV installations almost exponentially. The MW installations can afford to do soiling experiments as shown in section 3.1, but for smaller systems, especially the rooftop systems, it may not be affordable to do such experiments. Hence, there is a need to create a simple platform for the PV community to understand the soiling loss rate in their geographical location. This would guide in determining the cleaning frequency for that location. There has been lot of reported and unreported

studies done by various research organizations and companies. This data can be compiled onto one web platform as shown in the Figure 3.4. The world map shown in the figure consists of 64 data points from journals and conference papers through out the world discussing the soiling loss rates. The list of the journal and conference papers is provided in the Appendix A.

3.3 Conclusion

This chapter looked at the outdoor method to quantify the performance loss caused to the process of soiling. Then two strategies for quick estimation of the soiling rate at a given geographical location is discussed. In the following chapters, detailed look at the optical losses and the methodology to determine these losses are discussed.

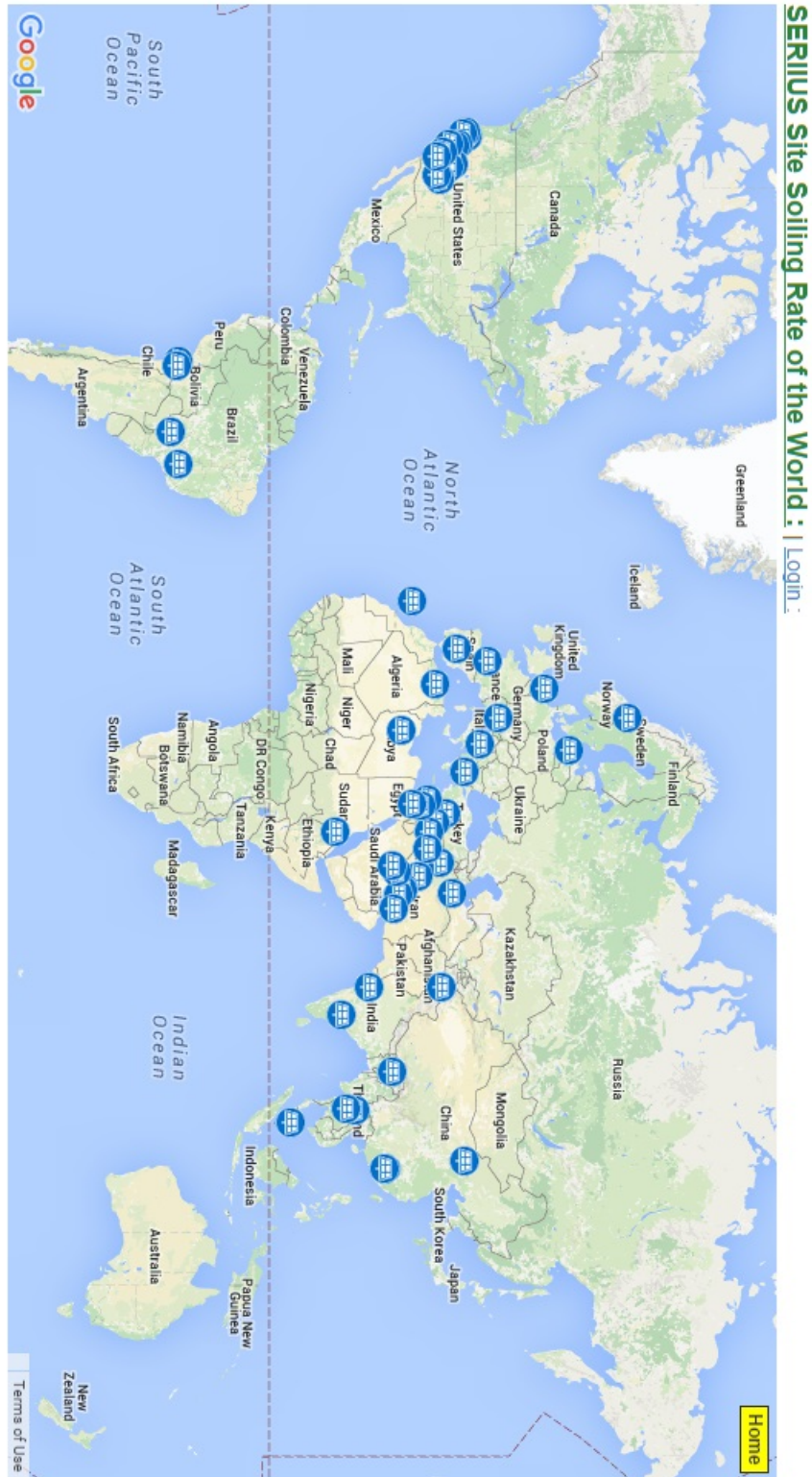


Figure 3.4: World PV Soiling Loss Rate Map with data from 64 literature, shown in Appendix A.

Chapter 4

Outdoor Characterization - Quantification and Modeling of Spectral and Angular Losses of Naturally Soiled PV Modules

In the previous chapter, the various factors that aid soiling and their impact on PV modules were discussed in detail. Soiling loss is usually discussed in terms of the reduction in I_{sc} or P_{max} , and/or in daily energy loss. In this chapter, the spectral and angular loss of soiled PV modules is discussed.

4.1 Introduction

Accumulation of dust on photovoltaic (PV) modules, referred to as “soiling”, is known to have detrimental effect on their performance. As the dust particles are opaque, the soil layer that is formed on PV modules is opaque and porous in nature, and transparent because of porosity and dust material type. At low AOI, the light reaching the glass superstrate depends on the transparent nature of the soil layer, whereas at high AOI, the opaque nature of soil layer is expected to dominate. The soil layer interferes with incident sunlight by both attenuating and scattering the light. The extent of interference depends on the AOI, dust particle size and shape, composition, and soiling density [42].

The physical properties and thickness of soil layer on the glass surface of PV modules

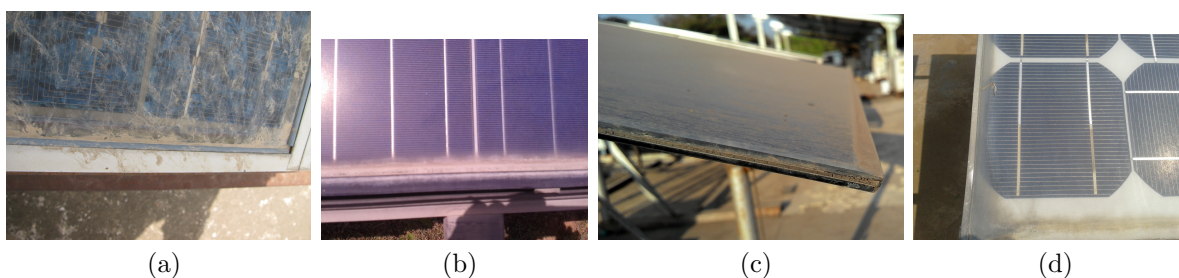


Figure 4.1: Different types of soil layer formation on PV modules at different sites in India. (a),(b) and (d) are c-Si PV modules, found in Delhi and (c) is a-Si PV module found in Mumbai.

are dependent on the front glass of the modules and on the location of installation. The degree to which an identical soil layer thickness affects various PV module technologies could depend on the spectral response of the solar cell used [26].

The random and non-uniform accumulation of dust on the module surface area can produce spots with different dust densities and shapes, as illustrated in Figure 4.1(a). The most common method of cleaning PV modules in the field is using water. If the water available for cleaning at the site is hard, it would result in damaging the module glass surface, as shown in Figure 4.1(b). The bottom region of the PV module glass is affected the most as the water tends to collect and become stagnant at the bottom edge of the tilted modules. The corrosion of the module glass in the bottom region of the module leads to difference in transmittance of light onto the cell as compared to the top region. It has also been observed that there can be higher accumulation of dust toward the bottom edge in some PV installations irrespective of the module being framed or frameless, as shown in Figure 4.1(c), which is a frameless module. The photograph shown in Figure 4.1(d) was obtained from an installation in Delhi, India, where a permanent discoloration at the edges of the PV module surface was observed. The reason for this discoloration on the module glass is not known but this may be because of the effect of stagnant wet soil layer formation leading to enhanced moisture ingress through the interface between the glass and frame. It is clear that the tilt angle of the module is a critical parameter determining the performance in dusty conditions. However, the tilt angle is typically determined based solely on the geographical coordinates with no consideration for the impact of soiling.

There are two ways the angle of incidence (AOI) influences the short-circuit current (I_{sc}) of the PV modules. The first is a geometrical effect, that is, the module's orientation

with respect to the incident sunlight, often referred to as the “cosine effect.” The second is because of the optical effects or surface characteristics of the PV module, referred to as the “optical effect”. Minimum optical losses on a cleaned or soiled module occur at around solar noon when the AOI is close to zero [39]. As the AOI increases, the optical losses caused by the soil layer increases.

A detailed study has been done on the change in the quantum efficiency curve at different AOI values for a small silicon solar cell encapsulated with ethylene vinyl acetate (EVA) [43]. In addition, several reports [11] [26] [39] have documented that there are spectral and AOI losses because of the formation of soil layer on small glass coupons and/or on small PV devices, which are naturally or artificially soiled. This study presents methods to characterize spectral and angular loss of large commercial size PV modules with different soil gravimetric densities. The QE measurements of these commercial modules were done indoor, whereas the AOI loss and reflectance measurements were done outdoor at the Arizona State University Photovoltaic Reliability Lab (ASU-PRL).

4.2 Methodology to Estimate the Spectral and Angular Loss

The modules used in this study were naturally soiled in the hot dry climatic condition of Mesa, Arizona, USA. One polycrystalline silicon module that was placed horizontally for more than 4 years showing different soil gravimetric densities was used for the spectral studies. Three soiled and one cleaned polycrystalline silicon PV modules were used for the AOI studies. Of these, heavily soiled and moderately soiled PV modules were soiled in the horizontal position between three and five years, whereas the lightly soiled PV module was soiled at a tilt angle of 23° for about three years. Although, the modules were from different manufacturers, the superstrate/encapsulant/substrate construction of all these modules was glass/EVA/cell/EVA/backsheet. Figure 4.2 shows the methodology followed in this study.

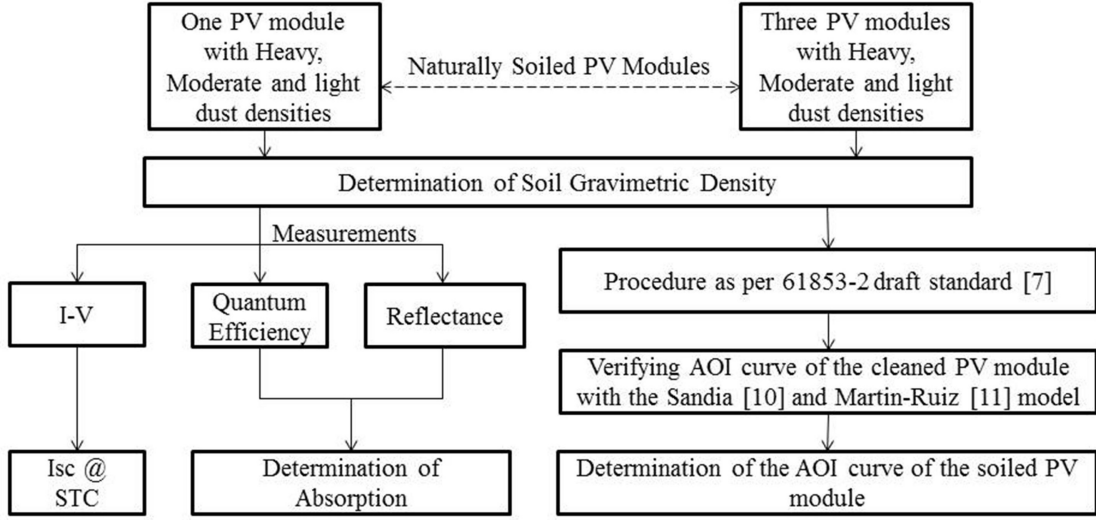


Figure 4.2: The methodology used in this study.

Table 4.1: Gravimetric density of soiled PV Module used in this study.

Type of Soil Sample	Spectral loss Study			Angular loss Study
	Soil Gravimetric Density (g/m^2)	$I_{sc}(STC)$ loss(%)	$P_{max}(STC)$ loss(%)	Soil Gravimetric Density (g/m^2)
Heavy ($>10g/m^2$)	74.6	41.3	34.4	11.80
Moderate ($2-10g/m^2$)	3.18	9.7	5.8	2.74
Light ($0-2g/m^2$)	0.6	3.3	3.0	1.71

4.2.1 Determination of Soil Gravimetric Density

Dry lint free cotton gauze was weighed (M) using Mettler Toledo balance (AG285, resolution 0.01mg). It was then dampened with water so that dusts from the PV module adhere to it well. The dampened cotton gauze was used to wipe on a pre-measured area (A). Later, it was dried in an oven and then weighed (M_{soiled}) again. The soil gravimetric density (SGD) of the PV modules was calculated using the equation 4.1 and is shown in Table 4.1. The accuracy of this method needs to be improved, but serves as a very close indicator of the soil gravimetric density.

$$SGD(g/m^2) = \frac{M_{soiled} - M}{A} \quad (4.1)$$

I_{sc} is affected by transmittance only whereas P_{max} may be affected by both transmittance and shunt resistance depending on the cell quality and technology. The shunt resistance and FF (Fill Factor) depend on the technology used by manufacturer. To avoid the shunt resistance influence and to obtain the true measure of transmittance due

to soiling, we are reporting all our data based on I_{sc} only. However, for the purpose of information, the influence on the P_{max} (Table 4.1) for the tested technologies is provided. It is again cautioned that the P_{max} loss is not an accurate measure of soiling loss as compared to I_{sc} loss. P_{max} is affected by many variables such as spectrum, broadband irradiance, temperature, AOI, etc. The corrections for all these factors will not be trivial as it can have impeded uncertainties.

4.2.2 Characterization of Spectral Loss

The cells from the test PV module were accessed from the backsheet by carefully cutting the backsheet and the back encapsulant. The exposed cell interconnects were soldered with tabbing wire to obtain Current – Voltage (I-V) and Quantum Efficiency (QE) data. I-V data of the cells were measured at Standard Test Conditions (STC) using a class AAA solar cell simulator (PV Measurement Inc., Model No. IV16K). The solar simulator is mounted on a custom built X-Y stage where the light source can be moved to the location of the test solar cell on the PV module. The losses in I_{sc} at STC of the soiled PV modules are shown in Table 4.1.

The QE measurements were carried out using PV Measurements QEX12M with custom-built X-Y stage, which can obtain QE at any spot on the entire test PV module. The measurements were taken for the wavelength range of 350 – 1100 nm at 5 nm increments. The beam width of the monochromatic light was set at 1.5 mm x 5 mm.

The reflectance spectra of the soiled solar cells were collected using an ASD Inc. handheld FieldSpec-4 general purpose spectroradiometer equipped with a high intensity contact probe accessory. The contact probe accessory has a halogen light source for reflectance measurement. The instrument can acquire visible and near-infrared (VNIR) and short-wave infrared (SWIR) spectra for the wavelength range of 350 – 2500 nm. The instrument is calibrated with a white reference panel before each reflectance measurement. The contact probe light opening (spot size 10 mm) was held very tightly to the surface of the sample to ensure that no light escapes from the contact probe. A total of 10 spectra were collected for each sample.

There are two types of QEs associated with solar cell, viz., Internal QE (IQE) and External QE (EQE). EQE is the ratio of the electrons collected as photocurrent and the incident photons on a solar cell. In a clean PV module, the above definition can be

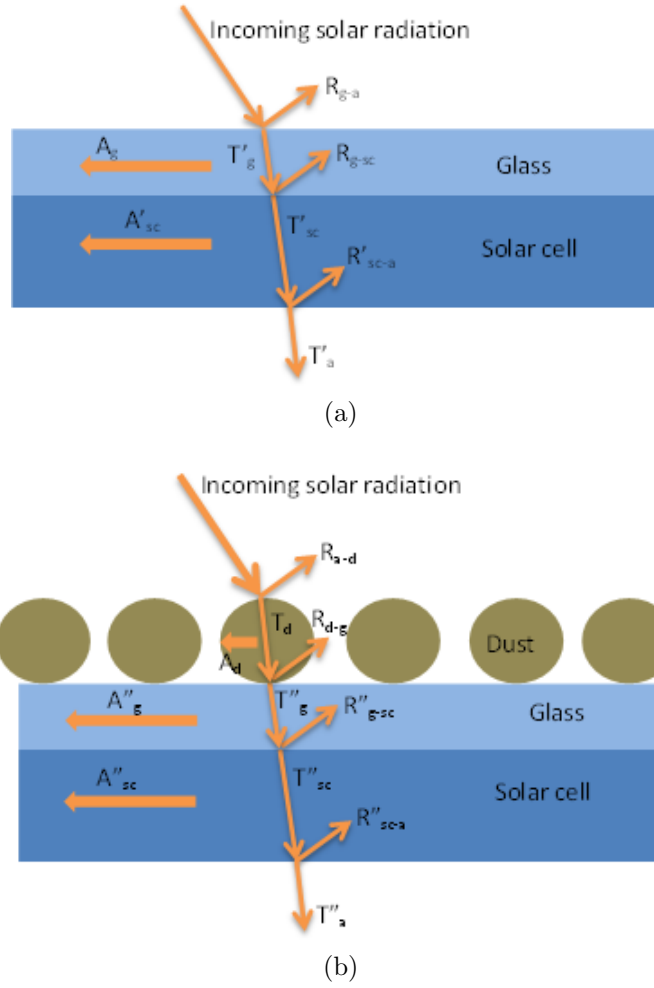


Figure 4.3: Illustration of optical losses on (a) cleaned and (b) soiled PV Module.

extended as follows. EQE_{CPVM} is the ratio of the electrons collected as photocurrent and the photons that entered the solar glass. Incident photons = photons that entered the glass (T'_g) + photons reflected (R_{g-a}) at the air and glass interface. Similarly, for a soiled PV module, EQE_{SPVM} is the ratio of the electrons collected as photocurrent and the photons that entered the solar glass. In this case, incident photons = photon reflected at the air and dust interface (R_{a-d}) + photons absorbed by dust (A_d) + photons reflected at the dust and glass interface (R''_{d-g}) + photons that entered the glass (T''_g). Both the EQE_{SPVM} and EQE_{CPVM} are difficult to measure. In the case of PV modules (or encapsulated solar cells), EQE that can be measured is the ratio of the electrons collected as photocurrent and the incident photons on the module which are termed as EQE_{MSPVM} and EQE_{MCPVM} . The definition of IQE will remain the same in the case of solar cell and PV module as it is the ratio of the electrons collected as photocurrent and the photons that are absorbed in the solar cell. Figure 4.3 shows the photon balancing diagram of a

cleaned and soiled PV module respectively. For ease of understanding, PV module here refers to a glass/solar cell system instead of a glass/encapsulant/solar cell system. The optical effect of the encapsulant layer is assumed to be negligible [43]. In Figure 4.3(a), some part of the incoming solar radiation is reflected (R_{g-a}) at the glass-air interface and the rest enters the glass (T'_g). Out of the photons that entered the glass, few photons would be absorbed by the glass (A'_g), some would get reflected at the glass-solar cell interface (R'_{g-sc}), and the rest would exit the glass (T'_{sc}). A portion of the photons that entered the cells would be absorbed by the solar cell (A'_{sc}) and remaining would be transmitted (T'_a) and reflected (R'_{sc-a}) at the bottom of the solar cell. Similarly, Figure 4.3(b) shows the optical path of the incoming solar radiation on a soiled PV module. Initially, some part of the incoming photons is reflected at the air-dust interface (R_{a-d}) and the remaining enters the dust (T_d). Out of the photons that enter the dust, some are absorbed (A_d), some are reflected at the dust - glass interface (R_{d-g}) and the remaining enters the glass (T''_g). Photons that enter the glass follow a similar optical path mentioned in the clean PV module. The reflectance that is measured using the spectroradiometer is the net reflectance of the cleaned (R_{MCPVM}) and soiled PV module (R_{MSPVM}), respectively. By equating the IQE obtained from the clean (IQE_{CPVM}) and the soiled (IQE_{SPVM}) PV module, we can determine the light absorbed by dust (A_d). ' ϕ ' is the spectral photon flux that is received by both the soiled and cleaned PV modules, and 'q' is the charge of one electron.

$$IQE_{CPVM} = IQE_{SPVM} \quad (4.2)$$

$$\frac{J_{CPVM}}{q\phi(1 - R_{MCPVM} - A'_g)} = \frac{J_{SPVM}}{q\phi(1 - R_{MSPVM} - A''_g - A_d)} \quad (4.3)$$

$$EQE_{MCPVM} = J_{CPVM}/q\phi \quad (4.4)$$

$$EQE_{MSPVM} = J_{SPVM}/q\phi \quad (4.5)$$

Substituting 4.4 and 4.5 in 4.3 and canceling common terms,

$$\frac{EQE_{MCPVM}}{(1 - R_{MCPVM} - A'_g)} = \frac{EQE_{MSPVM}}{(1 - R_{MSPVM} - A''_g - A_d)} \quad (4.6)$$

Beal et al. [43] show that absorption of low-iron soda-lime glass and glass with encap-

sulation is nearly zero from 350 to 1100 nm, that is, $A'_g = A''_g = 0$.

$$\frac{EQE_{MCPVM}}{(1 - R_{MCPVM})} = \frac{EQE_{MSPVM}}{(1 - R_{MSPVM} - A_d)} \quad (4.7)$$

By rearranging,

$$\text{Absorbed by dust, } A_d = [1 - R_{soiled}] - \left[\frac{EQE_{msoiled}}{EQE_{mclean}} (1 - R_{clean}) \right] \quad (4.8)$$

The following assumptions are made in deriving the above equation: 1) no photons entering the solar cell exited the solar cell, that is, $T'_a = T''_a = 0$; and 2) dust layer is considered as a transparent layer as they do not cover the glass surface completely. In addition, any amount of scattering that leads to current collection is accounted for in the transmission through dust.

The net light reflected by the soil layer can be determined by taking the difference of the measured reflectance of soiled and cleaned PV module. Now that the absorption and the reflectance by the soil layer are determined, the transmission through the dust layer can be calculated.

4.2.3 Characterization of Angular Loss

The experiment to determine the angle of incidence (AOI) curve on cleaned PV modules was performed by following the procedure described in the International Electrotechnical Commission (IEC) 61853-2 draft standard [44] and the report of Knisley et al. [45]. The modules were mounted on a two-axis-tracker co-planar to each other as shown in Figure 4.4. A sun-dial was used to verify the co-planarity of the modules when normal to the sun. To calculate the global and direct irradiances, a pyranometer (Kipp and Zonen) and a pyrhelimeter (Eppley) were employed. The pyrhelimeter was placed on another two-axis tracker and was continuously allowed to track the sun. T-type thermocouples were attached in order to measure the module temperature, while a multi-curve tracer (Daystar, DS3200) was used to sweep current-voltage (I-V) curves, along with the module temperatures and irradiances for AOI from 0° to 75° . An AOI measuring device (Microstrain, 3DM-GX3-25) which is an attitude heading reference system was used to determine the AOI. The calibrated AOI device was mounted on a non-magnetic arm to avoid magnetic interference that may influence AOI measurements. The experiment was conducted

on a clear sunny day when the ratio of direct normal irradiance (DNI) to global normal irradiance was 0.91 (above 0.9 as required by the IEC 61853-2 standard). The measurements were done in less than 30 minutes to minimize the influence of spectral variations during the measurements.



Figure 4.4: Outdoor experimental setup for AOI measurement [Soiling level: A – Heavy (11.8 g/m^2), B – Moderate (4.85 g/m^2), C – Moderate (2.74 g/m^2), D –Light (1.71 g/m^2); E – Cleaned].

During measurements, the tracker was operated manually to vary the AOI. Care was taken to ensure that there were no reflective surfaces nearby affecting the readings. Higher number of readings improved the accuracy; therefore readings were obtained at 24 different AOIs. The measurement was not extended beyond 75° AOI due to reflections from the surroundings and the limitation of the tracker. To verify the AOI curve measured is accurate, the typical cleaned silicon PV module curve obtained by Sandia model [46] and Martin-Ruiz model [47] were overlaid with obtained cleaned PV module AOI curve. If the curves overlapped each other, the corresponding soiled PV module AOI curve is considered.

4.3 Results and Discussions

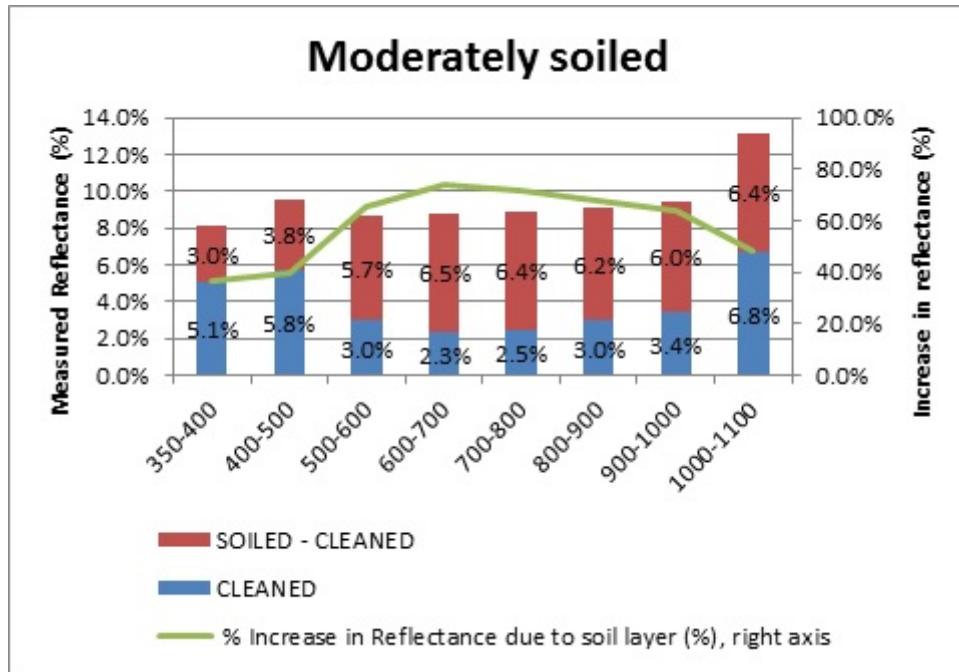
Energy loss of 50% from the PV system due to soiling has been reported in places such as Baghdad, Iraq [9]. Therefore it is possible to see a loss of I_{sc} close to 50%, which is represented in this experiment by the highly soiled PV module. Lightly soiled PV modules showed an I_{sc} loss of 3.3%.

The moderately and heavily soiled PV modules analyzed in this section have shown approximately 10% and 41% loss in I_{sc} , respectively. Energy generation loss associated with this is significant and additional expense on module cleaning or anti-soiling coatings may possibly be justified in terms of increased income generation.

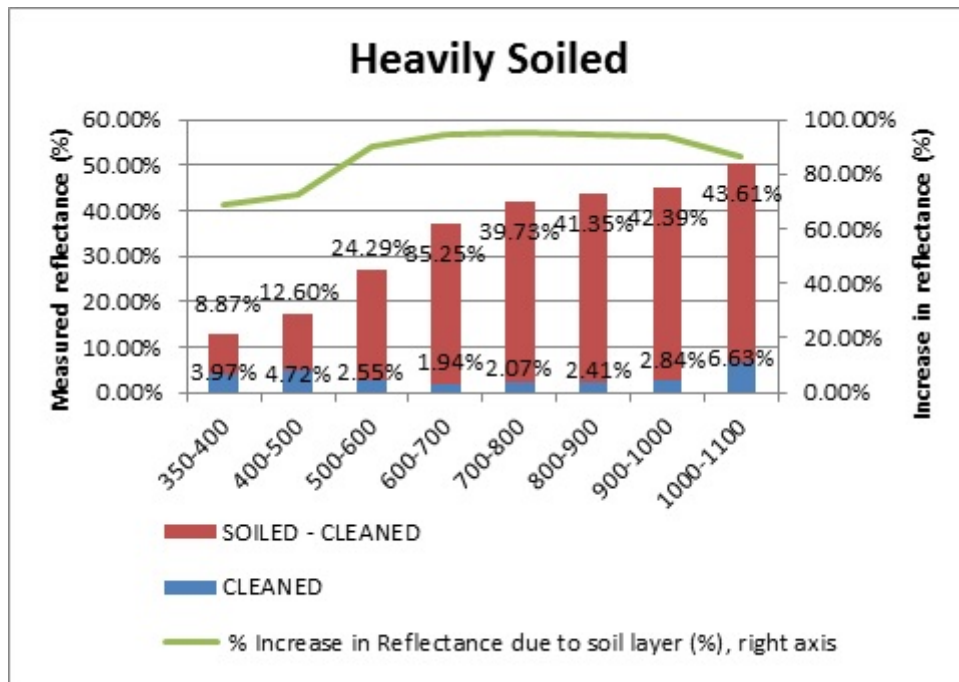
4.3.1 Comprehensive Spectral Loss Calculation of Soiled PV Module

The first step to quantify the spectral effect of soiled PV module in the field is to examine the reflectance spectra, which can be measured using the portable spectroradiometer identified in the above section. The reflectance measurements were carried out in the field for the soiled PV module before and after cleaning it. The increase in measured spectral reflectance of the moderately and heavily soiled PV modules because of the presence of soil layer is shown in Figure 4.5. Special care was taken to ensure that both the measurements (soiled and after cleaning) were made at the same location. For the cleaned PV module, the lowest reflectance is seen in the 600 – 700 nm range. This is expected as most antireflective coatings (ARCs) are designed to have minimum loss at approximately 600 nm. Moreover, high reflection is expected in the blue region (350 – 500 nm) for polycrystalline silicon PV module as compared to monocrystalline silicon PV module because of variation in thickness of the ARC layer. Because of the presence of the soil layer, the reflectance of both soiled modules increased overall in all measured wavelength bands (350 - 1100nm). In the moderately soiled PV module, there was relatively small increase in the measured absolute reflectance because of the soil layer at the 350 – 400 nm and 400 – 500 nm wavelength bands (3%, 3.8%), whereas at wavelength bands above 500 nm, the absolute reflectance approximately doubled (above 5.7%) and was consistent. Overall, the average reflectance because of the moderate soil layer increased by 58.4% (350–1100 nm) when compared to the clean PV module surface. In the heavily soiled PV module, the average reflectance of the soil layer increased dramatically by 87.2% in all wavelength ranges.

Optical absorption by the soil layer was calculated by using equation 4.8. As both absorbance and reflectance of the soil layer are known, the light transmitted through the dust layer can be determined because transmittance + absorbance + reflectance = 1.



(a)



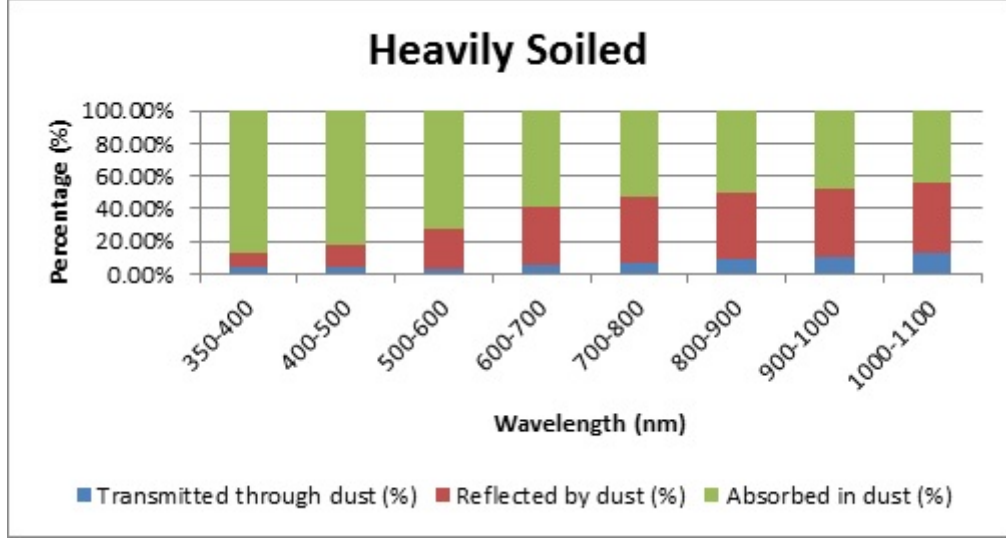
(b)

Figure 4.5: Spectral reflectance of the moderately (a) and heavily (b) soiled PV module before and after cleaning.

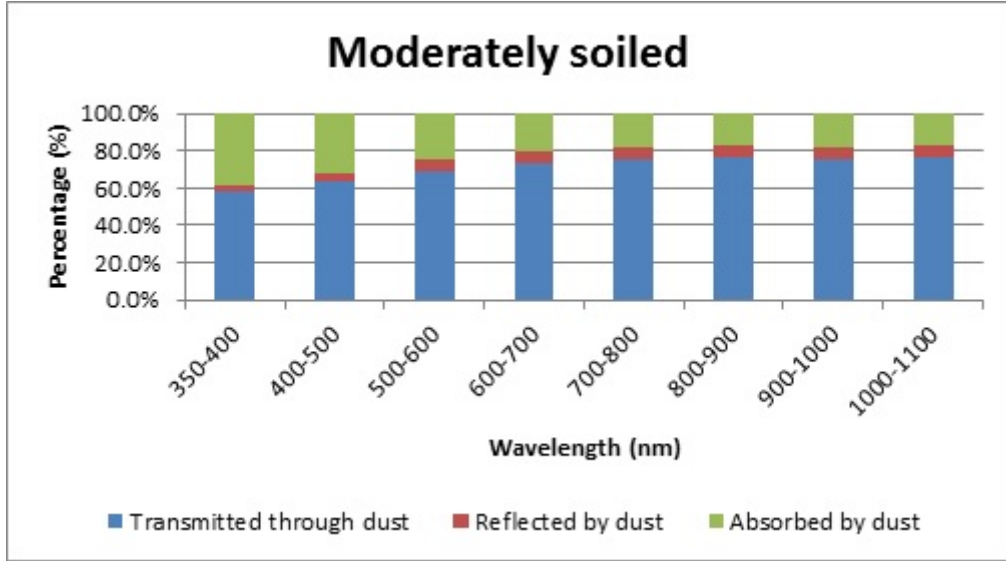
Figure 4.6 shows the optical absorption by the soil layers, net reflection because of the dust and the light transmitted through the soil layer. The spectral transmittance obtained showed similar trend as reported by Qasem et al. [48]. At wavelengths above 600 nm, the transmittance is less dependent on the wavelength band. This effect is explained

by the Mie scattering simulation [48], which showed that Mie scatter happens largely for small particle size ($< 6\mu\text{m}$) where the attenuation of the lower wavelengths becomes more significant. In a heavily soiled PV module, less number of photons is transmitted through the soil layer and hence the I_{sc} is reduced significantly (41% loss). From Figure 4.6(a), it can be observed that approximately 60% of the incoming photons are absorbed (or scattered in different directions) by the soil layer. In the lower wavelength range of 350 – 500 nm, the average absorption is maximum at 85%. In a moderately soiled PV module, an average of 71% of the incident photons transmits through the soil layer in all wavelength range. In Figure 4.6(b), absorption by soil layer was approximately 23% in all wavelength range and the highest average absorption (approximately 35%) was seen in the lower wavelength ranges from 350 to 500 nm.

As shown in Figure 4.7, the reflectance and EQE studies were carried out only on small heavily soiled areas, whereas the I_{sc} measurement has been carried out on the entire cell area. The transmittance loss of heavily soiled area of the cell is dictated by the heavy soil layer only, whereas the I_{sc} loss of the heavily soiled cell (HSC) is dictated by both heavily and less heavily soiled areas of the cell. Therefore in this case, it is expected that the loss in short circuit would be much less than the measured loss in transmittance. It is seen that the short circuit current (over the entire solar cell area) reduces by about 41 % (Table 4.1) and the transmittance (small heavily soiled area in the cell shown in Figure 4.7) reduced by approximately 90% over the whole spectral range [Figure 4.6(b)]. The difference between reduction of I_{sc} and transmittance value is attributed to the non-uniformity of the soil layer on the cell. In the case of HSCs, as shown in Figure 4.7, the cell is partially covered by a heavy soil layer and the remaining area of the cell is covered only by a moderately soiled layer. In order to determine the transmittance loss of the entire heavily soiled cell (HSC), the area weighted transmittance (T_{HSC}) of the solar cell is estimated by assuming that two types of dust density, viz. heavily (H') and moderately soiled (M') are seen in this solar cell. This assumption is made because visually, the less heavily soiled area shows similar soiling pattern as that of the moderately soiled solar cell (as per definition of Table 4.1). J_{sc} denotes short-circuit current density, and A is the area of the cell. Since the I_{sc} of the entire heavily soiled solar cell ($I_{sc,HSC}$) is a sum of the current generated by the heavily ($I_{sc,H'}$) and moderately ($I_{sc,M'}$) soiled portion of the solar cell, we have the following:



(a)



(b)

Figure 4.6: Reflectance, Absorption and Transmittance spectra of the heavily (a) and moderately (b) soiled PV module.

$$I_{sc,HSC} = I_{sc,H'} + I_{sc,M'} \quad (4.9)$$

$$J_{sc,HSC} \times A = (J_{sc,H'} \times A_{H'}) + (J_{sc,M'} \times A_{M'}) \quad (4.10)$$

Where, $A_{H'}$ and $A_{M'}$ are the areas of the heavily and moderately soiled areas on the cell, respectively, and $A = A_{H'} + A_{M'}$. J_{sc} generated by a soiled solar cell is a product of the J_{sc} generated by a cleaned solar cell and the incident radiation transmitted through the soiled layer, and hence $J_{sc,soiled} = J_{sc,cleaned} \times T_{soiled}$.

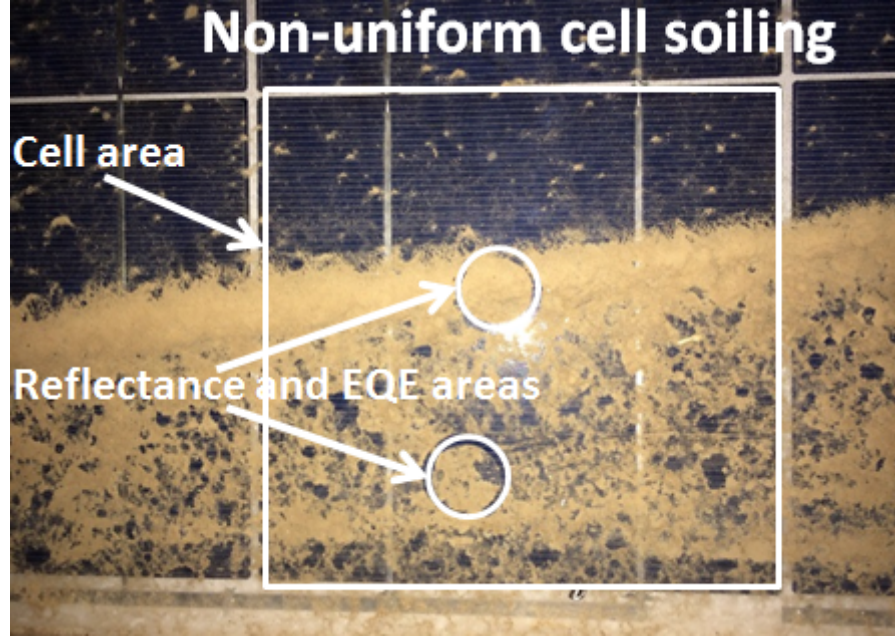


Figure 4.7: Non-uniform soiling of PV cells leading to difference in transmittance and I_{sc} data.

$$J_{sc,cleane\textit{d}} \times T_{HSC} \times A = (J_{sc,cleane\textit{d}} \times T_{H'} \times A_{H'}) + (J_{sc,cleane\textit{d}} \times T_{M'} \times A_{M'}) \quad (4.11)$$

Cancelling the common term $J_{sc,Cleaned}$, equation 4.11 is reduced to

$$T_{HSC} \times A = (T_{H'} \times A_{H'}) + (T_{M'} \times A_{M'}) \quad (4.12)$$

Using the imaging processing technique, $A_{H'}$ and $A_{M'}$ are estimated as 60.6% and 39.4%, respectively. Also, the average transmittance (averaged over the spectral range of 350 nm to 1100 nm) for the heavily soiled and moderately soiled area are calculated from Figure 4.6 as 7.05% and 71.2%, respectively. Substituting in the above equation 4.12, the area weighted average of the transmittance of the entire solar cell is estimated as 32.33% as opposed to 7.05% of the small heavily soiled area. This correlates well with the I_{sc} loss of 41%. More accurate correlation between the I_{sc} and spectral measurement can be obtained if the spectral measurements can be made with beams size similar to cell size. Another strategy to overcome this is to study the dust pattern, a more fine-grained version of the approach outlined in the previous paragraph. From the pattern, cell area could be binned to smaller areas based on soil gravimetric densities. Small area spectral

measurements could be made on selected areas.

Figure 4.8 shows the comparison of the measured EQE spectra of heavily, moderately, and lightly soiled PV module with the cleaned PV module. The lightly soiled PV module shows very small decrease in the EQE spectra with respect to the cleaned PV module, whereas the heavily and moderately soiled PV module showed significant reduction. The reduction in the EQE of the moderately soiled PV module is mainly because of the absorption in the dust and a small percentage is reflected. However, in the highly soiled PV module, reduction in EQE is largely dominated by the absorption of dust followed by reflection by the dust particles. As a result of the increase in QE, less photon reach the solar cell; this in turn reduces the I_{sc} of the PV modules.

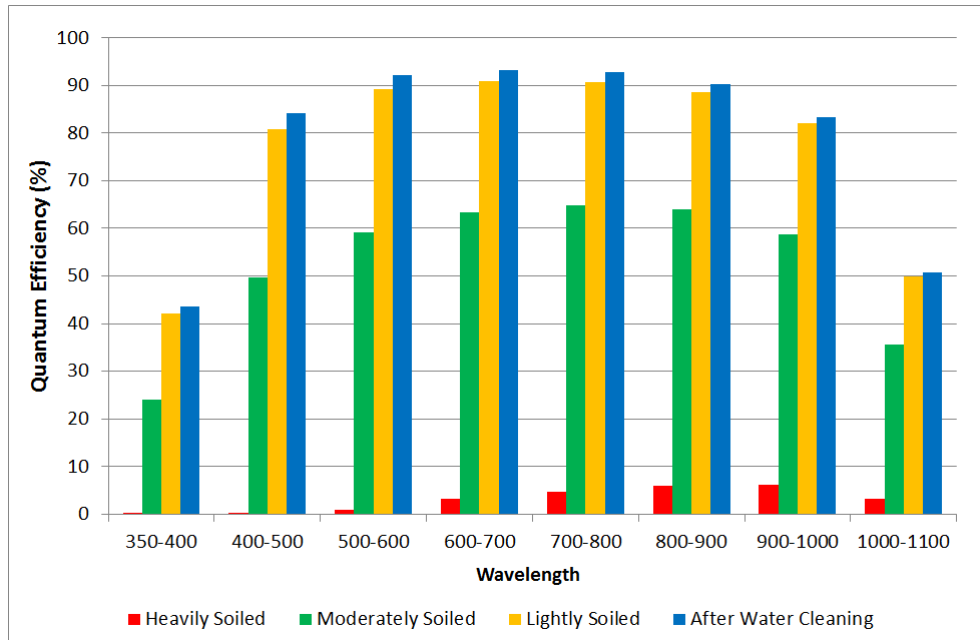


Figure 4.8: Comparison of quantum efficiency of heavily, moderately and lightly soiled PV module with the cleaned PV module.

4.3.2 AOI Loss of Soiled PV Module

In the previous section, we reported the spectral loss of the soiled PV module at 0° AOI. It is known that the reflectance increases beyond certain AOI, depending on the air/superstrate interface. This is true for both cleaned and soiled PV modules [49]. The Sandia model shown in the following is used for the determination of the AOI curve [45].

$$I_{scr} = I_{sc} \times \frac{E_o}{E_{poa}} \times (1 + \alpha_{I_{sc}}(T_c - 25)) \quad (4.13)$$

$$f_2(AOI) = \frac{[E_o * \frac{I_{sc}}{I_{scr} - (E_{poa} - E_{dni} \times \cos(AOI))}] \frac{I_{sc}}{1 + \alpha_{I_{sc}}(T_c - 25)}}{E_{dni} \times \cos(AOI)} \quad (4.14)$$

E_{dni} = Direct normal solar irradiance (W/m^2)

E_{poa} = Global solar irradiance in the plane-of-array (module) (W/m^2)

E_o = Reference global solar irradiance, typically $1000 W/m^2$

AOI = Angle between solar beam and module normal vector (deg)

T_c = Measured module (cell) temperature ($^{\circ}C$)

$\alpha_{I_{sc}}$ = Short-circuit current temperature coefficient ($1/^{\circ}C$)

I_{sc} = Measured short-circuit current (A)

$f_2(AOI)$ = Relative optical response

The values are normalized to obtain relative response, $f_2(AOI)$. This means that $f_2(AOI)$ at $AOI 0^{\circ}$ is 1. AOI curves of cleaned, lightly, moderately and heavily soiled PV module is shown in Figure 4.9.

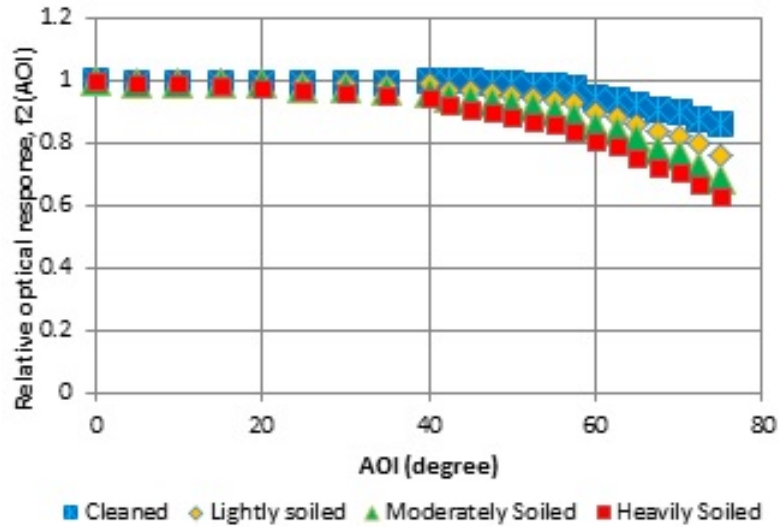


Figure 4.9: AOI curve of cleaned and moderately soiled PV module.

The Relative Difference (RD) between $f_2(AOI)$ and $f_2(0^{\circ})$ is very small for smaller AOIs and very high at higher AOIs. This is the case for both soiled as well as the cleaned modules. However, the value of RD at higher AOI is greater for soiled modules than cleaned modules at a particular AOI. The “critical angle” is defined as the angle above which there is a loss of 3%, or above, as compared with the 0° AOI. For cleaned poly-

Table 4.2: Comparing AOI curves of cleaned and soiled c-Si PV modules.

Sample Name (Soiling Level)	Critical Angle (3% and above loss)	RD (Relative Difference) ($f_2(0^\circ) - f_2(57^\circ)$)	Empirical Formula ($f_2(AOI)$)
Cleaned	57°	3%	$f_2(AOI) = -2E - 09(AOI)^5 + 4E - 07(AOI)^4 - 2E - 05(AOI)^3 + 0.0006(AOI)^2 - 0.0067(AOI) + 1.0062$
Lightly Soiled	42°	7%	$f_2(AOI) = -2E - 09(AOI)^5 + 4E - 07(AOI)^4 - 3E - 05(AOI)^3 + 0.0007(AOI)^2 - 0.0071(AOI) + 1.0072$
Moderately Soiled	38°	12%	$f_2(AOI) = -1E - 09(AOI)^5 + 2E - 07(AOI)^4 - 1E - 05(AOI)^3 + 0.0003(AOI)^2 - 0.0036(AOI) + 1.0041$
Heavily Soiled	20°	16%	$f_2(AOI) = -1E - 09(AOI)^5 + 2E - 07(AOI)^4 - 1E - 05(AOI)^3 + 0.0004(AOI)^2 - 0.0047(AOI) + 1.0046$

crystalline silicon PV modules, the critical angle is at about 57° , whereas for the lightly, moderately and heavily soiled PV module it is at about 42° , 38° , and 20° , respectively. The AOI curves in all cases can be fitted with a fifth order polynomial. This empirically derived function can be used in a PV system simulation tools. Table 4.2 shows the critical angle, RD, and the empirical formulas for determining the AOI curves of the cleaned and soiled PV module. It is observed that the AOI curves are heavily influenced by the air/soil/superstrate layer and is dependent on the thickness of the soiling layer. The critical AOI for the air/glass interface is about 57° , and it decreases dramatically as the soil gravimetric density (g/m^2) increases. The critical angle forms a good measure to indicate where the soiling loss is significant for a certain soil gravimetric density (g/m^2). This finding can be crucial for fixed tilt modules as they experience a wide range of AOI, especially on cloudy days.

4.4 Conclusion

Most of the earlier studies on the spectral effect of soiling were done on small glass coupons or small encapsulated solar cells that were naturally soiled outdoor or artificially soiled indoor. This study presents methods appropriate to characterize spectral and angular loss of large commercial size PV modules with different soil gravimetric densities. We

have reported that the moderately and heavily soiled crystalline silicon PV modules show a short-circuit loss of about 10% and 41%, respectively, with soil gravimetric density of approximately $3 \text{ gm}/m^2$ and $74 \text{ gm}/m^2$.

The increase in the reflectance of the moderately soiled PV module is the smallest in the 350–500nm wavelength bands and highest in the 600–700 nm wavelength bands. This is attributed to Mie scattering [48]. Because of the presence of the soil layer, the average reflectance of the moderately soiled and heavily soiled PV module was increased by 58.4% and 87.2%, respectively, in the 350 – 1100 nm range, compared to the clean module.

An equation to estimate absorption of light by soil layer was derived and used to obtain the absorption spectra. On an average, the absorption was 61% and 23% in the heavily and moderately soiled layer, respectively, in the 350–1100 nm range. Absorption in the soil would depend on the soil chemical composition, and hence, there is a need to repeat these experiments for different soil types.

The light transmitted through the soil layer was estimated from the absorption and reflectance spectra. On an average, 71% of the incoming light was transmitted through the moderately soiled layer, whereas only 7% was transmitted through the heavily soiled layer.

The reduction in the EQE of the moderately and heavily soiled PV module is largely dominated by the absorption (and scattered light) of dust, followed by reflection of the dust particles.

It is observed that the AOI curve is heavily influenced by the air/soil/superstrate layer. The critical AOI for the air/glass interface is about 57° , and it decreases dramatically to 20° as the soil gravimetric density (g/m^2) increased to $11.8 \text{ g}/m^2$. This influence is crucial for fixed tilt modules as they experience a wide range of AOI during its operation and a significant fraction of energy is generated at higher AOIs, especially on cloudy days.

Chapter 5

Indoor Characterization of Different Types of Dust found on PV Modules from India

In the previous chapter, methods to characterize spectral and angular loss of fielded large commercial size PV modules with different soil gravimetric densities was discussed. Even though this type of characterisation can lead to accurate estimation of the optical losses on PV modules, these techniques cannot be applied at all locations. In this chapter, an indoor method to estimate the effect of different soil types on PV module technology with various soil gravimetric densities is discussed.

5.1 Introduction

Estimation of soiling loss is difficult due to the variations in soil type [50], geographical locations and climatic conditions [42]. Prediction of the site-specific soiling loss and design of cleaning intervals is currently heuristic and hence prone to large errors. Studying the natural soiling loss on PV modules can be a very slow process. Accelerated soiling loss testing strategies have been reported in literature [51, 52] as an alternative to outdoor soiling methods. The main objective of these studies [48, 51, 52] and is to enable controlled laboratory experiments on the impact of soiling, thus reducing the time taken to understand the severity of the soiling loss due to the soil composition and soil gravimetric densities. Another advantage of accelerated soil testing is to quickly evaluate

the anti-soiling coatings for various properties including the particle adhesion strength on the surface and abrasion resistance property during cleaning using different cleaning methods. However, the accelerated deposition technique does not help in estimating the site-specific dependence of soiling rate ($\text{g}/\text{m}^2/\text{day}$ or $\text{g}/\text{m}^2/\text{month}$) as it can widely vary due to geographic location, season, tilt angle, whether it is rooftop or ground mounted, and height of installation from ground.

Studies have shown that the transmittance of the transparent cover and the spectral content of incoming solar radiation are altered depending on the soil type [48, 53]. It is important to understand the spectral alteration by the soil type especially when many research activities are focused on collecting a wider fraction of the solar spectrum to increase the efficiency. Many emerging PV technologies such as the organic PVs, multi-junction technologies, etc., try to enhance current collection at various part of the solar spectrum. Understanding the spectral loss due to soiling could offer better cell design and cost-effective deployment of these types of cells. Similarly, many research and development efforts that are made to develop anti-soiling and anti-reflective coatings on PV modules would also benefit from studies such as the one presented in this thesis. Laboratory techniques to determine the composition of the dust and its impact on performance would be valuable for such investigations.

Spectral losses due to soiling are difficult to predict without the knowledge of the soil type. Burton et al. [54] have shown an accelerated soiling test method that can be used to evaluate the response of PV modules coated with synthesized soil or grime in a controlled laboratory setting. In their study, they have shown that the red, Fe_2O_3 rich grime behaves like a neutral density filter and therefore attenuates the incident light spectrum uniformly. However, the yellow gothite rich grime forward scatters the light, showing less detrimental effect to the overall performance than the red grime.

In this chapter, a detailed study on the spectral sensitivity of naturally occurring soil/dust samples that were collected from PV modules installed in different parts of India, collected during the All India Survey of Photovoltaic Module Degradation 2014 [55], was conducted. These soil samples were artificially deposited to achieve various gravimetric densities. The spectral effect of dust on different PV technologies is demonstrated by calculating the short-circuit current (short circuit current density, J_{sc}) that would have been generated by the devices under AM1.5G spectrum.

5.2 Methodology

Different methodologies to correlate the reduction in PV module loss with dust have been summarized in [11]. In most cases, the study of the soiling loss on PV modules took many months or years. Our work provides a new approach to quantify soiling loss from different geographical regions, in this paper, sites from India. Figure 5.1 shows the detailed analysis procedure used in this work.

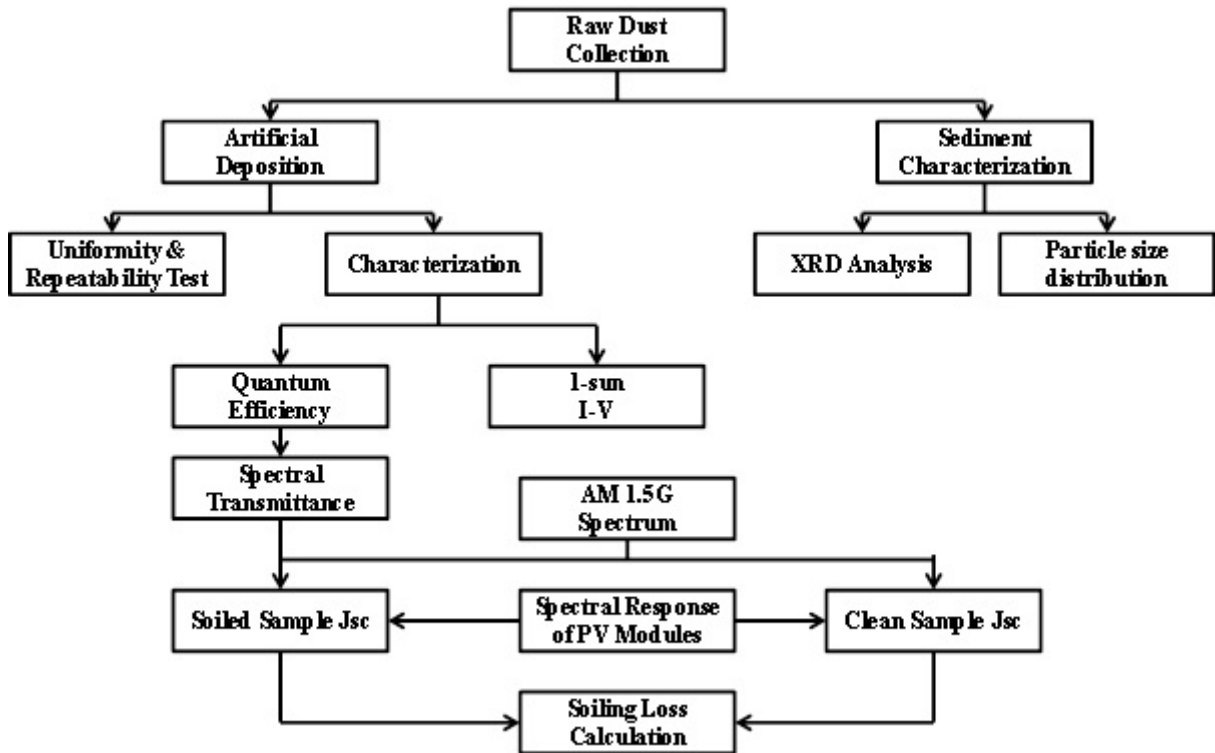


Figure 5.1: Detailed methodology used in this study.

Dust samples were collected from an existing PV module surface. This is because the particle size distribution from the PV module surface is different from the dust collected from the ground or airborne sample as shown in [19]. In this study, we have carried out optical and electrical characterization of dust collected from two major sites in India, viz. Jodhpur and Mumbai. Jodhpur is situated in the state of Rajasthan, which leads the installed PV power generation capacity in India due to the fact that it receives the highest solar insolation in the country [56]. Mumbai represents a typical urban city of India, situated in the state of Maharashtra, which is considered to be a city with significant potential for rooftop installations [57]. A limited quantity of dust samples from Gurgaon, Hanle, Agra and Pondicherry was collected, and optical characterization was done for a

gravimetric density of 1.8 g/m^2 . Some part of the dust samples were used to study the particle size distribution and its mineral compositions.



Figure 5.2: The experimental setup that was used to deposit dust on the solar glass samples.

5.2.1 Preparation of Soil Suspension

Acetonitrile (MERCK) is used as a carrier solvent for preparation of dust suspension. Sample dust of 1.2 gm was added to 100 ml of acetonitrile. This concentration of acetonitrile and dust was maintained for every deposition. A customized spray gun, shown in Figure 5.2, of 100 ml capacity was used for deposition. Borosilicate, low iron, solar glass from Borosil Glass Works Ltd. (India), of dimension 2 cm x 2 cm was used as the substrate. Substrate cleaning was done using a commercial degreaser followed by deionized water and isopropyl alcohol rinsing. Then the dry substrate was weighed using a microbalance (CITIZEN CX85S) of resolution 0.00001 g. The glass substrate is weighed before the deposition ($M_{cleaned}$) and after deposition (M_{soiled}). The area of the glass substrate (A) is also measured. The SGD is calculated using equation 4.1.

5.2.2 Artificial Dust Deposition

An airtight chamber was built to carry out deposition of dust. Dust in the solvent has a tendency to settle down in the course of few seconds resulting in nonuniform dispersion of dust in acetonitrile. To prevent this, a magnetic stirrer was used. The stirrer prevented the dust from settling down in the gun and thus helped maintain the uniformity of dust

in the suspension. The substrate was placed at 90° angle and at a distance of 20 cm from the gun, parallel to the nozzle (of diameter 1mm) of the gun.

Commercial grade Nitrogen (N_2) was connected from one end of the gun to create low pressure at the nozzle with respect to the pressure inside the spray gun. A flow meter of 20 standard liters per minute was used to control the flow of N_2 . This pressure difference ensured the suspension to flow out of the gun through the nozzle. Necessary safety arrangement for the exhaust was done to move acetonitrile vapors out of the chamber. N_2 flow was given at the intervals of 15 s, till the desired weight of dust was achieved on the substrate. An interval of 15 s ensured that the acetonitrile evaporates from the substrate and does not disturb the uniformity. The dust samples from various sites were deposited on the glass samples of desired gravimetric densities.

5.2.3 Characterization

Some part of the dust samples were used to understand the particle size distribution. Particle size of the dust samples were measured using Beckman Coulter Laser Diffraction Particle Size Analyzer. This system has the ability to measure particle sizes from $0.017\mu\text{m}$ to $2000\mu\text{m}$. An XRD elemental analysis was used to determine the mineral constituents of the dust samples. The XRD analysis was done using PANalytical Empyrean system. The XRD pattern was analyzed to identify the minerals using the PANalytical's XRD software suite.

The electrical performance loss at 1-sun was evaluated using a custom made solar simulator that is equipped with a 1 kW Xenon lamp, producing an AM 1.5G spectrum. The simulator was calibrated with a reference cell (RERA silicon reference cell). A Keithley 2400 source meter was used for the current - voltage (I-V) measurement. A 2 cm^2 mono crystalline silicon solar cell was placed on the chuck, and soiled glass samples were directly placed over the cell.

For measurement of the spectral response of the dust samples, one-side soiled glass was placed on a mono c-Si solar cell and measurement was carried out using a Bentham PVE300 quantum efficiency (QE) measurement system. QE scans were taken at 5 nm increments from 300 nm to 1100 nm wavelengths. The slit width ($1.5\text{ mm} \times 5\text{ mm}$) was chosen such that input light beam can be focused on the active area between the metallic fingers. Firstly, the QE of the cell, overlaid with clean glass substrate, was measured and

this is designated as QE_{clean} . This was considered as the reference for measurements of QE for the glass substrates with dust. Then QE was measured with substrates of different soil gravimetric densities overlaid on the cell and designated as QE_{soiled} . QE loss QE_{LOSS} , due to reflection and absorption by the dust layer, is defined as $QE_{clean} - QE_{soiled}$. J_{sc} of the soiled sample was calculated by integrating the measured QE curve (soiled) with the AM 1.5G spectrum as follows:

$$J_{sc,soiled} = \int_{300}^{1100} QE_{soiled} \times q \times \phi_{AM1.5G}(\lambda) d\lambda \quad (5.1)$$

where, q is the charge of the electron, $\phi_{AM1.5G}$ ($cm^{-2}s^{-1}$) is the incident photon flux of AM1.5G spectrum, and λ is the wavelength in nm. The spectral transmittance of the dust samples was calculated from the QE spectra of the soiled and clean glass samples, as follows:

$$Dust\ Spectral\ Transmittance, T_d(\lambda) = \frac{QE_{soiled}(\lambda)}{QE_{clean}(\lambda)} \quad (5.2)$$

This equation assumes that the reflectance of clean PV module is negligible (approximately 3%), which can be seen from Figure 4.5.

J_{sc} of various PV module technologies with soiling was calculated by integrating spectral response (SR, in AW^{-1}) of various PV module technologies with the spectral transmittance of the dust sample of interest (from Eq. 5.2) and AM 1.5G spectrum (in $Wm^{-2}nm^{-1}$). The measured SR data of various PV module technologies were taken from European Solar Test Installation [26]. The J_{sc} is calculated as follows:

$$J_{sc,soiled} = \int_{300}^{1100} T_d(\lambda) \times SR(\lambda) \times AM1.5G(\lambda) d\lambda \quad (5.3)$$

The respective J_{sc} was then used to calculate J_{sc} loss as follows:

$$J_{sc,loss} = 1 - \frac{J_{sc,soiled}}{J_{sc,clean}} \quad (5.4)$$

where $J_{sc,clean}$ is calculated by substituting T_d as 1 in equation 5.3.

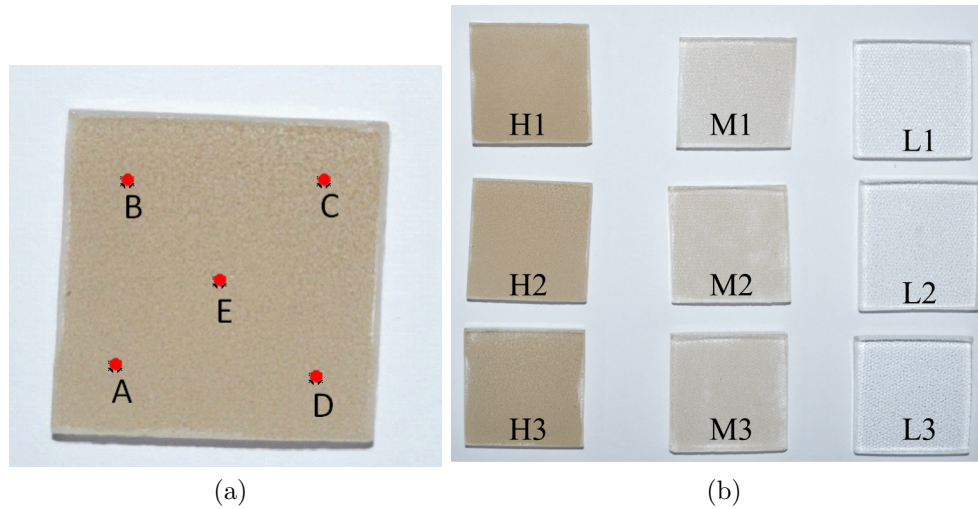


Figure 5.3: Uniformity of the sample was evaluated by calculating J_{sc} from QE spectra at 5 different locations in the sample. The sample shown in (a) has a SGD of 15 g/m^2 . Repeatability of the deposition technique was checked by depositing 3 soil gravimetric densities (H – Heavy (15 g/m^2), M - Moderate (5 g/m^2), L - Light (1 g/m^2)) thrice shown in (b) and J_{sc} value is calculated.

5.2.4 Uniformity and Repeatability

The uniformity of the dust sample deposition using the technique explained above is important because the QE measurement is carried out over a small area of $1.5 \text{ mm} \times 5 \text{ mm}$. These data would represent the individual soil gravimetric densities, which is measured over the glass sample area ($2 \text{ cm} \times 2 \text{ cm}$). Five spots in the sample (in Figure 5.33(a)) were chosen and respective J_{sc} values are shown in Table 5.1. The variation of the calculated J_{sc} values is 0.3% . Three soil gravimetric densities were selected, viz. heavy, moderate and lightly soiled samples showing 15 g/m^2 , 5 g/m^2 and 1 g/m^2 (Figure 5.3(b)), respectively, for the repeatability study. The selected gravimetric densities were deposited thrice and as shown in the Table 5.2 with suffix 1, 2 and 3. The variation of the J_{sc} values for the heavy, moderate and lightly deposited samples are 0.67% , 0.47% and 0.39% , respectively.

Table 5.1: Calculated J_{sc} of soiled glass sample in Figure 5.3(a) ($15 \text{ g}/m^2$), showing uniformity of deposition.

Positions	J_{sc} value estimated from QE measurement (mA/cm^2)
A	13.25
B	13.30
C	13.22
D	13.27
E	13.21

Table 5.2: Calculated J_{sc} of soiled glass sample in fig 5.3(a) ($15 \text{ g}/m^2$), showing repeatability of deposition.

Sample Number	J_{SC} value estimated from QE measurement (mA/cm^2)
H1	13.14
H2	13.27
H3	13.10
M1	24.08
M2	24.23
M3	24.01
L1	32.35
L2	32.32
L3	32.55

H – Heavy ($15 \text{ g}/m^2$), M-Moderate ($5 \text{ g}/m^2$), L-Light ($1 \text{ g}/m^2$)

5.3 Results and Discussion

5.3.1 Sediment Characterization

The dust samples collected from sites were analyzed to find the particle size distributions, and the results are shown in Table 5.3. The sediment type that dominates in the samples was of clay and different kinds of silts. Mumbai dust sample showed higher percentage of clay as compared to Jodhpur. Mumbai dust showed no presence of grained particles whereas Jodhpur dust samples showed small quantities (10.71%). The effect of the particle size has been studied by El-Shobokshy et al. [58], and they showed that dust containing small particles showed higher reduction in PV performance as compared to dust with large particles. The presence of grained particles may cause abrasions on the glass directly or on antireflective coatings on the glass [59], which may increase the opacity of the glass surface.

An XRD elemental analysis was used to determine the dust sample material composition, and the results are shown in Figure 5.4. The dominating component in all

Table 5.3: Particle size distribution and sediment types.

D (μm)	% of total Sample		Sediment Type
	Jodhpur	Mumbai	
0 - 4	9.26	22.31	Clay
4 - 8	5.09	15.74	Very Fine Silt
8 - 16	15.32	28.61	Fine Silt
16 -31	31.83	26.18	Medium Silt
31 - 63	27.78	7.15	Coarse Silt
63 - 125	10.71	0.00	Very Fine Grained
125 - 250	0.00	0.00	Fine Grained
250 - 500	0.00	0.00	Medium Grained
500 - 1000	0.00	0.00	Coarse Grained

the samples was quartz. Calcite was found in dust samples from Mumbai, Jodhpur and Hanle. Albite was found in Hanle, Jodhpur and Gurgaon. The next major constituent was Zeolite, which was found in Agra, Hanle, Jodhpur and Gurgaon. Illite was one of the major constituent of the dust samples found in Hanle. The optical absorption and reflection characteristics of these minerals are distinct and this can be expected to lead to differences in the performance of PV modules soiled with these dust.

5.3.2 Impact of Dust Samples from Mumbai and Jodhpur on Performance

5.3.2.1 1-Sun Response

The entire area of the test solar cell (2 cm^2) was covered by a soiled glass sample and subjected to I-V tests as explained in section 5.2.3. The soiled glass samples were of different soil gravimetric densities and from different locations.

Soiling loss, the percentage difference between the measured short circuit current (I_{sc}) of the soiled glass sample and a cleaned glass sample, was used to compare soiled glass samples with different soil gravimetric densities. The soiling loss increased with increase in soil gravimetric densities, as shown in Figure 5.5 and Figure 5.6. Initially, the loss increased rapidly with increase in the gravimetric density for both samples from Mumbai and Jodhpur. The loss gradually saturates at higher gravimetric densities. A similar observation was made by Eliminir et al. [28]. The dust sample from Mumbai appeared to show significant loss compared to dust from Jodhpur for all soil gravimetric densities. One main reason for this could be because dust from Mumbai had higher percentage of

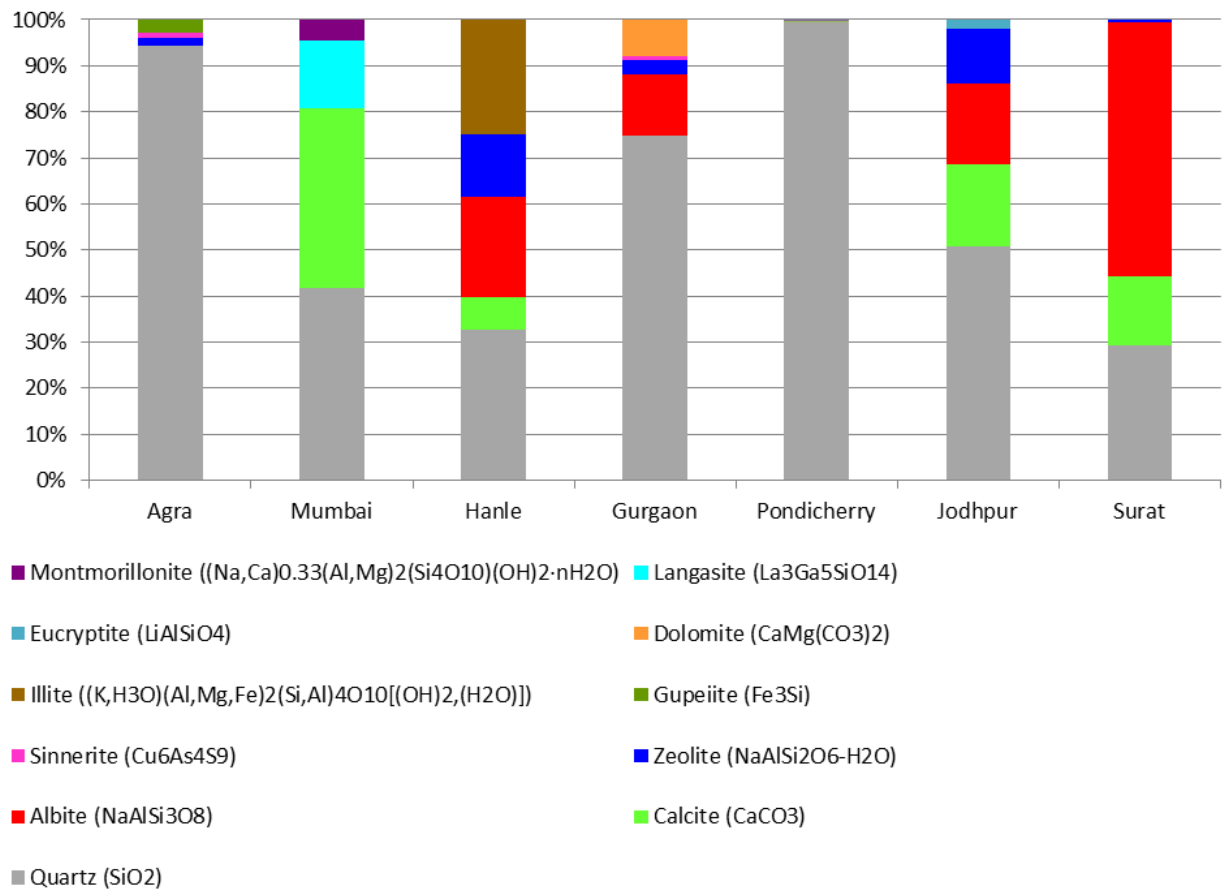


Figure 5.4: Analyzed XRD data of dust samples from Agra, Mumbai, Hanle, Gurgaon, Pondicherry and Jodhpur.

small particles (clay and very fine silt) as compared to dust from Jodhpur. El-Shobokshy et al. [58] attributed this to the more uniform distribution of small particles than of the coarser ones. This minimizes the gaps between the particles through which light can pass. The authors also reported that limestone particles (composed of calcite) tend to initially decrease fill factor (FF) which subsequently increases and reaches a maximum before decreasing again as the gravimetric density increases. This trend was also observed in both the dust from Mumbai and Jodhpur, which has calcite as one of its constituents. The maximum power (P_{max}) showed a similar trend as that of I_{sc} . The open circuit voltage (V_{oc}) remained nearly constant with increase in the SGD up to 3 g/m^2 . Above 3 g/m^2 , V_{oc} decreases (see Figure 5.6b) significantly for the dust collected from Mumbai as compared with Jodhpur.

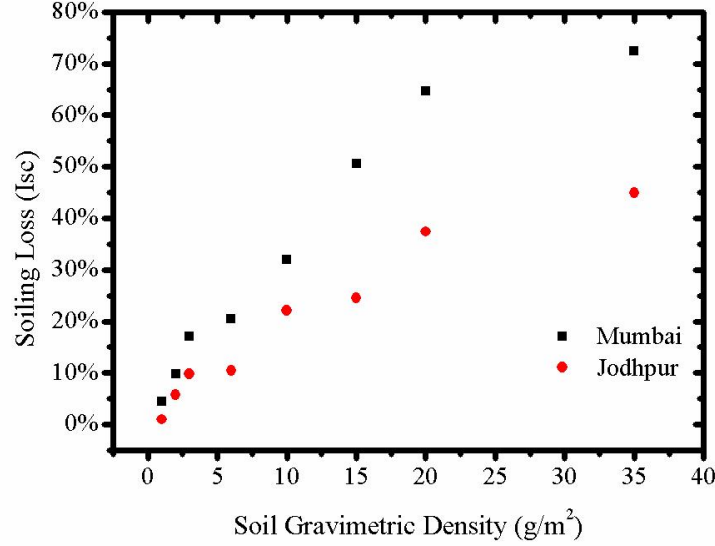


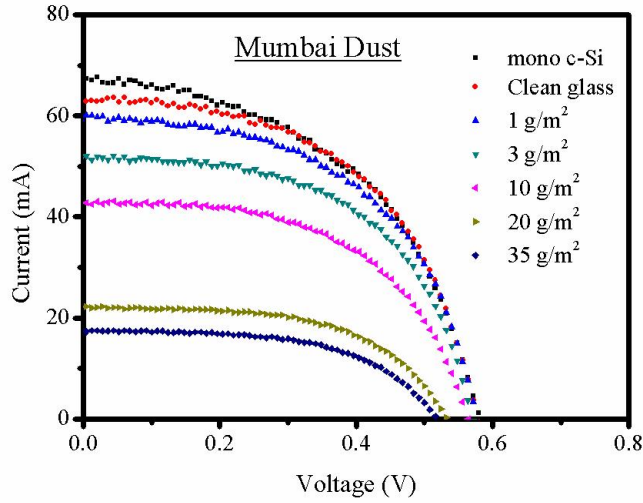
Figure 5.5: Comparison of soiling loss (using I_{sc}) of soiled glass samples from Mumbai and Jodhpur with different soil gravimetric densities.

5.3.2.2 Quantum Efficiency

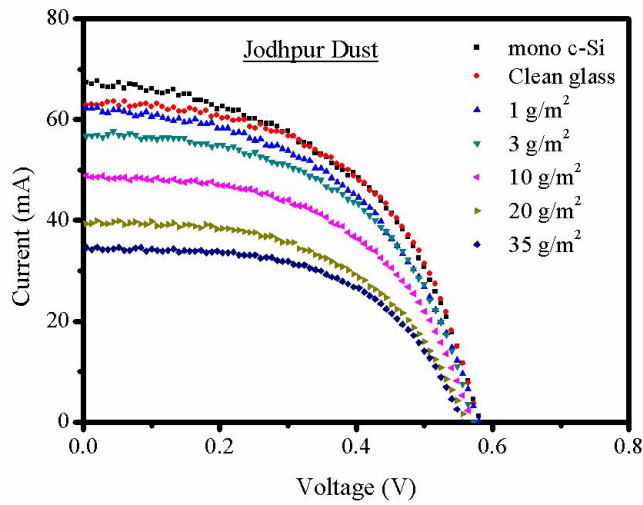
QE spectra were collected from 300 nm to 1100 nm using the test glass samples overlaid on a mono c-Si solar cell. Dust from Mumbai showed broader response (see Figure 5.7(a)), with highest loss corresponding approximately to the peak of the solar spectrum. In contrast, dust from Jodhpur showed a more pronounced response at 475 nm (see Figure 5.7(b)). The difference in the QE spectra of the clean and soiled glass samples (QE_{LOSS}) for the same gravimetric density is much higher for the samples from Mumbai compared with Jodhpur. This shows that dust from Mumbai will result in higher loss in performance as compared with dust from Jodhpur. A similar observation was made in the previous section for I_{sc} loss, shown in Figure 5.5. The response at the broad peak of 475 nm increases with increase in SGD for dust collected from Jodhpur.

5.3.3 Impact of Dust Samples from Gurgaon, Hanle, Agra and Pondicherry on PV Performance

Small quantities of dust samples were collected from Gurgaon, Hanle, Agra and Pondicherry. Hence, the effect of these dust samples with different soil gravimetric densities was not studied. The dust samples from each of these four sites were used to deposit 1.8 g/m^2 of dust on glass sample. QE measurements were done on these four samples and compared



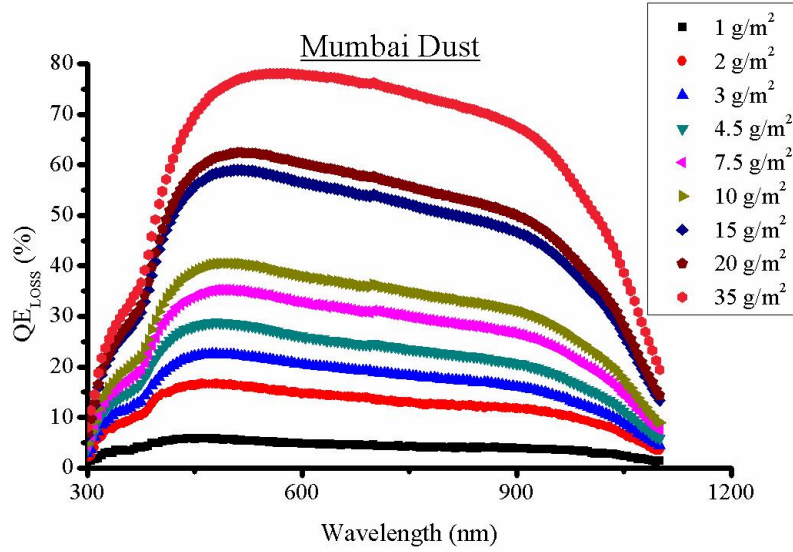
(a)



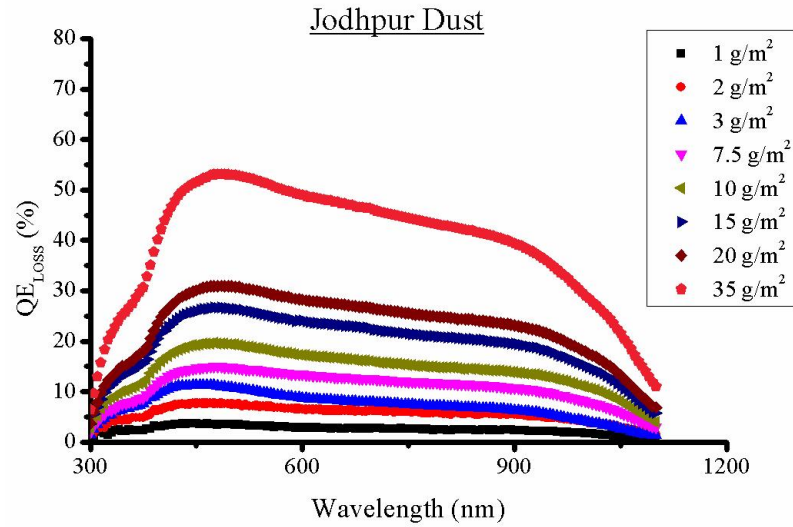
(b)

Figure 5.6: I-V curves of mono c-Si solar cell under clean and soiled glass samples from (a) Mumbai and (b) Jodhpur with different soil gravimetric densities.

with dust samples from Mumbai and Jodhpur of the same gravimetric density. I_{sc} loss of the six dust samples of 1.8 g/m^2 gravimetric density is shown in Figure 5.8. The dust sample from Mumbai shows the highest soiling loss followed by Pondicherry, Agra, Hanle, Jodhpur and Gurgaon. The high soiling loss shown by dust samples from Mumbai and Pondicherry can be explained by the QE spectra (see Figure 5.9), and the particle size distribution (see Table 5.4). QE spectra show that spectral sensitivity of the dust from Pondicherry and Mumbai at broad peak of 475 nm is similar. From Table 5.4, it can be seen that both dust types have high percentage of clay sediments (Mumbai – 22.31% and



(a)



(b)

Figure 5.7: Comparison of QE curve of mono c-Si solar cell with different dust densities from (a) Mumbai and (b) Jodhpur.

Pondicherry – 17.59%) consisting of particle size of less than $4 \mu\text{m}$. This may explain the reason for the QR_{LOSS} spectra of these two places show a matching pattern from 300-550 nm. However, the Mumbai dust showed higher QE loss at the longer wavelength as compared to Pondicherry dust. This difference may be due to the difference in the chemical composition of the dust as can be seen in Figure 5.4. Dust from Jodhpur (8.4%) and Gurgaon (8.3%) showed lowest soiling loss. The reason for this can be explained from QE spectra. Jodhpur dust exhibited highest difference in the QE spectra in the lower and middle wavelength range whereas Gurgaon dust had higher difference in the longer

Table 5.4: Sediment type classification of dust samples.

Dust samples from	% of Total Sample		
	Clay (0-4 μm)	Silt (4-63 μm)	Grained (63-1000 μm)
Jodhpur	9.26	80.02	10.71
Mumbai	22.31	77.68	0.00
Gurgaon	5.40	73.82	20.70
Hanle	10.93	82.69	6.37
Agra	16.03	71.54	12.48
Pondicherry	17.59	69.99	12.38

wavelength. As a result, the QE loss was similar which was reflected in the I_{sc} soiling loss. High percentage of grained sediments (compared to dust from other sites) was seen in these two types of dust (Jodhpur – 10.71%, Gurgaon – 20.7%), which means that there were larger gaps between these coarse particles through which light can pass. Dust sample from Pondicherry showed relatively high number of grained particle (12.38%) and hence should have showed similar response as that of Jodhpur and Gurgaon, but it had relatively high percentage of clay particles (17.59%), which may have filled the large gaps between the coarse particles. Dust samples from Agra and Hanle showed similar characteristics in the QE_{LOSS} spectra, except that the magnitude for Agra was higher than Hanle. This is reflected in the I_{sc} loss, where Agra shows higher loss compared to Hanle. Dust samples from Agra (16.03%) also showed higher percentage of clay sediments than Hanle dust samples (10.93%).

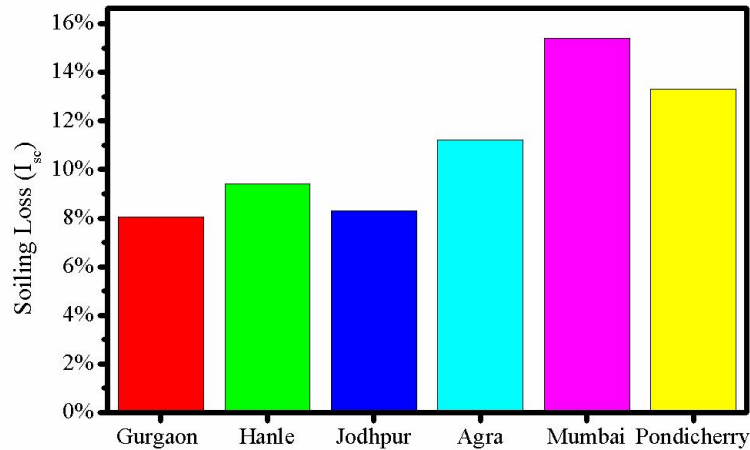


Figure 5.8: Comparison of soiling loss (I_{sc}) due to dust from Gurgaon, Hanle, Jodhpur, Agra, Mumbai and Pondicherry of same gravimetric density (1.8 g/m^2).

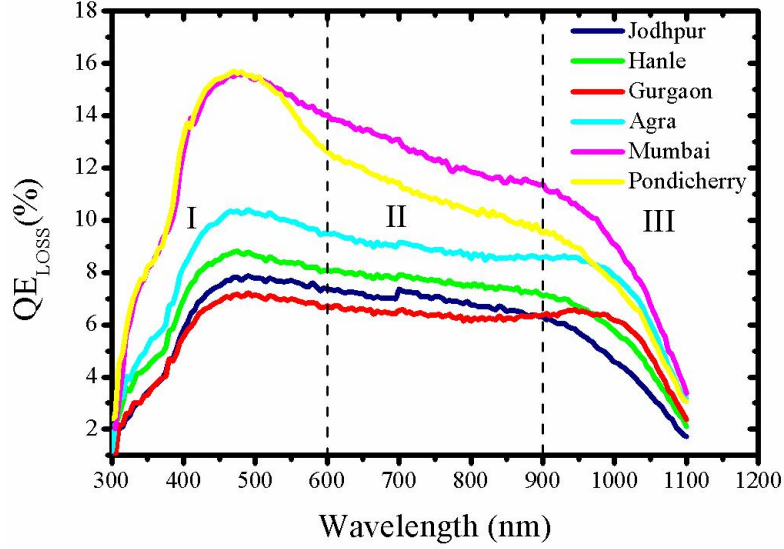


Figure 5.9: Comparison of difference in QE spectra from clean glass and dust deposited glass samples. The gravimetric density of 1.8 g/m^2 is maintained for all dust coated glass. Dust samples are collected from Gurgaon, Hanle, Jodhpur, Agra, Mumbai and Pondicherry. The graph is split into zones I, II and III.

5.3.4 Simulated Soiling Loss of Different PV Module Technologies

This spectral transmittance data (using equation 5.2) obtained from dust samples were also used to investigate spectral effects of these samples on various PV module technologies. The spectral effect on various types of PV technologies was studied by modifying the measured spectral response data [26] reported by European Solar Test Installation (see Figure 5.10) for mono c-Si, amorphous Silicon (a-Si), Copper Indium Gallium Selenide (CIGS) and Cadmium Telluride (CdTe) modules and calculating the J_{sc} that would have been generated under AM 1.5G spectrum [60]. The soiling loss was generated using J_{sc} for the various dust types and gravimetric densities.

5.3.4.1 Soiling Loss for Different Gravimetric Densities

The spectral sensitivity of the dust from Mumbai and Jodhpur on mono c-Si was shown in Figure 5.7. The bandgap of semiconductors used in PV modules vary and hence show different spectral response, as shown in Figure 5.10. Therefore, we expect that the soiling loss that will be exhibited by these technologies will be different. Table 5.5 and 5.6 shows the soiling loss of different PV module technologies with different soil gravimetric

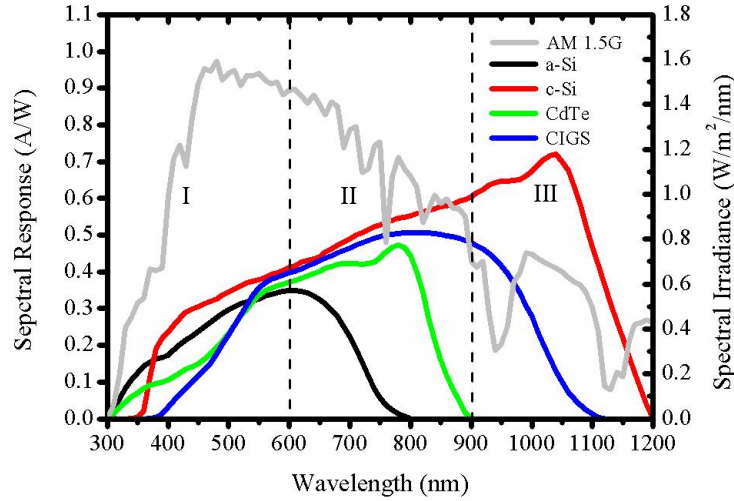


Figure 5.10: Spectral response of a-Si, mono c-Si, CdTe and CIGS modules, and AM1.5G spectrum divided into 3 zone- Zone I, Zone II and Zone III.

densities of dust collected from Mumbai and Jodhpur. It is seen that narrow bandgap of PV semiconductors such as c-Si shows lesser soiling loss compared to wider bandgap semiconductors (CdTe and a-Si) for all soil gravimetric densities. As observed in the earlier section, the soiling loss was much higher for dust collected from Mumbai as compared with Jodhpur.

Most of the locations where dust is a concern for energy yield from PV modules also have hot climatic conditions. The a-Si and CdTe technologies are considered more favorable for hot climatic conditions due to their lower thermal coefficient. Our data suggest that soiling losses may offset some of this advantage in locations that are both dusty and hot. In other words, a-Si and CdTe modules may need more frequent cleaning.

5.3.4.2 Soiling Loss for Different Dust Types

Table 5.7 shows the soiling loss on various PV module technologies with different dust types of same gravimetric density (1.8 g/m^2). Figure 5.9 has been divided into three zones- Zone I, Zone II and Zone III. Zone I is spread over 300 - 600 nm wavelength range that exhibits the highest variation in the QE spectra for various soil types. This zone also consist of the highest peak in the incident solar spectrum of AM 1.5G (see Figure 5.10). The dust type that exhibits highest spectral sensitivity in this zone tends to show highest soiling loss in the a-Si PV cell followed by CdTe, CIGS and c-Si solar cell. This is because

Table 5.5: Simulated soiling loss of dust samples from Mumbai.

Gravimetric Densities	Soiling loss (%) of PV Module Technologies			
	a-Si	CdTe	CIGS	c-Si
1 g/m ²	8.3	7.5	6.9	6.9
2 g/m ²	22.9	21.2	20.0	19.9
3 g/m ²	31.1	29.0	27.4	27.3
4.5 g/m ²	39.4	36.8	34.9	34.7
7.5 g/m ²	47.4	44.8	42.7	42.5
10 g/m ²	54.0	51.3	49.1	48.8
15 g/m ²	75.9	72.9	70.5	70.0
20 g/m ²	80.3	77.5	75.1	74.7
35 g/m ²	94.4	93.2	92.0	91.6

Table 5.6: Simulated soiling loss of dust samples from Jodhpur.

Gravimetric Densities	Soiling loss (%) of PV Module Technologies			
	a-Si	CdTe	CIGS	c-Si
1 g/m ²	5.3	4.7	4.3	4.3
2 g/m ²	10.9	9.8	9.1	9.1
7.5 g/m ²	20.9	19.3	18.2	18.1
10 g/m ²	27.7	25.5	23.9	23.8
15 g/m ²	37.1	34.4	32.5	32.4
20 g/m ²	42.8	39.9	37.8	37.7
35 g/m ²	71.4	67.4	64.4	64.0

Table 5.7: Simulated soiling loss of dust samples (1.8 g/m^2) from 6 locations.

Soil Samples collected from	Soiling loss (%) of PV Module Technologies			
	a-Si	CdTe	CIGS	c-Si
Mumbai	17.7	15.7	15.4	14.5
Pondicherry	15.5	13.8	12.7	12.4
Jodhpur	9.2	8.5	8.4	7.9
Hanle	10.2	9.5	9.5	8.9
Gurgaon	8.4	7.8	8.3	7.5
Agra	11.9	11.1	11.4	10.6

majority portion (62%) of the a-Si spectra response curve lies in Zone I. Zone II is from 600 nm to 900 nm. From the Figure 5.9 and earlier literatures [26, 51, 53] it can be seen that this zone behaves like a neutral density filter. CdTe PV cell shows major spectral response in this region as compared to other technologies. As a result, any considerable change in this zone due to any of the soil types can cause significant degradation in performance to CdTe, followed by CIGS, c-Si and a-Si. The spectral response in zone III (900 nm to 1200 nm) is dominated by c-Si followed by CIGS. As a result, spectral loss in this zone will affect c-Si the most and then CIGS technology.

5.4 Conclusion

Dust samples from fielded PV modules are collected from different geographical locations in India. These dust samples were artificially deposited on solar glass samples. Soiling loss due to I_{sc} was used to evaluate the performance of the soiled glass samples on mono c-Si solar cells. Spectral sensitivity of the dust samples from the different locations in India was studied.

Dust from Mumbai and Pondicherry showed the highest percentage of particle size less than $4\mu\text{m}$ (clay sediments). QE spectra (see Figure 5.7) are less spectrally sensitive at wavelengths above 600 nm. Qasem et al. [48] made a similar observation and explained it by Mie scattering where small particles ($< 3\mu\text{m}$) play a major role.

It is shown that the dust samples collected from different geographical locations in India attenuates the incoming irradiance in a spectrally dependent manner. These data are important as various PV technologies have very different spectral response (see Figure 5.10). As a result, the effect of soiling is not the same for all PV technologies. The spectrum of the incoming radiation is altered by the presence of the soiling layer on the

PV module surface. PV technologies with narrow spectral response and in Zone I and Zone II (a-Si and CdTe) are worse than technologies with broader spectral response in all three wavelength zones (Si and CIGS). For the same SGD, reduction in photocurrent was the lowest in CIGS and c-Si compared with a-Si and CdTe PV technologies. The advantages of thin film technologies like a-Si and CdTe in hotter climates due to low temperature coefficient of power may have to be offset in hot and dusty conditions due to the stronger response of these technologies to dust.

The soiling loss can be reproduced in the lab with the combination of collecting dust samples from specific region of interest, and spectral response of the PV technology. Rooftop PV installations may be the favored mounting option for the technology in urban areas, especially metro cities in India. However our data shows that the soiling losses are likely to be larger in one such city, i.e., Mumbai, we have analyzed. Coupled with the likely difficulty of accessing the roof mounted modules for cleaning, the necessity for developing anti-dust coatings assumes significance in such cases.

This study has considered the scenario when the density of the dust deposited is identical in different geographical locations. Future investigations should preferably consider the rate of dust deposition in actual conditions to incorporate the impact of dust and cleaning cycles on energy yield from PV power plants.

Chapter 6

Novel PV Module Cleaning System using Ambient Moisture

In the previous chapters, the severity of soiling on PV modules is discussed. The earlier chapter showed that the environmental conditions in which the modules are installed, play an important role in determining the energy output. For modules installed in countries near the equator, significant amount of dust can be accumulated on the panels, which lead to as much as 50% reduction in the energy output over 30 days. Degradation in PV system performance in the range of 15% - 65% for time duration varying from 6 days to 8 months in different parts of the world have been reported [61–63]. Decrease in the energy output reduces the yield which effectively increases the electricity price and the payback period. In addition, there could be module-level failures due to hot spots in unclean modules. Recommendations [42] to extenuate the impact of dust and other particulates like bird droppings and salt water stains on energy output include timely cleaning of the modules based on specific environmental conditions.

Manual cleaning of the modules in an installation would entail considerable time and efforts which may be over-whelming. Also at many installation sites, water may not be readily available for cleaning purposes. Keeping these factors in mind, this chapter discusses the design of an automated module cleaning system without any human intervention. The system would absorb moisture from the ambient atmosphere, which will then be filtered to be used for module cleaning. A chemical coating is also developed that will provide wiping action, that is required, after water is sprayed on the PV modules.

Table 6.1: Critical Relative Humidity of commonly available salts.

Material	CRH Value
Cesium Fluoride	6.20938
Lithium Bromide	7.75437
Zinc Bromide	9.28455
Lithium Chloride	11.2323
Sodium Hydroxide	11.5581
Potassium Hydroxide	16.7049
Potassium Acetate	22.4388
Lithium Iodide	22.8216
Calcium Bromide	23.5670
Calcium Chloride	32.0156
Magnesium Chloride	33.6686
Sodium Iodide	42.6040
Potassium Carbonate	43.1315
Magnesium Nitrate	60.3514
Sodium Bromide	64.7190
Cobalt Chloride	73.0330
Potassium Iodide	74.5466
Sodium Chloride	75.5164
Strontium Chloride	78.5322
Sodium Nitrate	79.5738
Ammonium Sulfate	81.7794
Ammonium Chloride	81.8777
Potassium Bromide	86.6424
Potassium Chloride	88.6190
Strontium Nitrate	94.2127

6.1 Concept and Approach

Deliquescence is the process by which a substance absorbs moisture from the atmosphere until it dissolves in the absorbed water and forms a solution. The deliquescence property of salts is the basic principle by which the absorption of moisture from the ambient atmosphere takes place. It is a known fact that when the humidity of the atmosphere is equal to or greater than the critical relative humidity (CRH) of a deliquescent material, the sample will absorb water until it is dissolved to yield a saturated solution. All deliquescent salts have characteristic critical relative humidity, which is a unique material property [64]. Table 6.1 shows the CRH values of various salts at 25°C. For this work, we selected salts taking into consideration the CRH values or average relative humidity, toxicity and cost of material.

The solution obtained after exposing the salts to ambient atmosphere (where the

humidity is equal to or greater than CRH) needs to be then filtered before it can be used for cleaning PV panels. The filtering process involves evaporation and condensation which is illustrated in Figure 6.1. The evaporation can be done with the help of solar radiation which can be trapped in a glass chamber to heat up the salt solution. Heating of the salt solution results in the formation of water vapor and then condense onto a relatively cooler surface to form water droplets. The water droplets are collected over a period of time which can then be used for cleaning PV modules. The evaporation of salt solution separates the salt from the solution, which can then be reused to absorb moisture from atmosphere. This process can be repeated to collect water.

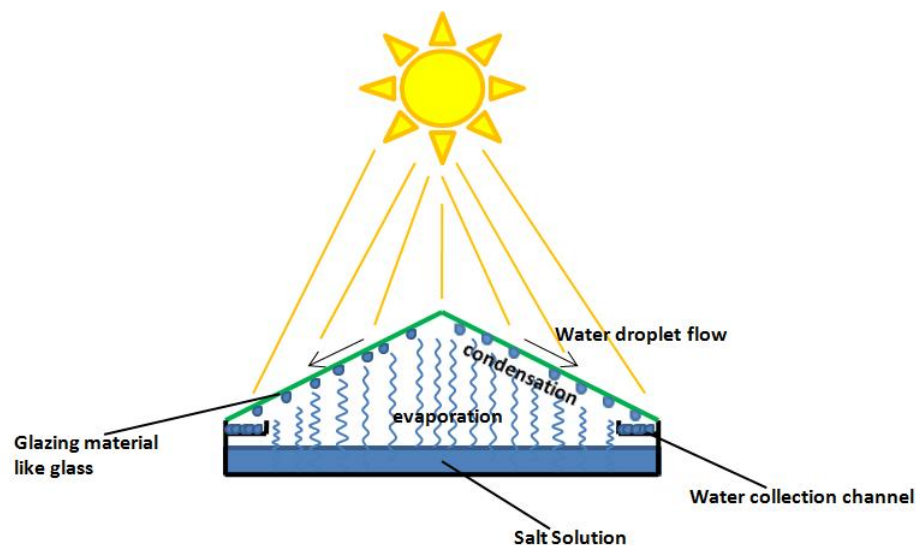


Figure 6.1: Illustration of a simple filtering process comprising of evaporation and condensation.

6.2 Average Annual Relative Humidity of the World

Relative humidity is a measure of how much water vapor is in the ambient. Relative humidity is defined as the ratio of the actual vapor pressure of water vapor to the saturation vapor pressure of water, in other words how much water is in the air divided by the most water that could possibly be there. This is an important parameter to deploy a mechanism that absorbs moisture from the air.

It can be seen from Figure 6.2 that most parts of the world and especially India show an average relative humidity of above 40% [65]. As a result, we have chosen calcium

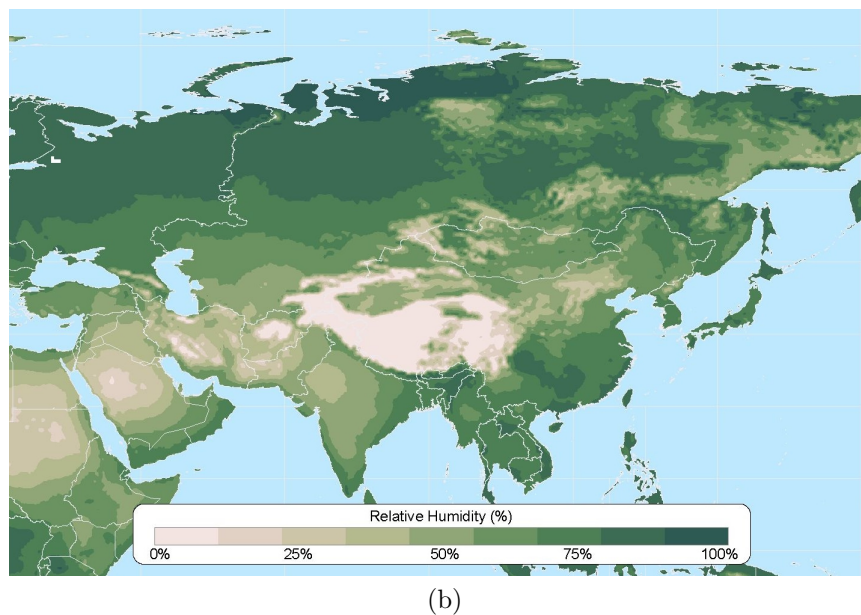
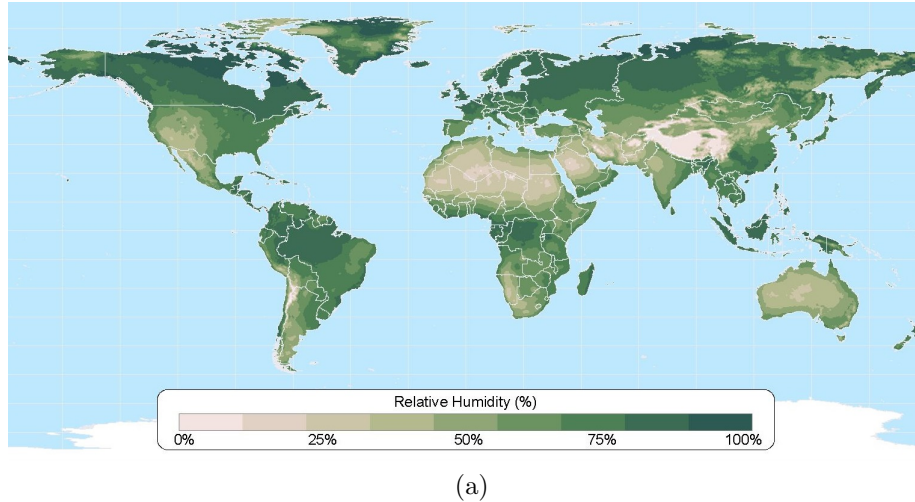


Figure 6.2: Average annual Relative Humidity seen in the (a)World and (b)Asia.

chloride, magnesium chloride and sodium chloride which has CRH values 32%, 33.6% and 75.5% to prove the concept.

6.3 Moisture Extraction

The extraction of moisture from the ambient depends on the relative humidity and ambient temperature. There are mainly two process involved in moisture extraction.

1. Moisture Absorption
2. Filtration

6.3.1 Moisture Absorption Experiments

Two sets of humidity absorption experiments were done over a period of 100 and 300 hours respectively. Separate experiments were conducted to evaluate the absorption efficacy of the salts under low humidity and high temperature conditions. As seen in the earlier section, major portion of the world, especially in India show average annual relative humidity greater than 40% throughout the year. Therefore, salts with CRH of less than 40% are suitable for the application. The selected salts such as $CaCl_2$ (Calcium Chloride) and $MgCl_2$ (Magnesium Chloride) satisfy this criterion.



Figure 6.3: Experiment setup to quantify the weight gain of various salts such as $NaCl$, $MgCl_2$ and $CaCl_2$, due to moisture absorption.

A plastic beaker was covered with a cloth and three types of salts such as $NaCl$, $MgCl_2$ and $CaCl_2$ are spread uniformly on the cloth, as shown in Figure 6.3. The initial weight for the 100 hour experiment of the $NaCl$ (Sodium Chloride), $MgCl_2$ and $CaCl_2$ are 21.45 gm, 17.27 gm and 17.2 gm respectively. Humidity and temperature sensors were used to monitor the humidity and temperature conditions. For the 100 hour experiment, temperature and the relative humidity varied from $27^{\circ}C$ to $34^{\circ}C$ and 74% to 84% respectively.

Figure 6.4 shows the hourly weight gain data of three salts for a duration of 100 hours. $NaCl$ has a high CRH value of 75%, the weight gain is very less (28% of the initial salt weight). On the other hand, $MgCl_2$ and $CaCl_2$ show a sharp initial increase, which then tends to settle down to a saturation value. The weight gain of $MgCl_2$ and $CaCl_2$ due to moisture absorption was 70% and 105% respectively. For all the salts, the weight gain was more appreciable during night and morning hours as compared to afternoon. High temperature conditions would result in increased evaporation during afternoon and hence reduced weight during those intervals.

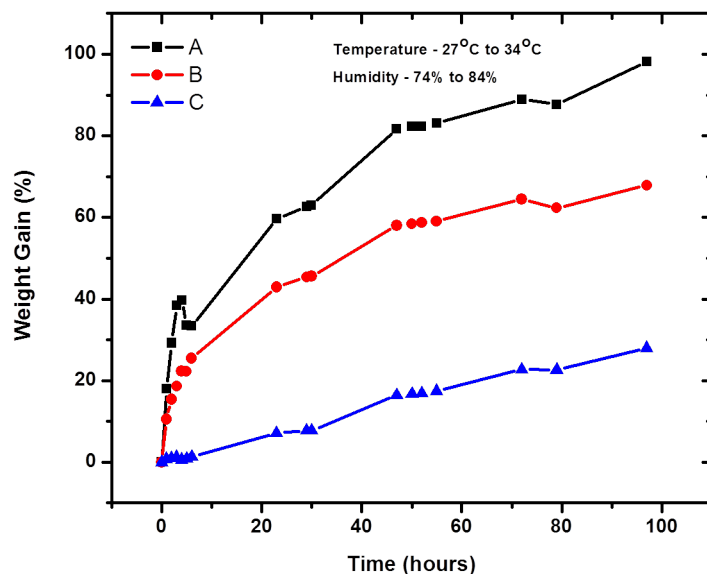


Figure 6.4: Weight gain data for 100 hours experiment for $CaCl_2$ (A), $MgCl_2$ (B) and $NaCl$ (C) (CRH = 75.5%).

Based on the encouraging results from initial experiments, elaborate tests for 300 hours duration were performed with more quantity of salt and combinations of salts as shown in Figure 6.5. The 300 hour experiment was done at an ambient of temperature and RH variation from $25^{\circ}C$ to $32^{\circ}C$ and 65% to 90% respectively. For samples involving $NaCl$, it can be observed that nearly after 200 hours of exposure, the weight gain started decreasing. It can be inferred that once the salt is saturated with moisture, the rate of evaporation outweighs the absorption rate and hence the net gain reduces. This is expected in the case of $NaCl$, since its CRH value was comparatively higher. Higher weight gain was obtained for $MgCl_2$ (62%), $CaCl_2$ (133%) and their combination. As in the initial experiment, best results were obtained for $CaCl_2$.

Experimental data at harsher ambient conditions for a duration of 170 hours are shown in Figure 6.6. $CaCl_2$ (103%) and equal mixture of $MgCl_2$ and $CaCl_2$ (89%) showed a gain comparable to previous results, while there was a severe loss in the case of $MgCl_2$ (30%). The reason for this loss in $MgCl_2$ is not known and it could be that CRH value of $MgCl_2$ salt is much higher than 33.66% as reported in the Table 6.1. Based on these results, it was concluded that $CaCl_2$ or mixture of $MgCl_2$ and $CaCl_2$ are the most suitable candidates for absorbing moisture from the ambient.

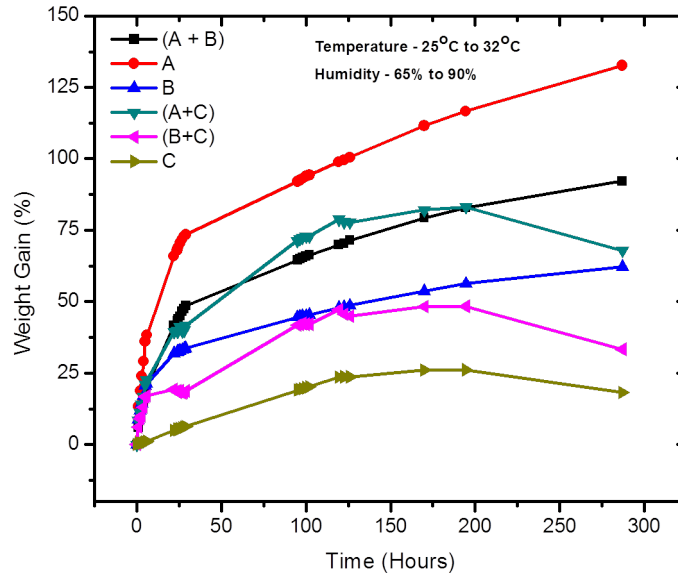


Figure 6.5: Weight gain data for 300 hours experiment for $CaCl_2$ (A), $MgCl_2$ (B), $NaCl$ (C) and equal mixtures of $MgCl_2$ and $CaCl_2$ (A+B), $NaCl$ and $CaCl_2$ (A+C), and $NaCl$ and $MgCl_2$ (B+C).

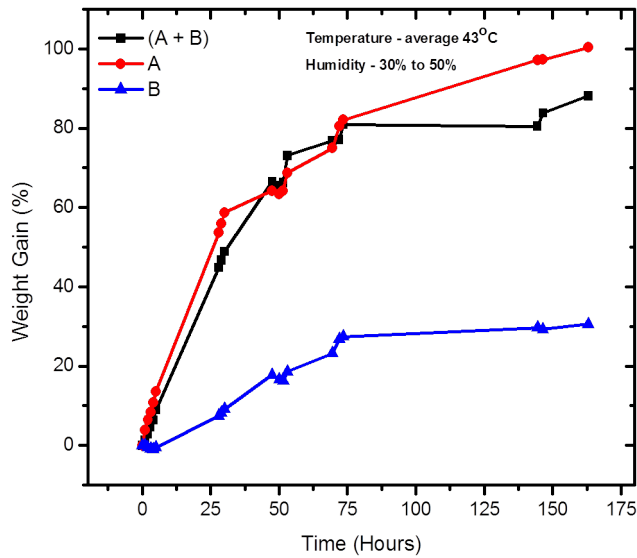


Figure 6.6: Weight gain data $CaCl_2$ (A), $MgCl_2$ (B), and equal mixture of $MgCl_2$ and $CaCl_2$ (A+B) for low relative humidity and high temperature.

6.3.2 Filtration

The schematic of the filtration process is shown in Figure 6.1. The filtration experiments were tried using the heat from sunlight and by using electric heaters as shown in Figure

6.7 and Figure 6.8.

In Figure 6.7(a), water droplets are formed due to the evaporation and condensation processes happening inside the glass pyramid. Evaporation of the calcium chloride solution due to the heat trapped in the glass pyramid, results in the formation of water vapor that condenses on the glass surface. The water droplets formed over a period of time is collected in a separate narrow channel towards the base of the pyramid. The circled area in Figure 6.7(b) shows the clean water collected in a narrow channel. For faster extraction of water droplets, electric heater was used as shown in Figure 6.8. The glass pyramid used in the electric heater experiment was relatively bigger and very narrow channels. As a result, a plastic pipe was attached to the channel so that water get collected in a clean container, circled as shown in Figure 6.8(a). After the extraction of water from the calcium chloride solution, the resultant anhydrous $CaCl_2$ is seen in Figure 6.8(b). The resultant $CaCl_2$ can be again used to collect water from the moisture.



Figure 6.7: Filtration experiment using solar energy image showing evaporation (a), and condensation happening on the glass surface (b). Circled area shows the clean water collected during the evaporation and condensation.

The collected or filtered water was tested to evaluate the quality. The test values are shown in Table 6.2. The measured values are compared to the potability range. It can be seen that all parameters of the filtered water was within the potability range. Since the salinity was very low, the water is ideal for cleaning PV modules which would otherwise aid in corroding the solar glass over the course of time.

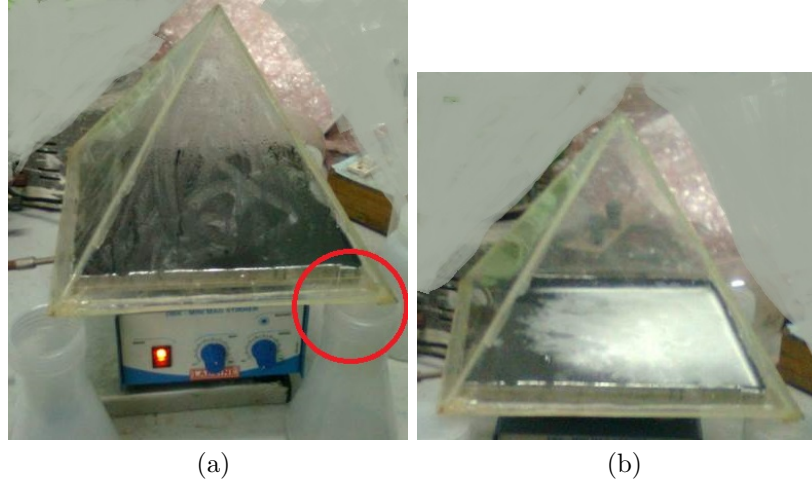


Figure 6.8: Filtration experiment using electric heater image showing evaporation and condensation happening on the glass surface (a). Circled area shows the container where the clean water gets collected during evaporation and condensation. The resultant anhydrous $CaCl_2$ is seen in (b) which can be reused for absorption.

Table 6.2: Test result of filtered water, compared with potability parameters.

Parameter	Measured Values	Potability Range (WHO Standard)
pH	8.2	6.5-8.5
Nitrate	23ppm	<45ppm
Chloride	7ppm	<250ppm
TDS	<128ppm	<500ppm
Salinity	11ppm	<410ppm
Conductivity	<200 μ Siemens	<780 μ Siemens

6.4 Prototype Design

The design of the prototype aims at meeting two important criteria with respect to cleaning of PV modules. The prototype discussed below has been designed for small or rooftop PV systems installed in places where the average annual relative humidity is above 40%.

The main function of PV panels is to produce useful electricity. If the cleaning process uses electricity, it reduces the amount of useful electricity generated by PV panels. The primary criteria was to reduce the use of electricity. Electricity is mainly used to pump water to water tanks, and from there to PV panel surface. The second criteria was to make it fully automated, i.e. no human intervention. Human involvement is used mainly for reaching the water to the PV panels, and for the wiping and drying process of the PV panel. Small PV systems, especially the rooftop PV systems are installed such that some panels are not easily accessible for cleaning.

In the previous sections, a mechanism to extract good quality water was discussed.

The water from humidity system can be used to eliminate the need for pumping water. It has been shown that this system works in two stages. The first stage involves the moisture absorption, which is achieved by using deliquescent salt, $CaCl_2$. The second stage involves the filtration stage where it would be mainly achieved by heat from sunlight. The amount of heat inside the glass pyramid can be increased by using concentrators.

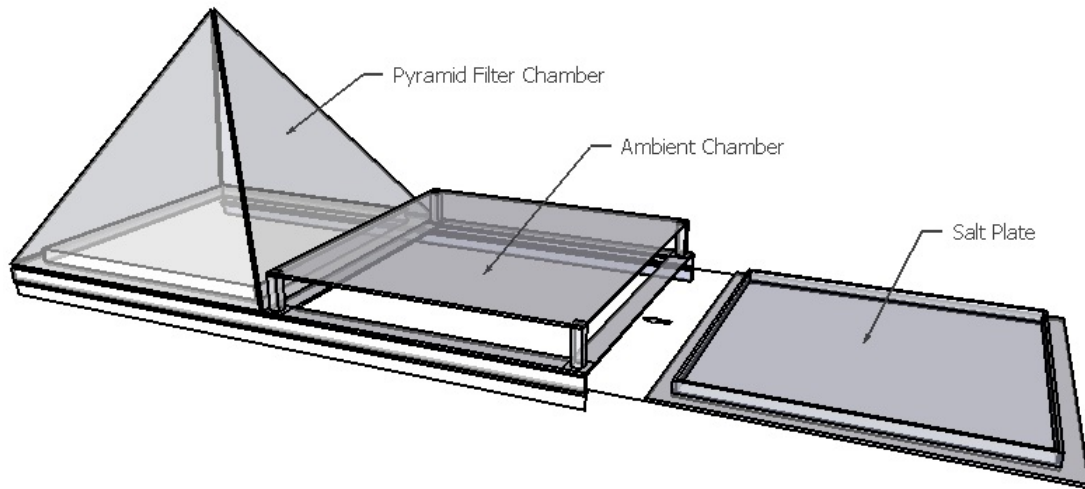


Figure 6.9: Schematic of the moisture absorbing and filtration stage, along with the salt plate

The moisture absorption and filtration stage of the prototype is shown schematically in Figure 6.9. The salt plate carries the crushed $CaCl_2$ salt. The salt is spread uniformly across the plate so that it is sufficiently exposed to the ambient. The ambient chamber holds the salt plate during the moisture absorption phase. The ambient chamber allows the salt to be exposed to the ambient and at the same time it should not be affected by environmental factors like dust and rain. Dust and rain water accumulation can adversely affect the water collection by contamination or loss of salt solution due to overflow.

A pyramidal chamber was selected for filtration of salt solution. Other shapes like a cone or hemisphere can also be used provided they are made of glazing material and it meets the design criterion similar to a solar still. Many experimental and numerical studies [66] have been done on solar stills to reach the optimum design by examining the effect of climatic, operational and design parameters on its performance. Since the filter function is similar to a solar still, the design parameters would be comparable. One of the crucial parameter that has been studied in detail is the cover tilt angle, which is the angle by the glazing material and the horizontal surface. The productivity of the filter

depends on number of factors. These include, but are not limited to the following:

- The volume available for evaporation above the salt solution surface; longer time is required for larger volumes.
- The increase of the tilt angle results in increased thermal losses from the cover, thereby increasing heat transfer area of the cover.
- Depending on the tilt angle, the pace at which the droplets travel along the interior surface of the cover towards the collecting channel will vary. Some droplets will fall into the basin if the angle is too low.
- The amount of radiation reflected by the cover may vary with seasons. Increasing the tilt angles may result in a decrease in the yield of the filter due to increased reflected radiation.

Figure 6.9 demonstrates horizontal motion of the salt plate. A vertical movement of the salt plate can be designed so that additional material to build the ambient chamber can be avoided, provided adequate environmental protection to the salt plate is provided. The function of the water from humidity system would be as follows:

- Salt powder is filled in the salt plate and kept in the ambient chamber for moisture absorption from late evening to early morning. Night time is chosen so that the humidity in the ambient will be relatively high and temperature will be lower compared to day, which facilitates maximum moisture absorption.
- As a result of moisture absorption, the salt powder has turned to salt solution. In the early morning, the salt plate is transferred to the pyramid filter chamber to extract clean water. The horizontal or vertical motion of the salt plate may require very small amount of electricity to run a motor for transferring the plate. The timing of the transfer can be based on light sensors.
- The filtration stage has made the calcium chloride solution less hydrous and as a result, would absorb more moisture during the next moisture absorption stage. Therefore, the salt powder need not be filled every day, and the cycle can continue.

The water channel inside the pyramid filter chamber is very narrow and do not have enough space to hold sufficient amount of water. Therefore, a storage tank is needed to store the water. It is not desirable to release the water immediately after the filtration process since the water quantity is very less. The storage tank is designed to release large quantity of water once the desired quantity to clean PV panel is reached. Stored water can be released through pipes with small holes placed near top of the PV panel. The prototype of water from humidity system, storage tank and pipe based dispersing mechanism is shown in Figure 6.10.



Figure 6.10: Prototype of water from humidity system, storage tank and pipe based dispersing mechanism.

PV panels are normally installed on fixed frames or movable frames with sun tracking systems. Hence the PV module cleaning system needs to cater to both fixtures. For a sun tracking dependent PV modules, the cleaning process can be done with the help of gravity. Depending on the inclination of the PV modules, the wiper mounted onto the ball screw mechanism can slide through the PV panels whereas for the fixed structure type a wiper has to be driven using motors. An external power source based on a dedicated PV module can be used to drive the DC motor circuitry. A schematic and prototype of the

tracker based design is shown in Figure 6.11.

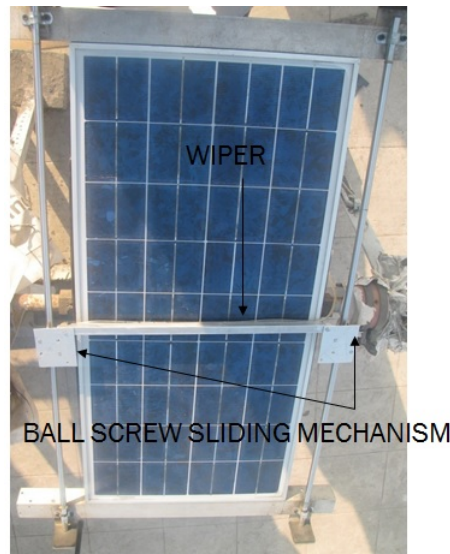
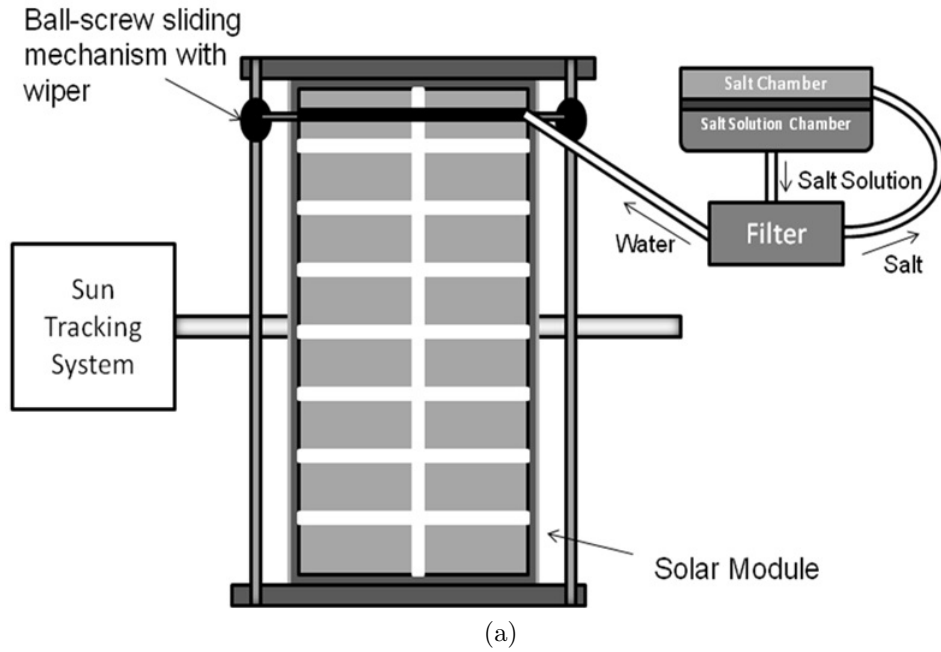


Figure 6.11: (Schematic (a) and Prototype (b) of the tracker based wiping mechanism.

6.5 Development of Wiping coating

In the previous section, a wiper mechanism is employed to wipe of the dirt of the PV modules. The wiper mechanism uses a motor to do the wiping action. This is undesirable because of two reasons. Firstly, energy from a battery or other sources is needed to run the motor. This might not be practical and economical because of the cost associated with

the batteries and the fixtures to keep them, especially for small PV systems. In addition, maintenance of the motor and the wiper mechanism will be important and would add to the cost during the life of its operation.

Keeping these factors in mind, self-cleaning coating is considered to eliminate the wiper mechanism with motors. The new schematic of the cleaning system with the self-cleaning/wiping coating is shown in Figure 6.12. Self cleaning coatings are being researched for extensive range of applications from window glass cleaning to cement and textiles. Researchers through the world are working to develop highly efficient and durable self-cleaning coating with enhanced optical properties for PV modules.

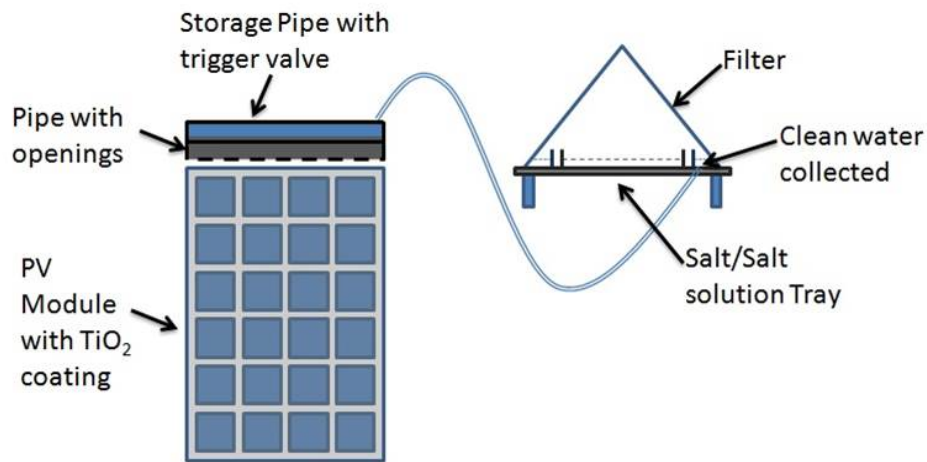


Figure 6.12: Illustration of the PV Module cleaning system prototype with the coating.

Self-cleaning coatings are broadly classified into two major categories [67]: superhydrophilic (water contact angle, WCA close to 0°) and superhydrophobic ($WCA > 150^\circ$) coatings. Both of the coatings clean themselves by the action of water. In a superhydrophilic coating, the water is made to spread over the surfaces (sheeting of water), which carries away dirt and other impurities, whereas in the superhydrophobic technique, the water droplets slide and roll over the surfaces thereby cleaning them. However, superhydrophilic coatings using suitable metal oxides have an additional property of chemically breaking down the complex dirt deposits by sunlight assisted cleaning mechanisms (photocatalysis). TiO_2 has been the main focus of study in self-cleaning applications because of its ability to clean the surfaces through two distinct properties: (1) photocatalysis and (2) superhydrophilicity. However other metal oxides like tungsten oxide (WO_3), zirconium oxide (ZrO_2), zinc oxide (ZnO), cadmium sulfide (CdS), etc. have also been investigated in recent years, but none of the materials could surpass TiO_2 , which uses only light to

activate the photocatalysis process.

Photocatalysis is a self-cleaning property which is shown by TiO_2 . As TiO_2 is a semiconductor, UV light can excite electron-hole pairs. The photogenerated electrons then react with molecular oxygen (O_2) to produce superoxide radical anions (O_2^-) and the photogenerated holes react with water to produce hydroxyl ($-OH$) radicals. These two reactive radicals work together to decompose organic compounds [68]. On the other hand, the $-OH$ groups can trap more photogenerated holes and improve the separation of electrons and holes which results in the enhancement of photocatalysis. It has been shown by Ganesh et al. [67] that TiO_2 coating developed using electrospinning show photocatalytic behavior.

Many techniques have been tried to deposit TiO_2 like chemical vapor deposition (CVD), sputtering, etc. However, these techniques are expensive. Sol-gel is a common and cheap technique used to deposit TiO_2 , but it is very difficult to control the thickness of the deposited films. Electrospinning is an alternative technique, which has been used to deposit metal oxide and polymer nanofibers [67].

Electrospinning is a cost-effective method for producing nanofibers by a simple setup comprising of three major parts: a high-voltage power supply, a syringe and a collector. This technique is used to produce a transparent, photocatalytic, and superhydrophilic TiO_2 coating on glass substrates.

6.5.1 Experiment

Firstly, a sol-gel solution is prepared for the deposition of TiO_2 on glass as follows:

- About 1.2gm of polyvinyl acetate (PVAc, Mw=500000) was added to 10 ml of N,N-dimethyl acetamide (DMAc, 99.8%)
- TiO_2 solution was prepared by mixing 2 ml of acetic acid (99.7%) and 1 ml of titanium isopropoxide (TiP, 97%).
- The above two solution were mixed and stirred at room temperature for 12 hours to acquire sufficient viscosity.

The soda-lime glass substrate was cleaned thoroughly by ultrasonication in DI water, acetone, ethanol and isopropanol, respectively, for about 10 min each and dried in an oven

at 80°C to ensure the glass is very clean before deposition.

In the electrospinning process [69], a high voltage is used to create an electrically charged jet of the solution, which dries or solidifies to leave a fiber. One electrode is placed into the spinning solution (or needle) and the other attached to a collector. Electric field is subjected to the end of a capillary tube that contains the fluid held by its surface tension. This induces a charge on the surface of the liquid. Mutual charge repulsion causes a force directly opposite to the surface tension. As the intensity of the electric field is increased, the hemispherical surface of the fluid at the tip of the capillary tube elongates to form a conical shape known as the Taylor cone. With increasing field, a critical value is attained when the repulsive electrostatic force overcomes the surface tension and a charged jet of fluid is ejected from the tip of the Taylor cone. The discharged solution jet undergoes a whipping process wherein the solvent evaporates, leaving behind a charged fiber, which lays itself randomly on a grounded collecting metal screen. The schematic of the electrospinning equipment is reproduced from [70] is shown in Figure 6.13.

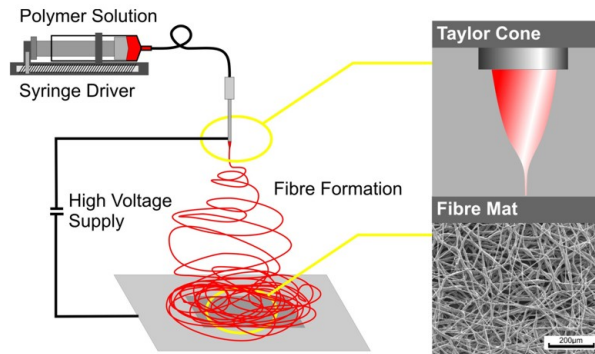


Figure 6.13: Schematic showing the electrospinning equipment.

The solution containing the TiO_2 precursor was loaded into the electrospinning system, as shown in Figure 6.14. The cleaned glass is mounted on top of the collector which is made of Aluminum foil. The applied voltage was fixed at 11.7 kV and the distance between the needle tip and the collector was about 10 cm. The needle inner diameter used was 22 gauge (0.7 mm inner diameter). The humidity level inside the electrospinning chamber needs to be controlled (RH - 50% – 60%). The electrospinning on glass was carried out for different time intervals (3 min, 1.5 min, 1 min). The PVAc- TiO_2 composite nanofiber coated glass samples was characterized using Zeta 3D microscope, as shown in Figure 6.15. This sample was further annealed at 450°C for 30 min in air. The annealing process

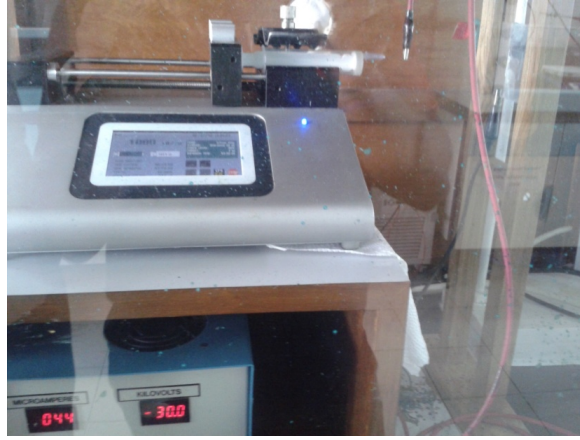


Figure 6.14: Electrospinning equipment used for this work.

evaporates the polymer and the solvent residues. The heating process also breaks the continuous fibers into TiO_2 nanoparticles on the glass, as shown in Figure 6.16. The resulting TiO_2 film was transparent, as shown in Figure 6.17.

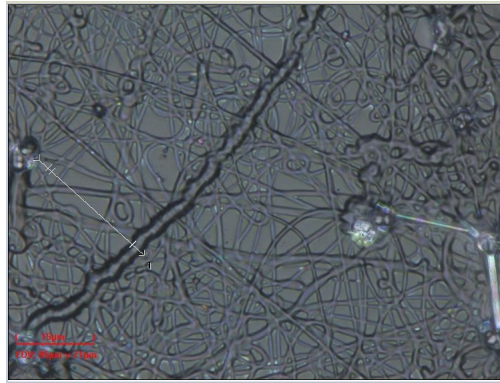


Figure 6.15: PVAc- TiO_2 composite nanofiber coated on glass sample. Image taken using Zeta 3D microscope.

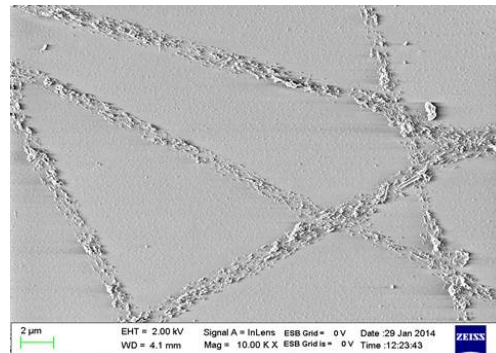


Figure 6.16: SEM image showing porous TiO_2 fibers with width of fiber $< 1\mu\text{m}$.



Figure 6.17: Image of the two solar glass coupons with TiO_2 coating (Right) and without TiO_2 coating (Left).

Table 6.3: WCA and weighted avg transmittance of TiO_2 samples on plain glass.

Sample. No	Flow Rate	Time (min)	Voltage (kV)	WCA	Transmittance
1.	40 $\mu\text{l}/\text{min}$	1	11.7	10.8°	87.37 %
2.	20 $\mu\text{l}/\text{min}$	1	11.7	11.6°	88.14%
3.	10 $\mu\text{l}/\text{min}$	1.5	11.7	21.7°	85.21%
4.	15 $\mu\text{l}/\text{min}$	3	11.7	23.4°	85.28 %
5		Plain Glass		53.5°	89.35 %

6.5.2 Results

Recipe for TiO_2 was prepared for both plain glass and textured glass. In both the experiments, voltage was fixed to 11.7 kV. Table 6.3 and Table 6.4 shows the water contact angle- WCA (indicator for hydrophilicity) and weighted average of transmittance from 300 – 1100 nm.

For the plain glass samples, it was observed that a flow rate of 40 $\mu\text{l}/\text{min}$ for a deposition time of 60 seconds yielded TiO_2 coated glass with the least WCA (10.8°) and highest transmittance (87.37%). It was seen that samples deposited with flow rates less than 40 $\mu\text{l}/\text{min}$ and deposition time above 60 seconds gave lesser transmittance. In textured glass samples, samples 1 and 5 yielded high transmittance values and low water contact angles.

Table 6.4: WCA and weighted avg transmittance of TiO_2 samples on textured glass.

Sample. No	Flow Rate	Time (min)	Voltage (kV)	WCA	Transmittance
1.	30 $\mu\text{l}/\text{min}$	1 min	11.7	7.2°	87.50%
2.	30 $\mu\text{l}/\text{min}$	2 min	11.7	22°	87.12%
3.	40 $\mu\text{l}/\text{min}$	1 min	11.7	13.7°	86.62%
4.	40 $\mu\text{l}/\text{min}$	2 min	11.7	15°	88.47%
5.	60 $\mu\text{l}/\text{min}$	1 min	11.7	13.9°	89.93%
6.	60 $\mu\text{l}/\text{min}$	30 sec	11.7	-nearly 0°	84.87%
7		Plain Glass		47.8°	90.42 %

6.6 Conclusion

This chapter discusses a novel PV module cleaning system using ambient moisture. The concept and approach in developing this is discussed initially. Since the cleaning system relies on humidity, a study on the average relative humidity seen in the world is discussed.

A ambient moisture extraction technique is presented. The deliquescent property of salts are used to absorb moisture from the humidity. The salt solution formed as a result of moisture absorption is filtered using a similar principle used in solar still. A pyramid made of glass is used to separate clean water from the solution. It is shown that the resultant water filtered is of good quality with very low salinity and chloride values.

The prototype design of the cleaning is discussed in detail. Salt powder is filled in the salt plate and kept in the ambient chamber for moisture absorption from late evening to early morning. As a result of moisture absorption, the salt powder has turned to salt solution. In the early morning, the salt plate is transferred to the pyramid filter chamber to extract clean water. The filtration stage has reduced the water content of the calcium chloride solution and as a result, would absorb more moisture during the next moisture absorption stage. Therefore, the salt powder need not be filled every day, and the cycle can continue.

For the cleaning process to be complete, after spraying water onto PV panels, a good wipe is needed to ensure no dust remains and the water residue evaporates off quickly. Bird droppings is an usual source of soiling on PV modules, hence it was decided to use a self-cleaning coating made of TiO_2 which shows high transmittance, superhydrophilicity and photocatalytic behavior. The development of TiO_2 and results obtained after deposition is discussed in this chapter.

Chapter 7

Summary

The need for PV technology is discussed in chapter 1. Given that electricity produced by PV technology is already contributing to 1% of world electricity demand in a short period, it is inevitable that this percentage is going to increase considerably. Solar radiation is abundant in the sun-belt countries and has huge scope of PV installations. But some of these countries have low frequency of rain which aids in dust accumulation on PV modules. Occurrence of dust storms and high concentration of airborne particles that may get accumulated on PV modules can further worsen PV performance.

From previous literature, it was understood that dust can be a mix of different particle sizes classified as clay, silt and grained sediments. The source of these dust can be immediate neighborhood or far away places, including other continents. The process of soiling on PV modules involve transportation of dust particles from one or many sources, initial adhesion mechanisms, changes in these adhesion mechanisms, alterations in surface and weak restorative strategies.

It was understood that the performance reduction in PV modules due to soiling is dependent on the geographical location. The factors that aid soiling on PV modules were boardly classified into PV module and system characteristics and geographical/environmental effects. Some of the factors are tilt angle, module direction, glazing material characteristics, PV technology, PV cell configuration, height of installation, average wind speed and direction, airborne dust concentration, dust storm frequency, distance of domestic dust sources, occurrence of dew, and dust particle size distribution.

Results of an outdoor PV modules experiment performed in Mumbai to understand the severity of soiling loss on PV modules is reported. Soiling loss observed in Mumbai

during the non-monsoon days is about 35-40% in about 100 days. Two different methods to quickly estimate the extent of soiling loss in a geographical location is proposed. The first method involves assigning scores to various parameters and calculating an index called "Site Soiling Index". There are lot independent research centers and private PV companies conducting experiments to determine the soiling rate at their location. A web platform was created to consolidate these result into a single web platform. This web platform can serve as a source of data for PV operators who are installing a PV system near these research centers or PV plants.

7.1 Outdoor Characterization of Spectral and Angular loss of Naturally Soiled PV Modules

Most of the earlier studies on the spectral effect of soiling were done on small glass coupons or small encapsulated solar cells that were naturally soiled outdoor or artificially soiled indoor. This study presents methods appropriate to characterize spectral and angular loss of large commercial size PV modules with different soil gravimetric densities. We have reported that the moderately and heavily soiled crystalline silicon PV modules show a short-circuit current loss of about 10% and 41%, respectively, with soil gravimetric density of approximately 3 gm/m² and 74 gm/m².

The increase in the reflectance of the moderately soiled PV module is the smallest in the 350 - 500 nm wavelength bands and highest in the 600 - 700 nm wavelength bands. This could be due to the particle size effect. Due to the presence of the soil layer, the overall reflectance of the moderately soiled and heavily soiled PV module was increased by 58.4% and 87.2% respectively.

The equation to estimate absorption of light by soil layer was derived and used to obtain the absorption spectra. On an average, the absorption was 61% and 23% in the heavily and moderately soiled layer respectively in the 350 to 1100 nm range. Absorption in the soil would depend on the soil composition and hence there is scope to repeat this for different types of soil.

The light transmitted through the soil layer was estimated from the absorption and reflectance spectra. An average 71% of the incoming light was transmitted through the moderately soiled layer whereas only 7% was transmitted through the heavily soiled layer.

The reduction in the QE of the moderately soiled PV module is mainly due to absorption in the dust and small percentage gets reflected. However, in the highly soiled PV module reduction in QE is largely dominated by the absorption of dust followed by reflection by the dust particles.

It is observed that the AOI curve is heavily influenced by the air/soil/superstrate layer. The critical AOI for the air/glass interface is about 57° and it decreases dramatically to 38° as the soil gravimetric density (g/m^2) increased to $3 \text{ g}/\text{m}^2$. This influence is crucial for fixed tilt modules as they experience a wide range of AOI during its operation and a major fraction of energy is generated at higher AOIs.

7.2 Development of Artificial Dust Deposition System and Indoor Characterization of Dust Samples Collected from PV Modules Installed in Different Parts of India

Dust samples from fielded PV modules are collected from different geographical locations in India. These dust samples was artificially deposited on solar glass samples. Soiling loss, calculated using I_{sc} , was used to evaluate the performance of the soiled glass samples on mono c-Si solar cells. Spectral sensitivity of the dust samples from the different locations in India was studied.

Dust from Mumbai and Pondicherry showed the highest percentage of particle size less than $4\mu\text{m}$. QE spectra are less spectrally sensitive at wavelengths above 600nm which was explained by Mie scattering where small particles ($< 3\mu\text{m}$) play a major role.

It is shown that the dust samples collected from different geographical locations in India attenuates the incoming irradiance in a spectrally dependent manner. This data is important as various PV technologies have very different spectral response. As a result, the effect of soiling is not the same for all PV technologies. The spectrum of the incoming radiation is altered by the presence of the soiling layer on the PV module surface. PV technologies with narrow spectral response (a-Si and CdTe) are worse than technologies with broader spectral response (Si and CIGS). For the same soil gravimetric density, reduction in photocurrent was the lowest in CIGS and c-Si compared to a-Si and CdTe

PV technologies. The advantages of thin film technologies like a-Si and CdTe in hotter climates due to low temperature coefficient of power may have to be offset in hot and dusty conditions due to the stronger response of these technologies to dust.

The soiling loss can be reproduced in the lab with the combination of collecting dust samples from specific region of interest, and spectral response of the PV technology.

Rooftop PV installations may be the favored mounting option for the technology in urban areas, especially metro cities in India. However our data shows that the soiling losses are likely to be larger in cities like Mumbai because of the presence of smaller particles (clay sediments) in the dust deposited on the modules. Coupled with the likely difficulty of accessing the roof mounted modules for cleaning, the necessity for developing anti-dust coatings assumes significance in such cases.

This study has considered the scenario when the density of the dust deposited is identical in different geographical locations. Future investigations should preferably consider the rate of dust deposition in actual conditions to incorporate the impact of dust and cleaning cycles on energy yield from PV power plants.

7.3 Novel PV Module Cleaning System Using Ambient Moisture

This chapter discusses a novel PV module cleaning system using ambient moisture. The deliquescent property of salts are used to absorb moisture from ambient air. The salt solution formed as a result of moisture absorption is filtered using a similar principle used in solar still. A pyramid made of glass is used to separate clean water from the solution. It is shown that the resultant water filtered is of good quality with very low salinity and chloride concentration.

The prototype design of the cleaning system is discussed in detail. Salt powder is filled in the salt plate and kept in the ambient chamber for moisture absorption from late evening to early morning. As a result of moisture absorption, the salt powder has turned to salt solution. In the early morning, the salt plate is transferred to the pyramid filter chamber to extract clean water. The filtration stage has reduced the water content of the calcium chloride solution and as a result, would absorb more moisture during the next moisture absorption stage. Therefore, the salt powder need not be filled every day, and

the cycle can continue.

For the cleaning process to be complete, after spraying water onto PV panels, a good wipe is needed to ensure no dust remains and the water residue evaporates off quickly. Bird droppings is an usual source of soiling on PV modules, hence it was decided to use a self-cleaning coating made of TiO_2 which shows high transmittance, superhydrophilicity and photocatalytic behavior.

Chapter 8

Future Works

8.1 Strategies for Quick estimation of the Extent of Soiling

One qualitative and another quantitative approach have been suggested in this thesis. Site soiling index is based on previous research, where the various parameters responsible for soiling on PV modules are scored based on their severity. This method even though qualitative can be used widely but may not be very accurate approach. The world soiling rate map are based on actual field measurements, and hence may be very accurate for the respective geographical location. The limitation of this is that few published data is available.

Some of the 12 parameters listed in Table 3.1 have not been well studied. Hence, there is a need for more research. Airborne dust concentration is measured mainly by PM2.5 and PM10 (indicator of air pollution), but Boyle et al. [33] showed that the correlation between accumulated dust and airborne particle concentration is vague and there is a need to build a better correlation or different measurement methodology. The effect of average wind speed parameter is highly dependent on the airborne particle concentration, and there is a need to understand the correlation between the average daily wind speed and the airborne dust particle concentration. A controlled experiment to understand the effect of dew which aids in soiling can be conducted. This mechanism is prominent in tropical countries. There is also a need to study the effect of various types of organic or inorganic dust particles on PV modules. It has been shown by El-Shobokshy et al. [50]

that carbon particles are more detrimental to PV performance as compared to limestone particles. In this thesis, it was identified that the most common minerals deposited on PV panels in India are Quartz, Calcite, Albite and Zeolite. More research with respect to various minerals found on PV modules and its effect on PV modules needs to be conducted. Further controlled experiments have the potential to increase the accuracy of SSI value which can provide more accurate cleaning frequency or suggest best type of preventive mitigation strategies.

Further, improvement in the methodology there is also need to address interdependence between parameters, like module direction and wind direction, and airborne dust concentration and wind speed. The current technique suggest an SSI for the non-rainy days but a monthly SSI maybe also envisaged.

The current number of 64 data points shown in the world is not enough. There is a need to accumulate more data. There are two strategies that could be considered:

1. The website can be hosted in an internationally known entity and can be made open for people to upload their data. Some security features have to be build-in so that authentic data gets uploaded.
2. Many more journal and conference papers maybe published which shows the soiling loss rate of various geographical locations. A collaborative effort may be needed by various entities so that this data can be made public for people to use.

I-V parameters such I_{sc} , P_{max} , and daily energy values have been used to evaluate the soiling loss rate. Research maybe needed to evaluate various parameters, and understand the errors introduced by each of these during uniform and non-uniform soiling.

8.2 Artificial Dust Deposition Using Water

The artificial dust deposition using acetonitrile is used in this thesis work. Acetonitrile was used so that uniform and repeatable deposition can be achieved, as it gets evaporated immediately after deposition. It can be seen from the FTIR results, see fig 8.1 that dust deposited using acetonitrile and water show different peaks, indicating that the composition of the dust is altered by acetonitrile. This FTIR result is of Mumbai dust sample and it is expected that the dust may contain organic compounds which may react

with acetonitrile. This change in dust composition may occur if there are lot of organic components in the dust, which maybe true for urban areas. Water based deposition was not used as the resultant deposition was highly non-uniform. Currently, an advance deposition system is being developed using water. Initial results are very encouraging.

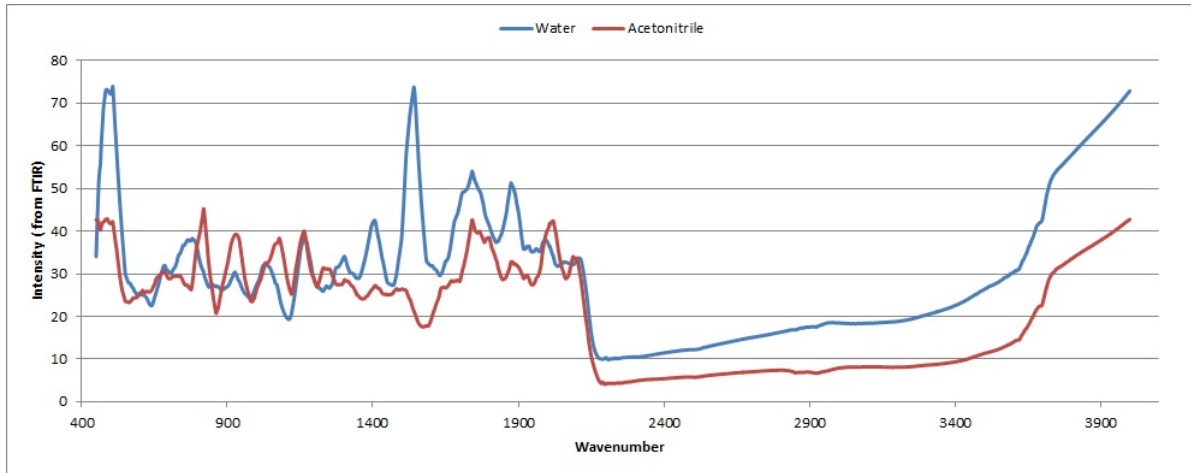


Figure 8.1: FTIR result of dust samples after artificial deposition using acetonitrile and water.

8.3 Improvements for the PV Module Cleaning System

The proof of the concept of collecting water from moisture for PV module cleaning is discussed in this thesis. The immediate future work include testing in the field, and depositing the wiping coating of TiO_2 on a large area like the PV module glass. Following improvements are envisaged for this system:

- Changing the CaCl powder to Poly(N-isopropylacrylamide) or PNIPAAm polymer. PNIPAAm polymer goes from being highly absorbent at lower temperatures, to dehydrating and shedding all its hydration at higher temperatures. The research by Yang et al. [71, 72] showed that cotton coated with PNIPAAm increased the material's absorbency to 340 percent its own weight (it was 18 percent without the coating). When the ambient temperature reaches $34^{\circ}C$, the change occurs and the polymer acts as a kind of waterproof barrier; the cotton becomes hydrophobic (water repellent) and sheds all the water it has absorbed.

- The wiping coating can be any other superhydrophilic or superhydrophobic coating which shows photocatalytic behavior.

Appendices

Appendix A

Literature Reviewed for the World PV Soiling Loss Rate Map (used in Section 3.2.2)

http://www.ncpre.iitb.ac.in/pages/SERIUS_Soiling_rate_of_the_World.html

Authors	Location	Latitude	Longitude	Type of Solar device	Period of study	Parameter	Max Soiling rate (at tilt angle similar to latitude)	Experiment Year	Remarks	Reference
Elhmnir et al.	Helwan, Cairo, Egypt	29,8500 N	31,3333 E	PV cells and glass	7 months	Efficiency	0.58	2005	Decreases in PV performance of about 17.4%/month.	Hamdy K. Elhmnir, Ahmed E. Ghias, R.H. Hamid, F. El-Hussainy, M.M. Beheary, Khaled M. Abdel-Moneim, Effect of dust on the transparent cover of solar collectors, Energy Conversion and Management, Volume 47, Issues 18–19, November 2006, Pages 3192-3203, ISSN 0196-8904, http://dx.doi.org/10.1016/j.enconman.2006.02.014 .
Kimber et al.	Los Angeles, Southern California	34.0522 N	118.2437 W	PV system (grid connected)	~ 1 year	Efficiency	0.19	2005	Average Annual soiling loss for Urban and suburban area is 5.6%, and 4.8%	Kimber, A.; Mitchell, L.; Nogradi, S.; Wenger, H., "The Effect of Soiling on Large Grid-Connected Photovoltaic Systems in California and the Southwest Region of the United States," in Photovoltaic Energy Conversion, Conference Record of the 2006 IEEE 4th World Conference on, vol.2, no., pp.2391-2395, May 2006, doi: 10.1109/WCPEC.2006.279690
Kimber et al.	San Diego, Southern California	32.7157 N	117.1611 W	PV system (grid connected)	~ 1 year	Efficiency	0.19	2005	Average Annual soiling loss for Urban and suburban area is 4.2%, and 3.6%	Kimber, A.; Mitchell, L.; Nogradi, S.; Wenger, H., "The Effect of Soiling on Large Grid-Connected Photovoltaic Systems in California and the Southwest Region of the United States," in Photovoltaic Energy Conversion, Conference Record of the 2006 IEEE 4th World Conference on, vol.2, no., pp.2391-2395, May 2006, doi: 10.1109/WCPEC.2006.279690
Kimber et al.	Sacramento, Central valley california	38.5816 N	121.4944 W	PV system (grid connected)	~ 1 year	Efficiency	0.21	2005	Average Annual soiling loss for Urban and suburban area is 6.2%, and 5.7%	Kimber, A.; Mitchell, L.; Nogradi, S.; Wenger, H., "The Effect of Soiling on Large Grid-Connected Photovoltaic Systems in California and the Southwest Region of the United States," in Photovoltaic Energy Conversion, Conference Record of the 2006 IEEE 4th World Conference on, vol.2, no., pp.2391-2395, May 2006, doi: 10.1109/WCPEC.2006.279690
Kimber et al.	Fresno, Central valley california	36.7468 N	119.7726 W	PV system (grid connected)	~ 1 year	Efficiency	0.21	2005	Average Annual soiling loss for Urban and suburban area is 4.8%, and 4.2%	Kimber, A.; Mitchell, L.; Nogradi, S.; Wenger, H., "The Effect of Soiling on Large Grid-Connected Photovoltaic Systems in California and the Southwest Region of the United States," in Photovoltaic Energy Conversion, Conference Record of the 2006 IEEE 4th World Conference on, vol.2, no., pp.2391-2395, May 2006, doi: 10.1109/WCPEC.2006.279690
Kimber et al.	San Francisco, Northern California	37.7749 N	122.4194 W	PV system (grid connected)	~ 1 year	Efficiency	0.16	2005	Average Annual soiling loss for Urban and suburban area is 6.05%, and 3.9%	Kimber, A.; Mitchell, L.; Nogradi, S.; Wenger, H., "The Effect of Soiling on Large Grid-Connected Photovoltaic Systems in California and the Southwest Region of the United States," in Photovoltaic Energy Conversion, Conference Record of the 2006 IEEE 4th World Conference on, vol.2, no., pp.2391-2395, May 2006, doi: 10.1109/WCPEC.2006.279690

Kimber et al.	petalumna, Northern California	38,2324 N	122,6367 W	PV system (grid connected)	~ 1 year	Efficiency	0.16	2005	Average Annual soiling loss for Urban and suburban area is 2.4%, and 1.5%	Kimber, A.; Mitchell, L.; Nogradi, S.; Wenger, H., "The Effect of Soiling on Large Grid-Connected Photovoltaic Systems in California and the Southwest Region of the United States," in Photovoltaic Energy Conversion, Conference Record of the 2006 IEEE 4th World Conference on , vol.2, no., pp.2391-2395, May 2006, doi: 10.1109/WCPEC.2006.279690
Kimber et al.	Las Vegas, Nevada	38.1699 N	115.1398 W	PV system (grid connected)	~ 1 year	Efficiency	0.31	2005	Average Annual soiling loss for Urban and suburban area is 4.2%, and 4.2%	Kimber, A.; Mitchell, L.; Nogradi, S.; Wenger, H., "The Effect of Soiling on Large Grid-Connected Photovoltaic Systems in California and the Southwest Region of the United States," in Photovoltaic Energy Conversion, Conference Record of the 2006 IEEE 4th World Conference on , vol.2, no., pp.2391-2395, May 2006, doi: 10.1109/WCPEC.2006.279690
Kimber et al.	Phoenix, Arizona	36.1699 N	112.0740 W	PV system (grid connected)	~ 1 year	Efficiency	0.31	2005	Average Annual soiling loss for Urban and suburban area is 4.1%, and 4.1%	Kimber, A.; Mitchell, L.; Nogradi, S.; Wenger, H., "The Effect of Soiling on Large Grid-Connected Photovoltaic Systems in California and the Southwest Region of the United States," in Photovoltaic Energy Conversion, Conference Record of the 2006 IEEE 4th World Conference on , vol.2, no., pp.2391-2395, May 2006, doi: 10.1109/WCPEC.2006.279690
Hassan et al	Saudi Arabia	33.4484 N		PV module (glass)	6 months	Efficiency	1.08	2004	33.5% and 65% reductions in efficiency after 1 month and 6 months.	A.H. Hassan, U.A. Rahoma, H.K. Elhimir, A.M. Fathy, Effect of airborne dust concentration on the performance of PV modules, J Astron Soc Egypt, 13 (1) (2005), pp. 24-38
Mastekbayeva et al	Pathum Thani, Thailand	14.0208 N	100.5250 E	Glazing material (LDPE)	30 days	Transmittance	0.4	2000	Experimental observations of natural dust accumulation on an inclined (15°) LDPE glazing at a tropical climatic condition during a 30-day period indicates a dust accumulation of 3.72 g/m ² and is found to reduce the global transmittance of the glazing from about 87.9% to 75.8%.	G.A. Mastekbayeva, S. Kumar, Effect of dust on the transmittance of low density polyethylene glazing in a tropical climate, Solar Energy, Volume 68, Issue 2, February 2000, Pages 135-141, ISSN 0038-092X, http://dx.doi.org/10.1016/S0038-092X(99)00069-9 .
Asl-Soleimani et al	Tehran, Iran	35.6892 N	51.3890 E	PV System	10 months	Power	0.2	2000	The influence of air pollution is quite considerable for a large city such as Tehran. Air pollution can reduce the energy output of solar modules by more than 60%.	E Asl-Soleimani, S Fathangi, M.S Zabih, The effect of tilt angle, air pollution on performance of photovoltaic systems in Tehran, Renewable Energy, Volume 24, Issues 3-4, November 2001, Pages 459-468, ISSN 0960-1481, http://dx.doi.org/10.1016/S0960-1481(01)00029-5 .
Hegazy	Minya, Egypt	28.0871 N	30.7618 E	Glass	1 month	Transmittance	0.6	2000	It is shown in the figure that for tilt angle of 30 degrees, the soiling loss increases to ~18% in 1 month	Hegazy AA. Effect of dust accumulation on solar transmittance through glass covers of plate-type collectors. Renewable Energy 2001 ; 22: 525-40.
Al-Helal et al	Riyadh, Saudi Arabia	25.0054 N	46.5448 E	Glazing material (Polyethylene)	1 month	Transmittance	0.13	2002	Reduction in GSR transmittance from 0.81 to 0.76 and 0.69 after 46 and 79 days respectively	Al-Helal I M, Al hamdan A M. Effect of arid environment on radiative properties of green house polyethylene cover. Solar Energy 2009; 83: 790-8.

Michels et al	Medianeira, Brazil	25.2953 S	54.0932 W	PV System	6 months	Power	0.09	2008	The dirty panel showed a power deficit of 16.3% compared to the cleaned panel for a period of six months	Roger Nabeyama Michels, Marcelo Giovanneti Cantieri, Marcelo Augusto de Aguiar e Silva, Estor Gronato, José Airtton Azevedo dos Santos and Mannel Messias Alvino de Jesus, "Yield from photovoltaic modules under real working situations in west Paraná - Brazil", v. 37, n. 1, p. 19-24, Jan.-Mar. 2015, Doi: 10.4025/actatechneol.v37n1.19191
Ju et al	Dameisha, Shenzhen, China	22.5991 N	114.3103 E	PV System	3 months	Power	0.09	2010	The mean PV-fouling coefficient in November, December and January is 0.956, the average PV fouling coefficient of February is 0.973.	Fali Ju; Xiangzhao Fu, "Research on impact of dust on solar photovoltaic(PV) performance," in Electrical and Control Engineering (ICECE), 2011 International Conference on , vol., no., pp.3601-3606, 16-18 Sept. 2011, doi: 10.1109/ICECENG.2011.6058487
Mohamed et al	Murzuq, Libya	25.9071 N	13.9461 E	PV System	4 months	Power	0.1	2011	Periodically weekly cleaning maintained performance losses between 2 – 2.5%. In Framework once a week cleaning intervals and rinse every three days from (February to May), then follows by once a month cleaning in other months, that help to reduce the dirt's and debris build up.	Ali Omar Mohamed, Abdulhazez Hasan, "Effect of Dust Accumulation on Performance of Photovoltaic Solar Modules in Sahara Environment", J. Basic. Appl. Sci. Res., 2(11)11030-11036, 2012
Rahman et al	Dhaka, Bangladesh	23.8103 N	90.4125 E	PV Module	1 month	Power	0.6	2011	It was found from the study that the accumulated dust on the surface of photovoltaic solar panel can reduce the system's efficiency by up to 35% in one month	Rahman et al. "Effects of Natural Dust on the Performance of PV Panels in Bangladesh", 11.Modern Education and Computer Science, 2012, 10, 26-32 Published Online September 2012 in MECS (http://www.mecs-press.org/) DOI: 10.5815/jmecs.2012.10.04
Cabanillas et al	Hermosillo, Sonora, Mexico	29.0730 N	110.9559 W	PV Module	3 months	Power	0.2	2010	The results indicate that the maximum reduction in potential is around of 6% for monocrystalline and polycrystalline modules and of 12% for the amorphous silicon.	R. E. Cabanillas and H. Munguia, "Dust accumulation effect on efficiency of Si photovoltaic modules, Citation: J. Renewable Sustainable Energy 3, 043114 (2011); doi: 10.1063/1.3622609
Ali et al	Taxila, Pakistan	33.7370 N	72.7994 E	PV Module	11 weeks	Efficiency	0.24	2014	the c-Si and p-Si PV module with dust deposition, showed 18.7% and 14.1% less output power respectively compared to the clean module of same type after 11 weeks	Hafiz Muhammad ALI, Muhammad Abdullah ZAFAR, Muhammad Anser BASHIR, Muhammad Ali NASIR, Muzaffar Ali and Aysha Maryam SIDDIQUI, EFFECT OF DUST DEPOSITION ON THE PERFORMANCE OF PHOTOVOLTAIC MODULES IN TAXILA, PAKISTAN, http://www.doiserbia.nb.rs/img/doi/0354-9836/2015%20Online-Fire/0354-98361500046A.pdf
Kaldellis et al	Athens, Greece	37.9839 N	23.7294 E	PV System	3 months	Efficiency	0.17	2009	5% power output reduction, even after a small period of time (i.e. a month) of PVs' exposure into the atmospheric air pollution.	Kaldellis, J. K., Kokala, A., and Kapsali, M., (2010), "Natural Air Pollution Deposition Impact on the Efficiency of PV Panels in Urban Environment, Fresenius Environmental Bulletin PSP 19 (12), pp. 2864-2872.
Zorrilla-Casanova et al	Malaga, Spain	36.7213 N	4.4213 W	PV Module	1 year	Energy	0.22	2010	In long periods without rain, daily energy losses can be higher than 20% over a 3 month period	J. Zorrilla-Casanova, M. Piffoigne J. Carretero, P. Bernola, P. Carpena, L. Mora-López, M. Sidrach-de-Cardona, Analysis of dust losses in photovoltaic modules, Proceedings of the world renewable energy congress 2011, p.2985–92.

Catehiani et al	Florence, Italy	43.7696 N	11.2558 E	PV Module	~ 1 month	Power	0.14	2011	For a tilt of 30deg. 3.43% soiling loss was seen over 24 days	Catehiani, M.; Gianni, L.; Cristaldi, L.; Fattori, M.; Lazzaroni, M.; Rossi, M., "Characterization of photovoltaic panels: The effects of dust," in Energy Conference and Exhibition (ENERGYCON), 2012 IEEE International , vol., no., pp.45-50, 9-12 Sept. 2012, doi: 10.1109/EnergyCon.2012.6348198
Pavvan et al	Puglia, Italy	40.7878 N	17.1033 E	PV System (Mega watt)	~55 days	Power	0.12	2010	For the first plant, built on a quite sandy site, the losses due to pollution were 6.9%, while for the second plant, built on a more compact ground, they were 1.1%. Experiment duration is about ~55 days	A. Massi Pavvan, A. Melilli, D. De Pieri, The effect of soiling on energy production for large-scale photovoltaic plants, Solar Energy, Volume 85, Issue 5, May 2011, Pages 1128-1136, ISSN 0038-092X, http://dx.doi.org/10.1016/j.solener.2011.03.006 .
Appels et al	Heverlee, Belgium	50.8639 N	4.6959 E	PV module (glass)	3 weeks	Transmittance/Power	0.13	2011	The results show a constant power loss between 3% and 4% for the optimal tilt angle and regular rainfall. Rain seems to have little cleaning effect on smaller dust particles (<10 µm), but on bigger particles (like pollen, ~60 µm) the effect was clearly visible. Water cleaning with soft water required (transmission loss due to hard water shown).	Appels, R.; Muhrirayan, B.; Beerten, A.; Praesen, R.; Driessen, J.; Poortmans, J., "The effect of dust deposition on photovoltaic modules," in Photovoltaic Specialist Conference (PVSC), 2012 38th IEEE, vol., no., pp.001886-001889, 3-8 June 2012 doi: 10.1109/PVSC.2012.6317961
Mejia et al	Hanford, California	36.3275 N	119.6457 W	PV Systems	~1 year	Efficiency	0.2	2010	The changes in conversion efficiency of 186 residential and commercial PV sites were quantified during dry periods over the course of 2010 with respect to rain events observed at nearby weather stations and using satellite solar resource data. Soiling losses averaged 0.051% per day overall and 26% of the sites had losses greater than 0.1% per day.	Felipe A. Mejia, Jan Kleissl, Soiling losses for solar photovoltaic systems in California, Solar Energy, Volume 95, September 2013, Pages 357-363, ISSN 0038-092X, http://dx.doi.org/10.1016/j.solener.2013.06.028 .
Lee et al	Thailand	15.8700 N	100.9925 E	PV module	9 months	Energy	0.52	2013	The soiling loss per month for Dec, Jan, Feb, Mar, Apr, May, July, Aug are 15.5%, 15.5%, 21.8%, 9.4%, 11.3%, 2.5%, 0%, 3.5% and 0%	Lee et al, An innovative approach to examine soiling impact on photovoltaic module performance, http://wiki-cleanitech.com/unecategorized/an-innovative-approach-to-examine-soiling-impact-on-photovoltaic-module-performance
Garcia et al	Tudela, Spain	42.0614 N	1.6063 W	PV System	1 year	Energy	0.2	2005	The highest optical energy losses are registered during the late winter months, when coincidentally the rainfall is the lowest and least intense. During the summer months the optical energy losses were lower, although it is observable how the losses augment as dry days go by. This energy loss increase is about 0.1-0.2% per day.	García, M., Marroyo, L., Lorenzo, E. and Pérez, M. (2011), Soiling and other optical losses in solar-tracking PV plants in Navarra. Prog. Photovolt: Res. Appl., 19: 211-217. doi:10.1002/ppp.1004

Caron et al	Carizzo Plain, California	35.1395 N	119.7426 W	PV System	1.5 years	Short-circuit current	0.12	2013	With soiling rates of less than 1.0% per month in the low desert and peak rates of 11.5% per month in heavy agricultural regions of the Central Valley, it is clear that soiling trends vary greatly across California	Caron, J.R.; Litmann, B., "Direct Monitoring of Energy Lost Due to Soiling on First Solar Modules in California," in Photovoltaics, IEEE Journal of , vol.3, no.1, pp.336-340, Jan. 2013 doi: 10.1109/JPHOTOV.2012.2216859
Caron et al	Southern California's Central Valley	34.06 N	118.2408 W	PV System	1.5 years	Short-circuit current	0.13	2013	With soiling rates of less than 1.0% per month in the low desert and peak rates of 11.5% per month in heavy agricultural regions of the Central Valley, it is clear that soiling trends vary greatly across California	Caron, J.R.; Litmann, B., "Direct Monitoring of Energy Lost Due to Soiling on First Solar Modules in California," in Photovoltaics, IEEE Journal of , vol.3, no.1, pp.336-340, Jan. 2013 doi: 10.1109/JPHOTOV.2012.2216860
Caron et al	Southern California's Colorado Desert	34.0000 N	117.0000 W	PV System	1.5 years	Short-circuit current	0.04	2013	With soiling rates of less than 1.0% per month in the low desert and peak rates of 11.5% per month in heavy agricultural regions of the Central Valley, it is clear that soiling trends vary greatly across California	Caron, J.R.; Litmann, B., "Direct Monitoring of Energy Lost Due to Soiling on First Solar Modules in California," in Photovoltaics, IEEE Journal of , vol.3, no.1, pp.336-340, Jan. 2013 doi: 10.1109/JPHOTOV.2012.2216861
Townsend et al	Davis, California	38.5449 N	121.7405 W	PV System	1 year	Energy	0.47	2000	In their study they measured annual soiling losses as high as 7% and monthly soiling losses as high as 20% both Isc and Voc of the solar cell were decreased under deposited dust through field exposure. Since, Isc is more decreased than Voc (2.78% and 0.863% respectively).	T. U. Townsend and P. A. Hutchinson, "Soiling Analysis at PVUSA," in Proceedings of ASES-2000, Madison, WI, 2000.
Ibrahim	Avar, Saudi Arabia	30.9599 N	41.0596 E	PV module	2 months	Short-circuit current	0.25	2010	Using a 17-day dry spell in mid-summer, the average rate of deposition during the dry summer months was estimated to be 0.045 g/m ² day. This level of deposition over 17 days reduced PV output about 4%. For the longest rainless period (28 days), upto 6% power loss might be faced.	A Ibrahim, "Effect of Shadow and Dust on the Performance of Silicon Solar Cell". J. Basic. Appl. Sci. Res., 1(3)222-230, 2011
Smith et al	Portland Oregon	45.5231 N	122.6765 W	PV System	17 days	Power	0.21	2010	By leaving one of the two panels of each pair exposed to natural conditions and always cleaning the other one, during the first week a decrease of the power output of about 2.2%, 2.5% and 1.7% for the monocrytalline, polycrytalline and amorphous silicon panels respectively, was observed.	Matthew K. Smith, Carl C. Wamser, Keith E. James, Seth Moody, David J. Sailor and Todd N. Rosenstiel, Effects of Natural and Manual Cleaning on Photovoltaic Output, J. Sol. Energy Eng 135(3), 034505 (Jun 11, 2013) (4 pages) doi:10.1115/1.4023927
Kalogirou et al	Limassol, Cyprus	34.7071 N	33.0226 E	PV modules	4 weeks	Power	0.31	2011		Soteris A. Kalogirou, Rafiada Agathokleous, Gregoris Panayiotou, On-site PV characterization and the effect of soiling on their performance, Energy, Volume 51, 1 March 2013, Pages 439-446, ISSN 0360-5442, http://dx.doi.org/10.1016/j.energy.2012.12.018 .

Cano et al	Mesa, Arizona	33.4152 N	111.8315 W	PV module	3 months	Short-circuit current	0.06	2012	For Mesa, Arizona (a hot-dry climate), the 0° tilt angle showed a 2.02% loss whereas 23° and 33° showed soiling loss close to 1% during the first three months of 2011.	Naeem, Mohammad Hussain, "Soiling of Photovoltaic Modules: Modeling and Validation of Location-Specific Cleaning Frequency Optimization," M.S. Thesis, Arizona State University, (2014). http://repository.asu.edu/attachments/140875/content/Naeem_asu_0010N14391.pdf
Schill et al	Gran Canaria island	27.9202 N	15.5474 W	PV module	5 months	Power	0.13	2010	The efficiency dropped to 20 % within 5 months before a heavy rain The maximum daily efficiency loss calculated for the silicon crystalline module tilted at 37° in northern Poland was equal to 0.8%. All modules investigated showed an average decrease in maximum power of 3%/year.	Schill, C.; Brachmann, S.; Heck, M.; Weiss, K.-A.; Koehl, M, "Impact of heavy soiling on the power output of PV-modules," Reliability of photovoltaic cells, modules, components, and systems IV : 22 - 25 August 2011, San Diego, California ISBN: 978-0-8194-8722-3
Klugmann-Radzemska et al	Gdansk, Poland	54.3520 N	18.6466 E	PV module	1 year	efficiency	0.8	2014	The maximum daily efficiency loss calculated for the silicon crystalline module tilted at 37° in northern Poland was equal to 0.8%. All modules investigated showed an average decrease in maximum power of 3%/year.	Ewa Klugmann-Radzemska, Degradation of electrical performance of a crystalline photovoltaic module due to dust deposition in northern Poland, Renewable Energy, Volume 78, June 2015, Pages 418-426, ISSN 0960-1481, http://dx.doi.org/10.1016/j.renene.2015.01.018 .
Amarnadh et al	Vellore, India	12.9165 N	79.1325 E	PV module	1 month	power	0.55	2013	Figure 8 shows that for a tilt angle of 0 deg and 30 deg, closest to optimum tilt angle (13 deg), soiling loss of 16.7% and 20% respectively	Gandhi Amarnadh T, Akshay Gupta, Vijay Shyam B, Investigation of the Effects of Dust Accumulation, and Performance for Mono and Poly Crystalline Silica Modules, INTERNATIONAL JOURNAL of RENEWABLE ENERGY RESEARCH, Vol.4, No.3, 2014
Boykiw et al	Arava Valley, Israel	32.6078 N	35.3068 E	PV module	2 weeks	efficiency	0.1	2010	NA	E Boykiw, "The Effect of Settling Dust in the Arava Valley on the Performance of Solar Photovoltaic Panels", https://sakal.allegheeny.edu/access/content/group/00093ca1-5eaf-4a09-be6e-f1bb5815f70/2011PDFs/boykiw_ehzaibeth.pdf
Adinoyi et al	Dhahran, Saudi Arabia	26.2361 N	50.0393 E	PV module	1.5 years	Power	0.27	2012	The study indicates that power decrease by as much as 50% can be experienced for solar PV modules that are left unclean for a period of over six months. Solar tracker improves power output and helps reduce dust accumulation effect by 50% at off-peak time.	Muhammed J. Adinoyi, Syed A.M. Said, Effect of dust accumulation on the power outputs of solar photovoltaic modules, Renewable Energy, Volume 60, December 2013, Pages 633-636, ISSN 0960-1481, http://dx.doi.org/10.1016/j.renene.2013.06.014 ,
John et al	Mumbai, India	19.0760 N	72.8777 E	PV module	~100 days	Energy	0.4	2012	daily energy based soiling loss calculation is consistently greater than Isc based as well as Pmax based calculations.	Jim J John, S. Chattopadhyay, R. Dubey, Anil K., J. Vasi, "Evaluation of Soiling Loss Measurement Methodologies for Different PV Module Technologies", presented at World Conference on Photovoltaic Energy Conversion, Kyoto, November, 2014
Al-Sabounchi et al	Abu Dhabi, UAE	24.2992 north	54.6973 east	PV System	1 year	Energy	0.87	2012	Monthly monitoring of PV system loss, July timeframe worst with 27% loss due to dust. Monthly cleaning cycle proposed.	Al-Sabounchi, Ammar M., Saeed A. Yalyali, and Hamda A. Al-Thani, "Design and performance evaluation of a photovoltaic grid-connected system in hot weather conditions.," Renewable Energy 53, 71-78 (2013), doi:10.1016/j.renene.2012.10.039.

Awward et al	Al-Qasral, Jordan	31.3296 N	37.3614 E	PV System	~4 months	Energy	0.03	2012	It can be inferred from the figure given in the paper, that about 2kWh was lost due to dust accumulation on the soiled panel as compared to cleaned panel(generated ~91kWh). This data was from 1st Feb 2013 to 19 April 2013. Author mentions that there is randomness in the data. Please take this data cautiously.	Awward, R., M. Shehadeh, and A. Al-Salaymeh, "Experimental investigation of dust effect on the performance of photovoltaic systems in Jordan." Proc. GCREEEDER 2013, Amman, Jordan,
Canada et al	Gila Bend, Arizona	32.9478 N	112.7168 W	PV System	10 years	NA	0.07	2012	From 1992 to 2012, the average annual soiling loss in Gila Bend, AZ has been 5.2%. From April to June there is an increase in soiling from 4% to 8% loss, i.e about 0.07%/day	Canada, Scott, "Quality assurance: Impact of soiling on utility-scale PV system performance." SolarPro Magazine, Issue 6.3, April/May 2013. http://solarprofessional.com/articles/operations-maintenance/impacts-of-soiling-on-utility-scale-pv-system-performance
Canada et al	Bullhead city, Arizona	35.1359 N	114.5286 W	PV System	11 years	NA	0.1	2012	From 1992 to 2012, the average annual soiling loss in Bullhead city, AZ has been 9.4%. From April to June there is an increase in soiling from ~8% to ~14% loss, i.e about 0.1%/day. Gila Bend gets 1.5 more rain events per year, and rainfall more evenly distributed throughout the year.	Canada, Scott, "Quality assurance: Impact of soiling on utility-scale PV system performance." SolarPro Magazine, Issue 6.3, April/May 2013. http://solarprofessional.com/articles/operations-maintenance/impacts-of-soiling-on-utility-scale-pv-system-performance
El-Din et al	Alexandria, Egypt	31.2001 N	29.9187 E	PV system	2 months	efficiency	0.34	2012	The average degradation of power and efficiency during the entire period of work (30 days) is 10.33%.	El-Din, A.M.A.M.S., A.K. Abdel-Rahman, A.H.H. Ali, and S. Ookawara, "Effect of dust deposition on performance of thin film photovoltaic module in harsh humid climate." Proc. 2013 International Conference on Renewable Energy Research and Applications (ICRERA), pp. 674-79 (2013). doi:10.1109/ICRERA.2013.6749839.
Ghazi et al	Baghdad, Iraq	33.3128 N	44.3615 E	PV module	3 months	Power	0.55	2012	The losses of the output power of the fixed solar panel at a tilt angle (35) can be reached 26% for one month and can be higher depending on the dust storm	Al-Ammri, A.S., A. Ghazi, and F. Mustafa, "Dust effects on the performance of PV street lights in Baghdad City." Proc. Renewable and Sustainable Energy Conference (RSSEC), 2013 International, 18-22, 2013. doi:10.1109/RSSEC.2013.6529687
Ndiaye et al	Dakar, Senegal			PV module	1 year	Power	0.22	2012	The maximum power output (Pmax) loss can be from 18 to 78% respectively for the polycrystalline module (pc-Si) and monocrystalline module (mc-si).	Ndiaye, A.C., M.F. Kébé, P.A. Ndiaye, A. Charaki, A. Kobi, and V. Sambou "Impact of dust on the photovoltaic (PV) modules characteristics after an exposition year in Sahelian environment: The case of Senegal." Intl. J. Phys. Sci. 8, 1166-73 (2013) DOI: 10.5897/IJPS2013.3921
Touati et al	Doha, Qatar	25.2854 N	51.5310 E	PV module	100 days	Efficiency	0.1	2012	The power efficiency of monocrystalline panels showed a faster degradation by around 10% for a dust exposure of 100 days only.	Touati, F., M.A. Al-Himi, and H.J. Boucheck, "Study of the effects of dust, relative humidity, and temperature on solar PV performance in Doha: Comparison between monocrystalline and amorphous PVs." International J. Green Energy 10, 680-689 (2013). DOI:10.1080/15435075.2012.692134

Sakhujia et al	Singapore	1.3521 N	103.8198 E	PV Module (Glass)	3 months	Efficiency	0.06	2013	Test conducted on 35m tall building, may not be true representation of soiling rate near the ground level.	Sakhujia, M., Son, J., Yang, H., Bhatia, C. S., Danner, A. J. "Outdoor performance and durability testing of antireflecting and self-cleaning glass for photovoltaic applications". Solar Energy 110, 231-238 (2014). http://dx.doi.org/10.1016/j.solener.2014.07.003
Sansui et al	Oghomosho, Nigeria	8.1227 N	4.2436 E	PV system	1 year	Energy	0.25	2011	NA	Y. K. Sansui, "The performance of amorphous silicon PV system under Hamattan dust conditions in a tropical area. Pac. J. Sci. Technol., 13 (1) (2012), pp. 168-175
Al-Busairi et al	Kuwait	29.3117 N	47.4818 E	PV module	6 months	Power	0.8	2009	Highest monthly losses due to dust accumulation were recorded in May from 4% for the vertical surface to 37% in Isc for the flat surface, mainly due to the presence of dusty rain or dry dust accumulation followed by light rain. Earlier observations have shown that yield losses can be even higher.	AlBusairi, H.A., Möller, H.J., 2010. Performance evaluation of CdTe PV modules under natural outdoor conditions in Kuwait. In: 25th European Photovoltaic Solar Energy Conference and Exhibition/5th World Conference on Photovoltaic Energy Conversion, 6-10 September, Valencia, Spain, pp. 3468-3470.
Mohammed et al	Riyadh, Saudi Arabia	25.0054 N	46.5448 E	PV module	3 months	Power	1	2011	NA	A.O. Mohamed, A. Hasan, Effect of dust accumulation on performance of photovoltaic solar modules in Sahara environment, J. Basic Appl. Scient. Res., 2 (11) (2012), pp. 11030-11036
Pang et al	Hongkong	22.3964 N	114.1095 E	PV module	3 months	Efficiency	0.18	2005	Maximum loss of 16.1% in 3 months was seen in CIGS PV module	Pang, H., Close, J., Lam, K., 2006. Study on effect of urban pollution to performance of commercial copper indium diselenide modules. In: 4th IEEE World Conference on Photovoltaic Energy Conversion, 7-12 May, Waikoloa, HI, pp. 2195-2198.
Liqun et al	Taiyuan, China	37.8706 N	112.5489 E	PV module (Glass)	2 weeks	Power	1.3	2011	18.2 and 32.6% soiling loss is seen at tilt angle of 45deg (south facing) and 0 deg respectively for a period of 2 weeks	Liqun, L., Zhiqi, L., Chunxia, S.Z.L., 2012. Degraded output characteristic at atmospheric air pollution and economy analysis of PV power system: a case study. Przegł. Elektrotech. (Electr. Rev.) 88 (9A), 281-284.
Senaoui et al	Ghardaia, Algeria	32.4902 N	3.6738 E	PV modules	2 months	Power	0.15	2013	It was found in this study, that the dust accumulation on the PV array surface for a period of several months can significantly reduce the PV array efficiency with an average power loss of about 4.38 %.	Senaoui, S., A. Hadj Arab, S. Bacha, H. Zerria, and E.K. Boudjelthia, "Sand effect on photovoltaic array efficiency in Algerian desert," in 2nd International Congress on Energy Efficiency and Energy Related Materials, A. Y. Oral, Z.B. Bahsi Oral, and M. Ozer, Eds. (Springer, New York: 2014), ISSN 2352-2434, ISBN 978-3-319-16901-9
Alnaser et al	Zallaq, Bahrain	26.0465 N	50.4980 E	PV system	7 months	Energy	1.08	2014	The accumulation of dust on PV panels became more significant in August (24.9%) and September (32.5%) due to humid weather during these two months with less wind speed that contributed to the adhesion (sticking) of dust on the panels, leading to loss of solar electricity production.	Alnaser, N.W., A. A. Dakhel, M.J. Al Othman, I. Batarseh, J. K. Lee, S. Najmali, and W. E. Alnaser, "Dust accumulation study on the Bapco 0.5MWp PV project at University of Bahrain," International Journal of Power and Renewable Energy Systems 2, 38-54 (2015). www.as-se.org/ijper/Download.aspx?ID=22792

Bhattacharya et al	Tripura, India			PV module	6 months	Efficiency	0.07	2014	Reduction of Voc, Isc, and efficiency reported (ranging from 9% to 13% loss in efficiency for 6 month duration. One module cleaned other left for exposure. As dust accumulates and ambient temperature increases, the rate by which the performance of mono-Si decreases is higher (-4 to -5%/month) compared to the situation of negative temperature gradient (-1.3 to -1.5%/month)	Bhattacharya, T., A.K. Chakraborty, and K. Pal, "Influence of environmental dust on the operating characteristics of the solar PV module in Tripura, India," <i>International Journal of Engineering Research</i> 4, 141-144 (2015). ISSN:2319-6890(online)
Ferrada et al	Antofagasta, Chile	23.6509 S	70.3975 W	PV System	1.5 years	Energy	0.17	2014	Thin-film module performance: Decreased due to the dust accumulation at a rate from 4.2%-3.7%/month (decreasing temperature conditions) and from 4.8%-4.4%/month (increasing temperature).	Pablo Ferrada, Francisco Araya, Aitor Marzo, Edward Fuentesalba, Cristóbal Parrado, and Carlos Portillo, "Photovoltaic performance and LCoE comparison at the coastal zone of the Atacama Desert, Chile," <i>Energy Conversion and Management</i> 95, 181-186 (2015). http://dx.doi.org/10.1016/j.enconman.2015.02.036
Fuentesalba et al	Atacama Desert, Chile	23.8634 S	69.1328 W	PV system	2 years	Energy	0.14	2014	the study showed that, for 11.60 and 21.50 tilt angles the total insolation losses were 21.92% and 16.78% respectively because of dust	Negash, Tanika and Tassew Tadiwose, "Experimental investigation of the effect of tilt angle on the dust photovoltaic module." <i>Internl. J. of Energy and Power Engineering</i> 4, 227-231 (2015) DOI: 10.11648/j.ijep.20150404.15
Negash et al	Bahir Dar, Ethiopia			PV module	~1 month	Energy	1.04	2013	reduction in transmission of 0.92% for untreated module glass and 1.1% with anti-soiling coating (no effectiveness of coating) over 1 week. Soiling due to snow	
Petersen	Evenstad, Norway			PV Module	1 week	transmittance	0.13	2014	power losses due to shading and soiling on photovoltaic (PV) modules," <i>Masters Thesis</i> (Norwegian University of Life Sciences, Norway; 2015) http://hdl.handle.net/11250/278807	Petersen, Anna Derås, "Simulation and experimental study of power losses due to shading and soiling on photovoltaic (PV) modules," <i>Masters Thesis</i> (Norwegian University of Life Sciences, Norway; 2015) http://hdl.handle.net/11250/278807
Shirakawa et al	Sao Paulo, Brazil			PV systems	18 months	Power	0.04	2014	power reductions due to soiling after 6, 12 (both 7%) and 18 (11%) months.	Shirakawa, M. A., Zilles, R., Moeelin, A., Christine, C. G., Gorbushina, A., Heidrich, G., Giundice, M. C., Negro, G. M. B. D., John, V.M. "Microbial colonization affects the efficiency of photovoltaic panels in a tropical environment." <i>Journal of Environmental Management</i> 157, p. 160-167 (2015) http://dx.doi.org/10.1016/j.jenvman.2015.03.050

Publications & Patents

Publications

Journal publications

1. John, J.J.; Rajasekar, V.; Boppana, S.; Chattopadhyay, S.; Kottantharayil, A.; TamizhMani, G., "Quantification and Modeling of Spectral and Angular Losses of Naturally Soiled PV Modules," in *Photovoltaics, IEEE Journal of*, vol.5, no.6, pp.1727-1734, Nov. 2015, doi: 10.1109/JPHOTOV.2015.2463745
2. Chattopadhyay, S.; Dubey, R.; Kuthanazhi, V.; John, J.J.; Solanki, C.S.; Kottantharayil, A.; Arora, B.M.; Narasimhan, K.L.; Kuber, V.; Vasi, J.; Kumar, A.; Sastry, O.S., "Visual Degradation in Field-Aged Crystalline Silicon PV Modules in India and Correlation With Electrical Degradation," in *Photovoltaics, IEEE Journal of*, vol.4, no.6, pp.1470-1476, Nov. 2014 doi: 10.1109/JPHOTOV.2014.2356717
3. John,J.J; Warade,S; TamizhMani,G; Kottantharayil,A, "Study of Soiling Loss on Photovoltaic Modules with Artificially Deposited Dust of Different Gravimetric Densities and Compositions Collected from Different Locations in India", in *Photovoltaics, IEEE Journal of*, vol.6, no.1, pp.236-243, Jan. 2016, doi: 10.1109/JPHOTOV.2015.2495208
4. Dubey,R; Chattopadhyay,S; Vivek, K, John,J.J, Solanki, C.S, Anil, K.; Arora, B M; Narsimhan,K L; Vasi,J, "Daylight Electroluminiscence Imaging by Image Difference Technique: Methodology and Field Application", under review at IEEE JPV

Conference Publications

1. John, J.J.; Raval, M.C.; Kottantharayil, A.; Solanki, C.S., "Novel PV module cleaning system using ambient moisture" in 26th European Photovoltaic Solar Energy Conference and Exhibition , pp.3569 - 3571, ISBN: 3-936338-27-2, doi: 10.4229/26thEUPVSEC2013.4AV.2.27
2. John, J.J.; Raval, M.C.; Kottantharayil, A.; Solanki, C.S., "Novel PV module cleaning system using ambient moisture and self-cleaning coating," in Photovoltaic Specialists Conference (PVSC), 2013 IEEE 39th, pp.1481-1483, 16-21 June 2013, doi: 10.1109/PVSC.2013.6744425
3. Vemula, M.G.; John, J.J.; Kuitche, J.; Tamizhmani, G., "Power rating of photovoltaic modules per IEC 61853-1 standard using a new outdoor test method," in Photovoltaic Specialists Conference (PVSC), 2013 IEEE 39th , vol., no., pp.0724-0728, 16-21 June 2013, doi: 10.1109/PVSC.2013.6744253
4. J J John, Sai Tatapudi, Govindasamy Tamizhmani, "Effect of soiling layer on QE, incident angle and Spectral Reflectance of c-Si PV Modules", NREL Reliability Workshop 2014
5. Cano, J.; John, J.J.; Tatapudi, S.; Tamizhmani, G., "Effect of tilt angle on soiling of photovoltaic modules," in Photovoltaic Specialist Conference (PVSC), 2014 IEEE 40th , pp.3174-3176, 8-13 June 2014, doi: 10.1109/PVSC.2014.6925610
6. J J John, Sai Tatapudi, Govindasamy Tamizhmani, "Influence of soiling layer on QE, Spectral Reflectance on c-Si PV Modules", IEEE PVSC 2014
7. J J John; V. Rajasekar; S. Boppana; S. Tatapudi; G. Tamizhmani, "Angle of Incidence effects on soiled PV modules",Proc. SPIE 9179, Reliability of Photovoltaic Cells, Modules, Components, and Systems VII, 91790D (8 October 2014); doi: 10.1117/12.2063351
8. Kazmerski, L.L.; Al Jordan, M.; Al Jnoobi, Y.; Al Shaya, Y.; John, J.J., "Ashes to ashes, dust to dust: Averting a potential showstopper for solar photovoltaics," in Photovoltaic Specialist Conference (PVSC), 2014 IEEE 40th , pp.0187-0192, 8-13 June 2014, doi: 10.1109/PVSC.2014.6925524

9. J J John, S. Chattopadhyay, R. Dubey, Anil K., J. Vasi, "Evaluation of Soiling Loss Measurement Methodologies for Different PV Module Technologies", presented at World Conference on Photovoltaic Energy Conversion , Kyoto, November, 2014
10. Dubey, R.; Chattopadhyay, S.; Kuthanazhi, V.; John, J.J.; Vasi, J.; Kottantharayil, A.; Arora, B.M.; Narsimhan, K.L.; Kuber, V.; Solanki, C.S.; Kumar, A.; Sastry, O.S., "Performance degradation in field-aged crystalline silicon PV modules in different indian climatic conditions," in Photovoltaic Specialist Conference (PVSC), 2014 IEEE 40th , pp.3182-3187, 8-13 June 2014 doi: 10.1109/PVSC.2014.6925612
11. Kuthanazhi, V.; Chattopadhyay, S.; Dubey, R.; John, J.J.; Solanki, C.S.; Kottantharayil, A.; Arora, B.M.; Narasimhan, K.L.; Vasi, J.; Kumar, A.; Sastry, O.S., "Linking performance of PV systems in India with socio-economic aspects of installation," in Photovoltaic Specialist Conference (PVSC), 2014 IEEE 40th , pp.1448-1451, 8-13 June 2014 doi: 10.1109/PVSC.2014.6925188
12. R. Dubey, S. Chattopadhyay, Vivek K., J. John, C. S. Solanki, Anil K., B. M. Arora, K.L. Narsimhan, J. Vasi, "Daylight Electroluminescence Imaging of Photovoltaic Modules by Image Difference Technique", presented at World Conference on Photovoltaic Energy Conversion , Kyoto, November, 2014
13. J J John, S Warade, A Kumar, A Kottantharayil, "Evaluation and Prediction of Soiling Loss on PV Modules with Artificially Deposited Dust", presented at 42nd IEEE PVSC New Orleans 2015
14. R. Dubey, S. Chattopadhyay, Vivek K., J. John, C. S. Solanki, Anil K., B. M. Arora, K.L. Narsimhan, J. Vasi, "Measurement of temperature coefficient of PV Modules in field and comparison with laboratory measurements", presented at 42nd IEEE PVSC New Orleans 2015
15. S. Chattopadhyay, R. Dubey, Vivek K., J. John, C. S. Solanki, Anil K., B. M. Arora, K.L. Narsimhan, V. Kuber, J. Vasi, "All India Survey 2014: Survey Methodology and Statistics", presented at 42nd IEEE PVSC New Orleans 2015

Patents

Jim J John, Anil Kottantharayil, “Novel PV Module Cleaning System using Ambient Moisture” Application number 2408/MUM/2011. PTC filing PCT/1N2011/000701, US Patent No. 14241279

Bibliography

- [1] UNDP. (2006) Millennium project fast facts: The faces of poverty. [Online]. Available: http://www.unmillenniumproject.org/resources/fastfacts_e.htm
- [2] J. Watson. (2015) Global market outlook for solar power 2015-2019. Solar Power Europe. [Online]. Available: <http://resources.solarbusinesshub.com/solar-industry-reports/item/global-market-outlook-for-solar-power-2015-2019>
- [3] S. Mittal. (2015) India achieves 4 gigawatts installed solar power capacity. Clean Technica. [Online]. Available: <http://cleantechnica.com/2015/06/22/indias-achieves-4-gw-installed-solar-power-capacity/>
- [4] T. Kapoor. (2015) Scaling up of grid connected solar power projects from 20,000 mw by the year 2021-22 to 1,00,000 mw by the year 2021-22 under national solar mission. Ministry of New and Renewable Energy India. [Online]. Available: <http://mnre.gov.in/file-manager/grid-solar/100000MW-Grid-Connected-Solar-Power-Projects-by-2021-22.pdf>
- [5] A. Kearney, J. Hauff, M. Verdonck, H. Derveaux, L. Dumarest, J. Alberich, and J.-C. Malherbe. (2010) Unlocking the sunbelt potential of photovoltaics. EPIA- European Photovoltaic Industry Association. [Online]. Available: http://www.mesia.com/wp-content/uploads/2012/08/EPIA-Unlocking_the_Sunbelt_Potential-of-PV.pdf
- [6] BRIDGE. (2010) Dirtmap - dust indicators and records of terrestrial and marine palaeoenvironments. Bristol Research Initiative for the Dynamic Global Environment (BRIDGE). [Online]. Available: <http://www.bridge.bris.ac.uk/projects/DIRTMAP>
- [7] V. Donkelaar, R. V. Martin, and M. Brauer, “Global estimates of ambient fine particulate matter concentrations from satellite-based aerosol optical depth

- development and application,” *Environmental Health Perspectives*, vol. 118, no. 6, pp. 847–855, 2010. [Online]. Available: <http://dx.doi.org/10.1289/ehp.0901623>
- [8] WHO. (2014) Exposure to particulate matter with an aerodynamic diameter of 10um or less (pm10) in 1600 urban areas, 2008-2013. Health Statistics and Information Systems (HSI). [Online]. Available: http://www.who.int/gho/phe/outdoor_air_pollution/phe_012.jpg?ua=1
- [9] I. T. AlAiawy, “Wind and other factor requirements to solar energy applications in iraq,” *Solar and Wind Technology*, vol. 7, pp. 597–600, 1990. [Online]. Available: [http://dx.doi.org/10.1016/0741-983X\(90\)90069-E](http://dx.doi.org/10.1016/0741-983X(90)90069-E)
- [10] S. Cattle, K. Hemi, G. Pearson, and T. Sanderson, “Distinguishing and characterising point-source mining dust and diffuse-source dust deposition in a semi-arid district of australia,” *Aeolian Res.*, vol. 6, pp. 21–29, 2012. [Online]. Available: <http://dx.doi.org/10.1016/j.aeolia.2012.07.001>
- [11] T. Sarver, A. Al-Qaraghuli, and L. Kazmerski, “A comprehensive review of the impact of dust on the use of solar energy:history, investigations, results, literature, and mitigation approaches,” *Renewable and Sustainable Energy Reviews*, vol. 22, pp. 698–733, 2013. [Online]. Available: <http://dx.doi.org/10.1016/j.rser.2012.12.065>
- [12] R. A. Bowling, “An analysis of particle adhesion on semiconductor surfaces,” *J. Electrochem. Soc.: Solid-State Science and Technology*, vol. 132, pp. 2208–2214, 1985. [Online]. Available: <http://dx.doi.org/10.1149/1.2114320>
- [13] R. Bagnold, *The physics of Blown Sand and desert dunes*, 1954, iISBN 978-94-009-5684-1 (Print) 978-94-009-5682-7 (Online).
- [14] S. J. Blott and K. Pye, “Particle size scales and classification of sediment types based onparticle size distributions: Review and recommended procedures,” *Journal of the International Association of Sedimentologists*, vol. 59, pp. 2071–2096, 2012. [Online]. Available: <http://dx.doi.org/10.1111/j.1365-3091.2012.01335.x>
- [15] NASA. (2013) Tracking dust across the atlantic. NASA Earth Observatory. [Online]. Available: <https://www.nasa.gov/content/goddard/tracking-saharan-dust-across-the-atlantic/#.VbD6-Pmqkko>

- [16] A. Buekens, *Pollution Control Technologies*, G. St Cholakov and B. Nath, Eds. Encyclopedia of Life Support Systems(UNESCO-EOLSS), 2009, vol. 3.
- [17] S. Engelstaedter, K. E. Kohfeld, I. Tegen, and S. P. Harrison, “Controls of dust emissions by vegetation and topographic depressions: An evaluation using dust storm frequency data,” *Geophysical Research Letters*, vol. 30, p. 1294, 2003. [Online]. Available: <http://dx.doi.org/10.1029/2002GL016471>
- [18] D. Schwela, “Guidlines for concentration and exposure-response measurement of fine and ultra fine particulate matter for use in epidemiological studies,” 2002. [Online]. Available: <http://apps.who.int/iris/handle/10665/67338>
- [19] L. Kazmerski, M. Al Jordan, Y. Al Jnoobi, Y. Al Shaya, and J. John, “Ashes to ashes, dust to dust: Averting a potential showstopper for solar photovoltaics,” in *Photovoltaic Specialist Conference (PVSC), 2014 IEEE 40th*, June 2014, pp. 0187–0192. [Online]. Available: <http://dx.doi.org/10.1109/PVSC.2014.6925524>
- [20] T. Claquin, M. Schulz, and Y. Balkanski, “Modeling the mineralogy of atmospheric dust sources,” *Journal of Geophysical Research*, vol. 104, pp. 243–256, 1999. [Online]. Available: <http://dx.doi.org/10.1029/1999JD900416>
- [21] A. S. Goudie and J. Middleton, *Desert Dust in the Global System*. ISBN-10 3-540-32354-6 Springer Berlin Heidelberg New York.
- [22] J. F. Kok, E. J. R. Parteli, T. I. Michaels, and D. B. Karam, “The physics of wind-blown sand and dust,” *Rep. Prog. Phys*, vol. 75, no. 106901, 2012. [Online]. Available: <http://dx.doi.org/10.1088/0034-4885/75/10/106901>
- [23] M. J. Mcpherson. (2011) Svee background to subsurface ventialation, part v, aerodynamic , sources, and control of dust. [Online]. Available: http://www.minewiki.org/index.php/SVEE.-_The_aerodynamics,_sources_and_control_of_airborne_dust
- [24] E. F. Cuddihy, “Theoretical considerations of soil retention,” *Solar Energy Materials*, vol. 3, pp. 21–33, 1980. [Online]. Available: [http://dx.doi.org/10.1016/0165-1633\(80\)90047-7](http://dx.doi.org/10.1016/0165-1633(80)90047-7)

- [25] T. Negash and T. Tadiwose, “Experimental investigation of the effect of tilt angle on the dust photovoltaic module,” *International Journal of Energy and Power Engineering*, vol. 4, no. 4, pp. 227–231, 2015. [Online]. Available: <http://dx.doi.org/10.11648/j.ijepe.20150404.15>
- [26] H. Qasem, T. R. Betts, H. Mullejans, H. Al-Busari, and R. Gottschalg, “Dust induced shading on photovoltaic modules,” *Progress in Photovoltaics: Research and Application*, vol. 22, pp. 218–226, 2014. [Online]. Available: <http://dx.doi.org/10.1002/pip.2230>
- [27] J. Cano, J. John, S. Tatapudi, and G. Tamizhmani, “Effect of tilt angle on soiling of photovoltaic modules,” in *Photovoltaic Specialist Conference (PVSC), 2014 IEEE 40th*, June 2014, pp. 3174–3176. [Online]. Available: <http://dx.doi.org/10.1109/PVSC.2014.6925610>
- [28] H. K. Elminir, A. E. Ghitas, a. E.-H. F. Hamid, R H, M. M. Beheary, and K. M. Abdel-Moneim, “Effect of dust on the transparent cover of solar collectors,” *Energy Conservation and Management*, vol. 47, pp. 3192–203, 2006. [Online]. Available: <http://dx.doi.org/10.1016/j.enconman.2006.02.014>
- [29] D. Goosens, Z. Y. Offer, and A. Zangvil, “Wind tunnel experiments and field investigations of eolian dust deposition on photovoltaic solar collectors,” *Solar Energy*, vol. 50, pp. 75–84, 1993. [Online]. Available: [http://dx.doi.org/10.1016/0038-092X\(93\)90009-D](http://dx.doi.org/10.1016/0038-092X(93)90009-D)
- [30] T. Sample, J. Lopez-Garcia, and A. Pozza, “Long-term soiling in a moderate subtropical climate,” *Photovoltaic Module Reliability Workshop*, 2015. [Online]. Available: http://www.nrel.gov/pv/performance_reliability/pdfs/2015_pvmrw_58_sample.pdf
- [31] T. N. Quang, C. He, L. Morawska, L. D. Knibbs, and M. Falk, “Vertical particle concentration profiles around urban office buildings,” *Atmos. Chem. Phys.*, vol. 12, p. 5017–5030, 2012. [Online]. Available: <http://dx.doi.org/10.5194/acp-12-5017-2012>
- [32] H. A. McGowan and A. Clark, “A vertical profile of pm10 dust concentrations measured during a regional dust event identified by modis terra, western queensland,

- australia,” *Journal of Geophysical Research: Earth Surface*, vol. 113, no. F2, 2008, f02S03. [Online]. Available: <http://dx.doi.org/10.1029/2007JF000765>
- [33] L. Boyle, H. Flinchbaugh, and M. Hannigan, “Ambient airborne particle concentration and soiling of pv cover plates,” in *Photovoltaic Specialist Conference (PVSC), 2014 IEEE 40th*, June 2014, pp. 3171–3173. [Online]. Available: <http://dx.doi.org/10.1109/PVSC.2014.6925609>
- [34] R. Muthyal. (2013) Lessons learned through installation of solar pv systems in typical indian hot climatic zone. [Online]. Available: <https://firstgreenconsulting.wordpress.com/2013/06/01/lessons-learned-through-installation-of-solar-pv-systems-in-typical-indian-hot-climatic-zone>
- [35] UNCCD, “Global alarm: Dust and sandstorms from the world’s drylands,” Online, <http://www.unccd.int/Lists/SiteDocumentLibrary/Publications/Global%20Alarm%20eng.pdf>, August 2001.
- [36] C. Sioutas, R. J. Delfino, and M. Singh, “Exposure assessment for atmospheric ultrafine particles (ufps) and implications in epidemiologic research,” *Environmental Health Perspectives*, vol. 113, no. 8, pp. 947–955, 2005. [Online]. Available: <http://dx.doi.org/10.1289/ehp.7939>
- [37] H. Vuollekoski, M. Vogt, V. A. Sinclair, J. Duplissy, H. Järvinen, E. M. Kyrö, R. Makkonen, T. Petäjä, N. L. Prisle, P. Räisänen, M. Sipilä, J. Ylhäisi, and M. Kulmala, “Estimates of global dew collection potential on artificial surfaces,” *Hydrol. Earth Syst. Sci.*, vol. 19, p. 601–613, 2015. [Online]. Available: <http://dx.doi.org/10.5194/hess-19-601-2015>
- [38] M. Gostein, T. Duster, and C. Thuman, “Accurately measuring pv soiling losses with soiling station employing module power measurements,” in *Photovoltaic Specialist Conference (PVSC), 2015 IEEE 42nd*, June 2015, pp. 1–4. [Online]. Available: <http://dx.doi.org/10.1109/PVSC.2015.7355993>
- [39] J. Zorilla-Casanova, M. Piliouline, J. Carretero, P. Bernaola, P. Carpena, L. Mora-Lopez, and M. Sidrach-de Cardona, “Analysis of dust losses in photovoltaic

- modules,” in *World renewable Energy Congress Sweden*, Sweden, 2011. [Online]. Available: http://www.ep.liu.se/ecp/057/vol11/039/ecp57vol11_039.pdf
- [40] J. Caron and B. Littmann, “Direct monitoring of energy lost due to soiling on first solar modules in california,” *Photovoltaics, IEEE Journal of*, vol. 3, no. 1, pp. 336–340, Jan 2013. [Online]. Available: <http://dx.doi.org/10.1109/JPHOTOV.2012.2216859>
- [41] C. Y. Lee, J. K. Chiang, P. C. Lin, K. Suzuki, and F. Chen. (2014) An innovative approach to examine soiling impact on photovoltaic module performance. [Online]. Available: <http://wiki-cleantech.com/uncategorized/an-innovative-approach-to-examine-soiling-impact-on-photovoltaic-module-performance>
- [42] M. Mani and R. Pillai, “Impact of dust on solar photovoltaic (pv) performance: Research status, challenges and recommendations,” *Renewable and Sustainable Energy Reviews*, vol. 14, pp. 3124–3131, 2010. [Online]. Available: <http://dx.doi.org/10.1016/j.rser.2010.07.065>
- [43] R. J. Beal, B. G. Potter, and J. H. Simmons, “Angle of incidence effects on external quantum efficiency in multicrystalline silicon photovoltaics,” *IEEE Journal of Photovoltaics*, vol. 4, pp. 1459–1464, 2014. [Online]. Available: <http://dx.doi.org/10.1109/JPHOTOV.2014.2350672>
- [44] “Photovoltaic module performance of testing and energy rating - part 2: Spectral response, incidence angle and module operating temperature measurements,” IEC 61853-2 (Draft) Standards, Tech. Rep., 2012.
- [45] B. Knisely, S. Janakeeraman, J. Kuitche, and G. Tamizhmani, “Validation of iec 61853-2 standard (draft): Angle of incidence effect on photovoltaic modules,” in *Photovoltaic Specialists Conference (PVSC), 2013 IEEE 39th*, June 2013, pp. 0675–0680. [Online]. Available: <http://dx.doi.org/10.1109/PVSC.2013.6744239>
- [46] D. King, J. Kratochvil, and W. Boyson, “Measuring solar spectral and angle-of-incidence effects on photovoltaic modules and solar irradiance sensors,” in *Photovoltaic Specialists Conference, 1997., Conference Record of the Twenty-Sixth*

- IEEE*, Sep 1997, pp. 1113–1116. [Online]. Available: <http://dx.doi.org/10.1109/PVSC.1997.654283>
- [47] N. Martin and J. M. Ruiz, “Annual angular reflection losses in pv modules,” *Progress in Photovoltaics*, vol. 13, pp. 75–84, 2005. [Online]. Available: <http://dx.doi.org/10.1002/pip.585>
- [48] H. Qasem, “Effect of accumulated dust on the performance of photovoltaic modules,” Ph.D. dissertation, Loughborough University. [Online]. Available: <https://dspace.lboro.ac.uk/dspace-jspui/bitstream/2134/11735/4/Thesis-2013-Qasem.pdf>
- [49] J. J. John, V. Rajasekar, S. Boppana, S. Tatapudi, and G. TamizhMani, “Angle of incidence effects on soiled pv modules,” SPIE Optics Photonics Conference, San Diego, California, 2014. [Online]. Available: <http://dx.doi.org/10.1117/12.2063351>
- [50] H. F. M. El-Hobokshy M S, “Degradation of photovoltaic cell performance due to dust deposition on it surface,” *Renewable Energy*, vol. 3, pp. 585–590, 1993. [Online]. Available: [http://dx.doi.org/10.1016/0960-1481\(93\)90064-N](http://dx.doi.org/10.1016/0960-1481(93)90064-N)
- [51] P. Burton and B. King, “Artificial soiling of photovoltaic module surfaces using traceable soil components,” in *Photovoltaic Specialists Conference (PVSC), 2013 IEEE 39th*, June 2013, pp. 1542–1545. [Online]. Available: <http://dx.doi.org/10.1109/PVSC.2013.6744438>
- [52] K. Brown, T. Narum, and N. Jing, “Soiling test methods and their use in predicting performance of photovoltaic modules in soiling environments,” in *Photovoltaic Specialists Conference (PVSC), 2012 38th IEEE*, June 2012, pp. 001 881–001 885. [Online]. Available: <http://dx.doi.org/10.1109/PVSC.2012.6317960>
- [53] J. John, S. Tatapudi, and G. Tamizhmani, “Influence of soiling layer on quantum efficiency and spectral reflectance on crystalline silicon pv modules,” in *Photovoltaic Specialist Conference (PVSC), 2014 IEEE 40th*, June 2014, pp. 2595–2599. [Online]. Available: <http://dx.doi.org/10.1109/PVSC.2014.6925462>
- [54] P. Burton and B. King, “Spectral sensitivity of simulated photovoltaic module soiling for a variety of synthesized soil types,” *Photovoltaics, IEEE*

- Journal of*, vol. 4, no. 3, pp. 890–898, May 2014. [Online]. Available: <http://dx.doi.org/10.1109/JPHOTOV.2014.2301895>
- [55] S. Chattopadhyay, R. Dubey, V. Kuthanazhi, J. J. John, C. S. Solanki, A. Kottantharayil, B. M. Arora, K. L. Narasimhan, V. Kuber, J. Vasi, A. Kumar, and O. S. Sastry, “Visual degradation in field-aged crystalline silicon pv modules in india and correlation with electrical degradation,” *IEEE Journal of Photovoltaics*, vol. 4, pp. 1470–1476, 2014. [Online]. Available: <http://dx.doi.org/10.1109/JPHOTOV.2014.2356717>
- [56] NREL and NISE. (2015) Updated india solar resource maps. [Online]. Available: http://www.nrel.gov/international/images/india_ghi_annual.jpg
- [57] R. Singh and R. Banarjee, “Estimation of rooftop solar photovoltaic potential of a city,” *Solar Energy*, vol. 115, pp. 589–602, 2015. [Online]. Available: <http://dx.doi.org/10.1016/j.solener.2015.03.016>
- [58] M. S. El-Shobokshy and F. M. Hussein, “Effect of dust with different physical properties on the performance of photovoltaic cells,” *Solar Energy*, vol. 51, pp. 505–511, 1993. [Online]. Available: [http://dx.doi.org/10.1016/0038-092X\(93\)90135-B](http://dx.doi.org/10.1016/0038-092X(93)90135-B)
- [59] S. C. Pop, V. Abbaraju, B. Brophy, Y. S. Yang, S. Maghsoodi, and P. Gonsalves, “A highly abrasive-resistant, long-lasting anti-reflective coating for pv module glass,” *Photovoltaic Specialist Conference (PVSC), IEEE 40th*, pp. 2715–2719, 2014. [Online]. Available: <http://dx.doi.org/10.1109/PVSC.2014.6925490>
- [60] “Photovoltaic devices - part 3: Measurement principles for terrestrial photovoltaic (pv) solar devices with reference spectral irradiance data,” IEC 60904 Standards, Tech. Rep., 2008.
- [61] A. Salim, F. Huraib, and N. Eugenio, “Pv power-study of system options and optimization,” in *8th European PV solar energy conference, Florence, Italy*, 1988.
- [62] F. Wakim, “Introduction of pv power generation to kuwait,” Tech. Rep., 1981.
- [63] A. H. Hassan, “Effect of airborne dust concentration on the performance of pv modules,” *J Astron Soc Egypt*, vol. 13, pp. 24–38, 2005.

- [64] A. Jabbar and N. Khalifa, “On the effect of cover tilt angle of the simple solar still on its productivity in different seasons and latitudes,” *Energy Conversion and Management*, vol. 52, pp. 431–436, 2011. [Online]. Available: <http://dx.doi.org/10.1016/j.enconman.2010.07.018>
- [65] U. E. A. Climate Research Unit. (2005) Average annual relative humidity. Nelson Institute Centre for Sustainability and the Global Environment. [Online]. Available: <http://nelson.wisc.edu/sage/data-and-models/atlas/data.php?incdataset=Average%20Annual%20Relative%20Humidity>
- [66] P. V. Kumar, A. Kumar, O. Prakash, and A. K. Kaviti, “Solar stills system design: A review,” *Renewable and Sustainable Energy Reviews*, vol. 51, p. 153–181, 2015. [Online]. Available: <http://dx.doi.org/10.1016/j.rser.2015.04.103>
- [67] A. Ganesh, “Photocatalytic superhydrophilic tio₂ coating on glass by electrospinning,” *RSC Advances*, vol. 2, p. 2067 – 2072, 2012. [Online]. Available: <http://dx.doi.org/10.1039/C2RA00921H>
- [68] K. Guan, “Relationship between photocatalytic activity, hydrophilicity and self-cleaning effect of tio₂/sio₂ films,” *Surface Coat Technology*, vol. 191, pp. 155–160, 2005. [Online]. Available: <http://dx.doi.org/10.1016/j.surfcoat.2004.02.022>
- [69] G. Wilkes. (2004) Electrospinning. [Online]. Available: <http://www.che.vt.edu/Faculty/Wilkes/GLW/electro-spinning/electr spinning.html>
- [70] Nanotec-ufrn. (2012) Nanotechnology and regenerative medicine. [Online]. Available: <http://nanotec-ufrn.blogspot.in/2012/11/nanotecnologia-e-medicina-regenerativa.html>
- [71] H. Yang, H. Zhu, M. Hendrix, N. Lousberg, G. de With, A. C. C. Esteves, and J. H. Xin, “Temperature-triggered collection and release of water from fogs by a sponge-like cotton fabric (adv. mater. 8/2013),” *Advanced Materials*, vol. 25, no. 8, pp. 1149–1149, 2013. [Online]. Available: <http://dx.doi.org/10.1002/adma.201370052>
- [72] S. Alkhazraji, S. Aldhaheri, and F. Alhameli, “Device for water collection from atmospheric moisture,” Patent US Patent App. 14/331,614, 2015. [Online]. Available: <http://www.google.com/patents/US20150020687>